

DOE FILE COPY

FILE 8.3  
SAN/0499-9  
MDC G7864

STMPO-119

10 MWe Solar Thermal  
Central Receiver Pilot Plant

SOLAR FACILITIES DESIGN INTEGRATION

INDEPENDENT FEASIBILITY ASSESSMENT  
(RADL ITEM 4-4)

June 1979

WORK PERFORMED UNDER CONTRACT  
DE-AC-03-79SF10499

FOSTER WHEELER DEVELOPMENT CORP  
JOHN BLIZARD RESEARCH CENTER  
12 PEACH TREE HILL ROAD  
LIVINGSTON, N. J. 07039

RECEIVED  
JUN 21  
STMPO



U.S. Department of Energy



FOSTER  WHEELER



Solar Energy

**10 MWe Solar Thermal  
Central Receiver Pilot Plant  
Solar Facilities Design Integration**

---

---

**INDEPENDENT FEASIBILITY ASSESSMENT  
(RADL ITEM 4-4)**

---

---

**June 1979**

**DISCLAIMER**

This report was prepared as an account of work sponsored by the United States Government. Neither the United States nor the United States Department of Energy, nor any of their employees, makes any warranty, express or implied, or assumes any legal liability or responsibility for the accuracy, completeness, or usefulness of any information, apparatus, product, or process disclosed, or represents that its use would not infringe privately owned rights. Reference herein to any specific commercial product, process, or service by trade name, mark, manufacturer, or otherwise, does not necessarily constitute or imply its endorsement, recommendation, or favoring by the United States Government or any agency thereof. The views and opinions of authors expressed herein do not necessarily state or reflect those of the United States Government or any agency thereof.

**FOSTER WHEELER DEVELOPMENT CORP  
JOHN BLIZARD RESEARCH CENTER  
12 PEACH TREE HILL ROAD  
LIVINGSTON, N. J. 07039**

**PREPARED FOR THE  
U.S. DEPARTMENT OF ENERGY  
SOLAR ENERGY  
UNDER CONTRACT DE-AC-03-79SF10499**

## TABLE OF CONTENTS

<u>Section</u>		<u>Page</u>
1	INTRODUCTION	1-1
2	DOCUMENTS REVIEWED	2-1
3	SUMMARY OF REVIEW AND ASSESSMENT	3-1
	3.1 Structural Design and Analysis	3-1
	3.2 Mechanical Design	3-3
	3.3 Thermal/Hydraulic Design	3-5
	3.3.1 Design Correlations	3-5
	3.3.2 Static Stability, Flow Sensitivity, and Tube Wall Temperature	3-6
	3.3.3 Dynamic Stability	3-8
4	RECOMMENDATIONS	4-1
5	REFERENCES	5-1
<u>Appendix</u>		
A	PERSONNEL CONTRIBUTING TO THE REVIEW	
B	LETTER TO FILE 9-41-6023, 10-MWe PILOT PLANT RECEIVER DESIGN EVALUATION, I. BERMAN, FOSTER WHEELER DEVELOPMENT CORPORATION, APRIL 2, 1979	
C	COMMENTS ON RECEIVER SUBSYSTEM ANALYSIS PLAN FOR 10-MWe SOLAR THERMAL CENTRAL RECEIVER PILOT PLANT, PROPOSED REVISION, MARCH 16, 1979	
D	REPORT ON REVIEW OF HEAT TRANSFER AND PRESSURE DROP COR- RELATIONS USED BY ROCKETDYNE IN DESIGN OF PILOT PLANT RECEIVER	
E	MCDONNELL DOUGLAS PILOT PLANT RECEIVER PANEL STATIC STABILITY	
F	SUMMARY REPORT ON PILOT PLANT RECEIVER EVAPCRATOR/ SUPERHEATER PANEL DYNAMIC STABILITY ANALYSIS	

SECTION 1  
INTRODUCTION

Section 1

INTRODUCTION

On March 12, 1979, Foster Wheeler received approval to proceed on this subcontract as receiver subsystem evaluator and technical advisor to McDonnell Douglas Astronautics Company and was directed to utilize the first 90 days to conduct an independent assessment of the basic receiver concept. This assessment, performed by the Foster Wheeler personnel listed in Appendix A, included review and analyses of critical design areas to determine whether the proposed receiver has any serious design deficiencies or operating limitations that would require major modifications. This report describes this independent assessment.

SECTION 2  
DOCUMENTS REVIEWED

## Section 2

## DOCUMENTS REVIEWED

The following documents were reviewed in the course of this assessment:

- Central Receiver Solar Thermal Power System, Phase I, CDRL Item 2, Pilot Plant Preliminary Design Report, Volume 2, System Description and System Analysis, SAN/1108-8/1; and Volume 4, Receiver Subsystem, SAN/1108-8/4, October 1977
- 10-MWe Solar Thermal Central Receiver Pilot Plant, Plant Integration and Solar Facilities Subsystems, Volume 1, Technical Proposal, Book 1, MDC G7375P, May 1978
- Receiver Subsystem Analysis Plan for 10-MWe Solar Thermal Central Receiver Pilot Plant, Energy Technology Engineering Center, December 1978, proposed revision, March 16, 1979
- Rocketdyne CRTF test panel as-built drawings 99 RS 010501; 010502 (Sheet 1); 010503 (Sheets 1, 2, 3, and 4); 010504, 010505; 010506, 010508, 010510, 010522; 010523, 010524, 010525, 010527, 010528
- Performance Analysis for the MDAC Rocketdyne Pilot and Commercial Plant Solar Receivers, General Electric Company, SAND 78-8183, September 1978
- MDAC/Rocketdyne Solar Receiver Design Review, Combustion Engineering Inc., SAND 78-8188, November 1978
- R. N. Schweinberg, STMPO, letter to Ray W. Hallet, Jr., MDAC, March 6, 1979, Subject: Pilot Plant Receiver Material Meeting Report
- Receiver Boiler/Superheater Panel Performance at Derated Steam Conditions, MDAC Memorandum A3-374-E000-M-011, January 21, 1979
- Water/Steam Loop Parametric Analysis, MDAC Memorandum A3-374-E000-M-003, January 23, 1979
- Parametric Thermal Analysis of the Central Receiver Boiler/Superheater Panel, MDAC Memorandum A3-228-DELTA-78014, January 23, 1979
- Boiler/Superheater Panel Thermal Performance--Analysis of Wall and Flow Temperature Distribution, MDAC Memorandum A3-374-E000-M-008, January 26, 1979
- R. W. Hallet, Jr., MDAC, letter to R. N. Schweinberg, STMPO, April 30, 1979, Subject: Pilot Plant Receiver Material.

SECTION 3  
SUMMARY OF REVIEW AND ASSESSMENT

---



## Section 3

## SUMMARY OF REVIEW AND ASSESSMENT

3.1 STRUCTURAL DESIGN AND ANALYSIS

Reference 1 states that in terms of design and analysis, the pilot plant is to meet the following ASME Boiler and Pressure Vessel Code requirements:

- Absorber Boiler Panel
  - Section I
  - Fatigue Analysis Criteria from Section III plus Code Case N-47 (1592)
  - Section VIII-Division 2 (for thermal ratcheting evaluation)
- Pressure Vessels
  - Section VIII.

The use of Section III, Code Case N-47 (1592), and Section VIII-Division 2 are decisions of the owner and are not required for a Section I Code Stamp. It is important that the codes established for nuclear components are not blindly used. These nuclear codes should be modified to relate their reliability level to the requirements of the CRSTPS.

This question of Code rules was addressed in various places.<sup>2-4</sup> The general philosophy is given in the comments on the ETEC Receiver Subsystem Analysis Plan.<sup>3</sup> The proposed analysis plan seems to be written with the idea that creep damage need not be considered in fatigue calculations. In a telephone conversation, Lee and Chandler of Rocketdyne indicated they believe compressive hold times would not be damaging, and therefore there was no need to

evaluate the effect of creep damage in reducing fatigue life. This is not true for Incoloy 800<sup>5</sup> although it is true for Types 304 and 316 stainless steel. In addition, it was once assumed that the maximum tube wall temperature was about 1080°F.<sup>6</sup> At that temperature the creep damage which would be calculated from the creep rupture curve might not be too severe. Creep damage would be substantial at 1250°F, the maximum tube temperature calculated by Foster Wheeler during this review. Thus, any analysis plan must include creep fatigue and not solely fatigue evaluation.

If it is decided that ratcheting is a mode of failure that must be considered, it should be creep ratcheting at elevated temperatures and not the ratcheting of Section VIII-Division 2. However, it is recommended that neither ratcheting nor creep ratcheting be considered.

In designing the receiver, the first step is to clearly define the tube design temperature and then the tube material. Assume that the maximum tube wall temperature to be considered is 1250°F. When one looks at various related items, the relationship of the properties of Incoloy 800 and Incoloy 800H conflict. The Code indicates that at 1150°F the allowable stress is the same for each. Below 1150°F the values for Incoloy 800 are higher. Above 1150°F, the values for Incoloy 800H are higher. This was demonstrated at the Meeting on Pilot Plant Receiver Material Selection at STMPO, on February 27, 1979.<sup>6</sup> However, it is stated in Reference 7 that strength and fatigue properties are superior for Incoloy 800 from 800 to 1200°F.

Once the temperature and material properties are defined, some of the Code design problems must be addressed. With the modifications suggested in Reference 4, including a clear definition of creep fatigue requirements, the proposed revision of the analysis plan should be a good basis for design. Implementation of these modifications should then include the use of Reference 8 especially for creep fatigue analysis.

There is another item in Reference 2 which should be emphasized. There is very little reliable test information on the creep fatigue life of actual structures. It may be necessary to limit the design life, or to use less conservative criteria in order to pass the creep fatigue requirements for the hottest panels. As pointed out on Page 7 of Reference 2, tests would be the best tool for design. Even if performed after the design is complete and fabrication is begun on the 10-MWe unit, these tests would alert us to cycle-time limitations and permit evaluation of the necessity for replacement of the hot panels. Thus, accelerated structural creep fatigue tests on the five tubes and full panel would be extremely valuable.

### 3.2 MECHANICAL DESIGN

The Rocketdyne CRTF test panel as-built drawings were reviewed along with a sketch of the redesigned 10-MWe boiler steam manifold included in Attachment 1 to Reference 9. The following comments and recommendations are offered.

- Welded rather than flanged piping connections should be used at the steam outlet of each panel. It is difficult to keep a flanged connection tight with a large number of thermal cycles and rapid thermal transients in which bolt temperature lags behind flange temperature.

- The use of low-melting-point metals (aluminum, zinc, cadmium, tin, and lead) should be avoided in the design and in the shop during fabrication. These metals can penetrate and embrittle austenitic stainless at temperatures above their respective melting points. This occurs by selective intergranular attack of the material. In one case which Foster Wheeler experienced, the zinc from galvanized identification tags rubbed off on Type 321 superheater tubing. After the tubes were put in service at temperatures ranging from 1000 to 1200°F, extensive cracking of the Type 321 material occurred in less than 3 months. There have also been numerous cases in the petrochemical industry where galvanized structural members have abraded against or been attached to austenitic stainless steel vessels and catastrophic cracking of the material has occurred. Current nuclear standards for the breeder reactor program have recognized this problem and it is now specified that no low-melting-point materials be used which can come in contact with austenitic stainless steels. We strongly recommend that all low-melting-point materials be banned from the fabrication area and that all construction materials specified on the drawings which involve low-melting-point plating or other coating methods be eliminated.
- All welded attachments (lugs, etc.) to the tubes of the panel are points of stress (strain) concentration. We suggest that the clips and lugs be redesigned so they attach to the weld between tubes rather than directly to the tubes. It would also be wise to minimize the number of attachments.
- Rolling the tube before welding (Drawing 99RS 010503, Sheet 2, Views B and E) can lead to porosity in the fillet welds joining the tubes to the manifold unless extreme cleanliness is achieved. If any contaminants (hydrocarbons, water) exist in the crevices between the tube and the manifold and the tube is rolled, there is no escape path for the gases formed by decomposition of the material and the exit path of escape is through the weld, leading to porosity. If extreme cleanliness is maintained, it is possible to lightly roll the tubes prior to welding and avoid the problem. However, it has been our experience that it is more desirable to stake the tube in place, preferably for a full 360 deg utilizing a specially designed tool. We would also strongly recommend that once the manifold and tubes have been thoroughly cleaned the material be kept warm and above the dew point at all times during assembly and completion of the tube welding operation. In addition, the tube weld edge preparation shown will cause bridging at the root. If edge preparation is used, a J-groove is needed.
- Regarding Section C-C on Drawing 99RS 010505A, there is a possible root cracking problem with Incoloy 800 material and Inconel 82 weld rod. The pipe must be raised in the socket to allow for weld contraction.

- Assuming that the pipe plugs in the inlet header in Drawing 99RS 010501 are Incoloy 800, there could be a galling problem. Technically, galling is a substantial increase in the coefficients of friction between the mating parts. Foster Wheeler has experienced a number of occurrences where stainless steel studs were inserted into stainless steel flanges with significant galling occurring either during insertion or attempted removal of the studs. It is advisable that there be a relatively large difference in the hardness of the two mating materials.
- Dissimilar welds between ferritic Cr-Mo valve bodies and austenitic stainless steel piping are indicated. These have proved to be a problem in the boiler industry if not correctly designed and welded. These should be checked to avoid potential catastrophic cracking.
- Note 8 on Drawing 99RS 010501 calls for passivation of internal surfaces. If passivation with nitric acid is contemplated, it should be recognized that ferritic valve bodies are present.
- Three problems are apparent with regard to the redesigned boiler steam manifold (panel outlet header). The sketch shows a 90-deg countersunk hole 0.70 in. in diameter. If this countersink is intended to be the edge preparation for the tube-to-manifold weld, it is our opinion that this joint design is not satisfactory, since it is very difficult to obtain complete fusion at the root. We suggest that the edge preparation be changed to a modified J-groove to permit full root fusion. We also do not understand the reason for the heavy chamfer on the tube holes at the outer wall of the manifold; all that should be required is a breaking of the corner of the drilled hole. In addition, each end of the large manifold support lug approaches the manifold radially and accordingly forms a 90-deg angle with the outer surface of the manifold. This represents a significant stress concentration and the design should at least provide for a generous radius at this point. We would recommend designing this particular area with the lug attached in the vicinity of the circumferential butt weld joining the caps to the manifold. It may even be possible to design the structure so that these supports can be wrapped completely around the manifold and attached or keyed mechanically to the manifold.

### 3.3 THERMAL/HYDRAULIC DESIGN

#### 3.3.1 Design Correlations

The heat transfer and pressure drop correlations used by Rocketdyne in the design of the pilot plant receiver, as reported in the CRSTPS Phase 1 Preliminary Design Report, were reviewed. The correlations used for single and

two-phase flow are generally accepted in the boiler industry. The only heat-transfer correlations that have significant impact on receiver design are those for film boiling and superheated steam. Rocketdyne has reported that they use two-thirds of the saturated vapor heat-transfer coefficient as the minimum coefficient in film boiling, and that this procedure has been substantiated by experiments on a single-tube panel. This is acceptable if the tests were properly designed to get accurate data over the full range of anticipated receiver operation. Foster Wheeler would use the Bishop-Sandberg-Tong correlation<sup>10</sup> and we suggest this be checked against Rocketdyne's procedure. For superheated steam, we recommend the Heineman correlation<sup>11</sup> rather than the Dittus-Boelter correlation<sup>12</sup> used by Rocketdyne. However, since the Dittus-Boelter correlation yields more conservative heat-transfer coefficients, its use does not jeopardize the design of the receiver.

Further details on review of the correlations can be found in Appendix D.

### 3.3.2 Static Stability, Flow Sensitivity, and Tube Wall Temperature

The receiver preheater and evaporator/superheater panels were analyzed to determine static stability and panel sensitivity to heat flux variations across the panel width. For the purpose of analysis the FWEC pressure drop computer program EQPRSDRP was used. The program incorporates the following:

- Moody friction factors for single phase flow
- Martinelli-Nelson two-phase frictional multiplier  $\phi_{fo}^2$  evaluated at zone average conditions
- Flow acceleration static pressure changes computed from zone inlet and outlet velocity head assuming no slip between phases

- Computational capability for multiple circuits, zones, flows, and absorptions.

The general procedure followed for analysis was to compute and plot the static pressure difference between panel inlet and outlet headers as a function of mass flow rate for different heat absorption rates. These curves were analyzed to determine whether negative sloping regions exist, indicating static Leginegg instability, and to determine increases or decreases in flow rate per tube as a function of heat absorption variations across the width of the panel.

Header configuration induced flow imbalances and the maximum evaporator/superheater panel tube wall temperature were also investigated.

Analysis of the preheater and evaporator/superheater panel sensitivity to heat flux variations across the panel width revealed the following:

- The up-flow preheater panels are stable at the design, minimum, and maximum load conditions, and no instability is expected from heat flux variations.
- The down-flow preheater panels are unstable and will be subject to flow stagnation or reversal at the design and minimum load conditions. At the maximum load conditions, the pressure drop will be positive and the flow will be stable. However, the margin of safety is quite small.
- The boiler panels are relatively stable at the design, minimum, and maximum loads for the expected heat flux variations. Flow variations are less than 5 percent. However, since the average enthalpy change from panel inlet to outlet is large (approximately 974 Btu/lb at the design load), relatively small percentage heat absorption increases combined with a small flow reduction can result in a large increase in final steam temperature, and consequently, in tube wall temperature for that tube in the panel which receives the greatest heat absorption.

- Of the boiler panel load conditions analyzed (design, minimum, maximum) the worst steamside conditions (the highest leaving steam temperature) result in panel 18 at the design load. For a 9.1 percent incident heat flux variation, the absorbed heat flux increases 5.4 percent, the flow is reduced by 4.1 percent, and the leaving steam temperature is 1129°F.
- The highest boiler panel mean tube wall temperature (1242°F) was computed at a location 38.5 ft from the heated inlet of panel 18 at the design load.
- No header-configuration-induced flow imbalances are expected for the preheater and boiler panels over the operating load range.

Details of the analytical procedures and results are given in Appendix E.

### 3.3.3 Dynamic Stability

The receiver evaporator/superheater panels were analyzed to evaluate the overall thermal performance and the tube-side pressure drop. The thermal/hydraulic conditions thus obtained were then used to establish the static and dynamic stability characteristics of the tube-side boiling flow. The analyses were performed at three levels of total incident thermal power per panel to examine the thermal performance and flow stability of the panels under the following conditions:

- Panel 13 at 3.218 Mwt
- Panel 21 at 1.728 Mwt
- Panel 21 at 0.625 Mwt.

The overall thermal performance of the boiler panels was examined using an existing FWEC solar boiler performance computer code, which was modified to accommodate the MDAC/Rocketdyne boiler configuration and thermal/hydraulic



conditions. In the analysis, the entire 45 ft active tube length was divided into 45 elements. For each element under consideration, the energy balance equation was first solved using an iterative procedure to calculate the outside tube-wall temperature and the fluid enthalpy at the exit of the element. The thermal resistance of the tube and convection inside the tube were calculated based on the local conditions of the element. The tube-side pressure drop through the element was computed simultaneously. The thermal performance results were then used in static and dynamic stability analyses.

A one-tube model was analyzed to simulate the conditions of panel 13 with 3.218 Mwt incident power to assess static stability. The results of the analysis showed that the curve of water/steam pressure drop versus the normalized water/steam flow rate has a positive slope throughout the flow-rate range and, therefore, the boiler panel is statically stable under a given circumferentially uniform heat flux condition.

A density-wave type of dynamic instability was investigated in the dynamic stability analysis. This type of instability is due to the feedback and interaction between the various pressure drop components and is caused specifically by the lag introduced through the density head term due to the finite speed of propagation of density waves. The density wave oscillation can be analyzed by the conventional linear feedback theory in the frequency domain. For this study, two computer codes, DYNAM<sup>13</sup> and NUFREQ<sup>14</sup> were used to evaluate dynamic stability. For both codes the Nyquist stability criteria used in control system theory were applied to determine if the boiling channel was stable.

The flow stability analyses indicate that the boiler panels are statically stable, but dynamically unstable under various levels of incident thermal power. Reducing the inlet water subcooling and increasing the water flow rate improved the dynamic stability of the boiling channel, but the results were still unsatisfactory. Inlet orificing of individual boiler tubes was required to achieve dynamic stability. However, the required orifice sizes were extremely small and were prohibited by the consideration of scale deposition. If the boiler panel configuration could be modified, it is suggested that the heated subcooled section be separated from the evaporator/superheat panel by modifying the preheat panel and the superheat section be separated from the present combined evaporator/superheater panel by introducing a proper plenum between evaporation and superheat. This will require a rearrangement of the boiler circuits. In other words, there would be three groups of flow panels (preheat, boiling, superheat) in series connection and in each group a number of panels would be connected in parallel.

The CHF/DNB thermal stress analysis needs more precise high-cycle fatigue data for Incoloy 800. This task is beyond the present work scope, and further efforts on CHF/DNB thermal analysis are necessary.

Within the limit of the current funding, Foster Wheeler will continue dynamic stability analysis for separate preheater boiler and superheater panels to find a way to stabilize the flow circuit and perform a limited analysis for the DNB-induced thermal oscillation.

The dynamic stability analysis and results are discussed in more detail in Appendix F.

SECTION 4  
RECOMMENDATIONS

## Section 4

## RECOMMENDATIONS

Based on the results of the first 90-day feasibility assessment reported here, Foster Wheeler recommends that the following steps be taken to assure trouble-free operation of the receiver.

- Make certain that the design tube wall temperature is equal to the maximum steady-state tube wall temperature that will be encountered in service. It is apparent from the analyses reported here that the maximum tube wall temperature is considerably higher than previously reported.<sup>6</sup>
- Consider creep fatigue in the choice of tube material.
- Use the Interim Structural Design Standard,<sup>8</sup> modified to utilize Code Section I as the basis of the Receiver Subsystem Analysis Plan.
- Run elevated-temperature, accelerated creep-fatigue tests on the five-tube panel and also, if possible, on the CRTF full panel.
- Use only up-flow panels in the preheater section of the receiver.
- Use welded rather than flanged piping connections at the steam outlet of each panel.
- Redesign tube support clips so that they do not attach directly to the tubes, and minimize the use of attachments.
- On the panel outlet manifold, as redesigned,<sup>9</sup> the edge preparation for the tube-to-manifold weld should be changed to a modified J-groove to permit full root fusion.
- The large support lugs on the panel outlet manifold should be redesigned to reduce stress concentration and thermal stresses at the lug-to-manifold interface.
- Investigate the dynamic stability of the evaporator/superheater panels further in view of the instability indicated in the analyses reported here. Tests should be run on the full-scale panel at CRTF as soon as possible to check these analyses, with care being taken that the test

panel is adequately instrumented to detect dynamically unstable flow conditions. Analytical work to find a practical way to stabilize the flow should continue.

- To prevent excessive steam and tube wall temperatures during transients, the panel steam outlet temperature control system must be highly responsive to changes in incident power because of the high sensitivity of steam temperature to changes in power and flow. It is likely that a feedforward signal responsive to incident power on each panel will be required. This can be determined in the full-scale tests at CRTF.

SECTION 5  
REFERENCES

## Section 5

## REFERENCES

1. Record of Discussion, Kick-Off Meeting: Receiver Design Evaluation by Foster Wheeler, March 21, 1979, MDAC Memorandum A3-226-MLJ-EP-221.
2. Letter to File 9-41-6023, 10-MWe Pilot Plant Receiver Design Evaluation, I. Berman, Foster Wheeler Development Corporation, April 2, 1979.\*
3. Proposed Revision to Receiver Subsystem Analysis Plan for 10-MWe Solar Thermal Central Receiver Pilot Plant, March 16, 1978.
4. Comments on Receiver Subsystem Analysis Plan for 10-MWe Solar Thermal Central Receiver Pilot Plant by I. Berman, Foster Wheeler Development Corporation, May 11, 1979.\*
5. S. Majumdar, "Compilation of Fatigue Data for Incoloy 800 and 800H Alloys," Argonne National Laboratories, Report No. ANL/MSD-79-3, March 1978.
6. Report of February 27, 1979 meeting on Pilot Plant Receiver Material, Enclosure 2 to letter from R. N. Schweinberg, STMPO, to R. W. Hallett, Jr., MDAC, March 6, 1979.
7. Letter to R. N. Schweinberg, STMPO, from R. W. Hallett, Jr., MDAC Memorandum A3-202-EP-GCC-323, April 30, 1979, Subject: Pilot Plant Receiver Material.
8. Sandia Laboratories, "Final Report Phases 1 and 2 - An Interim Structural Design Standard for Solar Energy Application," SAND-79-8183, January 1979.
9. Letter to R. N. Schweinberg, STMPO, from R. W. Hallett, Jr., MDAC, Memorandum A3-373-EP-RLG-383, May 11, 1979, Subject: Action Item Response, Initial Project Design Review, May 2, 1979.
10. A. A. Bishop, R. O. Sandberg, and L. S. Tong, "Forced Convection Heat Transfer at High Pressure After the Critical Heat Flux," ASME Paper No. 65-HT-31.
11. J. B. Heineman, "An Experimental Investigation of Heat-Transfer to Superheated Steam in Round and Rectangular Channels," Argonne National Laboratories, Report No. 6213, 1960.
12. F. W. Dittus and L. M. K. Boelter, "Heat Transfer in Automobile Radiators of the Tubular Type," University of California, Publications in Engineering, Vol. 2, No. 13, 1930, pp. 443-461.

\* Reference 2 is included as Appendix B and Reference 4 as Appendix C.

13. L. G. Efferding, "DYNAM, A Critical Computer Program for Study of the Dynamic Stability of Once-Through Boiling Flow with Superheated Steam," GAMD-8656, 1968.
14. R. T. Lahey, Jr. and G. Yadigaroglu, "NUFREQ, A Computer Program to Investigate Thermo-Hydraulic Stability," General Electric Company, Report No. NEDO-133344, July, 1973.



APPENDIX A

## Appendix A

## PERSONNEL CONTRIBUTING TO THE REVIEW

The individuals from Foster Wheeler Development Corporation (FWDC) and Foster Wheeler Energy Corporation (FWEC) involved in this assessment are listed below along with their titles and areas of responsibility or expertise.

- R. J. Zoschak, Technical Director, Applied Thermodynamics Research, FWDC - Thermal/hydraulic analysis and design\*
- Dr. I. Berman, Technical Director, Engineering Science and Technology, FWDC - Structural analysis and design
- W. R. Apblett, Jr., Technical Director, Materials Technology, FWDC; and Chief Metallurgist, Foster Wheeler Corporation (the parent company of FWDC and FWEC) - Materials, metallurgy, and fabrication
- W. P. Gorzegno, Divisional Vice President, Engineering, Equipment Division, FWEC - Overall steam generator design and operation
- Dr. S. M. Cho, Manager, Thermal Hydraulics and Systems Engineering; Dr. T. T. Kao and H. L. Chou, Staff Engineers, Engineering Technology Department, Nuclear and Advanced Technology Operations, Equipment Division, FWEC - Dynamic stability analysis
- F. M. Talmud, Manager, Functional Design; S. Goidich and G. Nedelka, Staff Engineer, Staff Engineering Department, Equipment Division, FWEC - Fluid and thermal analysis.

---

\*R. J. Zoschak serves as Project Manager for this assessment.

APPENDIX B

## INTER OFFICE CORRESPONDENCE

9-41-6023

April 2, 1979

To: FILE

From: I. Berman

cc: W. R. Apblett, Jr.  
S. Cho  
A. C. Gangadharan  
W. P. Gorzegno  
G. D. Gupta  
G. M. Kohler  
T. V. Narayanan  
R. J. ZoschakSubject: 10-MWe Pilot Plant Receiver Design EvaluationINTRODUCTION

On March 21, 1979, R. J. Zoschak, W. P. Gorzegno, S. Cho, and I. Berman visited MDAC in Huntington Beach, California, in order to participate in a review of the receiver design for the 10-MWe pilot plant to be erected at Barstow. These notes relate mainly to the area of structural design and analysis with some material and fabrication information as well as other items that seem pertinent.

FWDC first spoke briefly to Raymond W. Hallet (Director of the 10-MWe pilot plant effort, MDAC), Pete Drummond (Vice President of Energy, MDAC), and Gerry Coleman (Technical Director of 10-MWe pilot plant, MDAC). The all day technical discussions were chaired by Gerry Coleman. In addition to the FW personnel the following participated in part or fully:

Gerry Coleman	MDAC
Chic Finch	MDAC
Pete Guzelis	MDAC
Larry Joy	MDAC
Jerry Freifeld	Rocketdyne
Ron Pauckert	Rocketdyne

ATTACHMENTS

- I Agenda
- II Questions to MDAC Regarding Structural Analysis (developed by I. Berman)
- III Overall MDAC Subsystem Design Concepts
- IV Record of Discussion - Receiver Material Meeting, STMPO, February 27, 1979

To: File  
Subject: 10-MWe Pilot Plant Receiver Design Evaluation

April 2, 1979  
Page 2

#### SUMMARY ITEMS

- The Rocketdyne approach to Code is inconsistent and incomplete.
- Incoloy 800 will be used. Questions concerning consistency of properties, fatigue life for compressive hold times, and the thermal expansion coefficient of the compatible weld material must be answered.
- A definite number must be obtained for the material design temperature and the operating pressure and temperature conditions for which the analysis is to be carried out. In the range of temperature of operation there are sharp changes in some parameters for fairly small changes in temperature.
- The thickness chosen 0.115 in. is much greater than any requirement of Section I. The large thickness does reduce the creep-fatigue life.
- Creep fatigue is a failure mode that must be guarded against in the panels. The method to be used by Rocketdyne is unclear. The method of N-47 recommended by STMPO is extremely expensive and time consuming. The much simpler and less expensive method suggested in the proposed Interim Design Code needs some substantiation. A first level of substantiation can be done by some analysis of typical conditions. In addition the fatigue and creep damage curves and creep-fatigue damage allowable values need substantial study.
- If the ratcheting behavior is to be investigated it should be creep ratcheting as in Code Case N-47 since the thermal ratcheting as in Section VIII-Division 2 does not apply at the operating temperature. It is recommended that no ratcheting calculations be required.
- Structural tests would be invaluable. The five panel specimen as well as the full panel can be used for an accelerated creep-fatigue test after other tests are run. An analysis would be run to determine if our prediction techniques have validity.
- Tube-to-tube welds and attachments to tubes need further study.

#### GENERAL DISCUSSION

The meeting opened with a description of the program by Gerry Coleman. There were many side discussions so that the sequence of items was not as shown in the Agenda. In addition the Rocketdyne group had to leave at 1:00 p.m. so some of the questions by W. R. Apblett could not be discussed. These were given to the Rocketdyne people so that they would respond in writing.

One important point brought out at the beginning by Coleman was that we are to look at the pilot plant and not the commercial plant. This is particularly important structurally because the condition of higher flux in the commercial plant would greatly affect the creep-fatigue results as well as other structural considerations.

To: File  
Subject: 10-MWe Pilot Plant Receiver Design Evaluation

April 2, 1979  
Page 3

Question: What are the Code requirements that are to be met by the pilot plant?

Answer: Section I - They intend getting a Section I stamp as they did on the test panel. They also intend using the analysis methods of Section VIII-Division 2, Section III, and Code Case N-47 (1592) to supplement Section I. These are guides. There is no Code review of these methods other than meeting Section I.

Comments: In the Proposal for the Receiver Subsystem, MDAC indicates the approach to Code Design in their Stress Analysis Section. Although difficult to follow, the explicit items seem to indicate the following:

- Thickness design by Section I. Stress levels under operating conditions, both normal and abnormal will be used to predict life based on fatigue and thermal ratcheting. There seems to be some question as to whether or not creep will be included.
- All panels will be designed to operate for 30 years and to survive any single point failures in the pilot plant system.
- Rocketdyne used methods for life analysis from Section VIII-Division 2, Section III, and Code Case N-47. They analyzed the existing SRE panel and preliminary design of the pilot plant panels. They indicate that they met greater than 30-year life on fatigue using these methods. They do not indicate creep fatigue.
- There are no Code data for fatigue for Incoloy 800 in the Code. Case N-47 does have fatigue data for Incoloy 800H. Rocketdyne generated their own design curves for low cycle fatigue using "ASME Methods from experimental data."
- Rocketdyne indicates that they will check thermal ratcheting of panel tubing using the method of Section VIII-Division 2, Appendix 5, and the "latest" creep data of the material. Section VIII-Division 2 does not include creep ratcheting.
- Rocketdyne indicates that the panels will be sized so that strains occurring from possible oscillations of the DNB position will be below the endurance limit. This brings up the general question of high cycle fatigue and determination of an adequate curve for Incoloy 800 which may or may not have an endurance limit.

FWDC suggested that the proposed Interim Structural Code developed by FWDC for DOE through Sandia be used as a consistent basis for design. This proposed Code is not as restrictive as the use of the Nuclear Codes. Even though Section VIII is the basis of the proposed Interim Structural Code, Section I could be used rather than Section VIII-Division 1.

G. Coleman indicated that MDAC and Rocketdyne would review the Interim Code and discuss it with STMPO at a meeting the following week. STMPO will define the Code requirements.

The use of the Code by MDAC in their design is discussed in more detail in subsequent parts of this note.

To: File  
Subject: 10-MWe Pilot Plant Receiver Design Evaluation

April 2, 1979  
Page 4

Question: Is Incoloy 800 still going to be used?

Answer: Yes. They realize that there are some questions with limited boiler experience and with availability of material property data for analysis. However, they have developed all their fabrication techniques and feel locked into Incoloy 800 unless it can be definitely shown that it is not adequate.

Comment: The initial Incoloy 800 data from ANL (Figure A) shows a large variance in number of cycles to failure for Incoloy 800 material from the same heat of material. ANL believes that there is variation in chemical composition even in one heat of material. ANL data also shows that compressive hold time in the cyclic test is more damaging than tensile hold time for Incoloy 800. This is important because the primary cyclic strain that may cause failure is the high axial compressive value. The ANL results seem to be in accord with other data. Finally, ANL says that data that they have seen shows that the creep-fatigue interaction curve for Incoloy 800H in N-47 of the Code (Figure B) is not valid. Namely, rather than a single straight line in which creep damage plus fatigue damage is equal to unity, small amounts of creep damage may substantially reduce the fatigue life. This should also be true of Incoloy 800.

The Incoloy 800 material data needs much clarification. As shown on the last page of Attachment IV MDAC is considering the specification of additional limits on the chemistry of Incoloy 800.

Question: Is there going to be any reduction in tube thickness?

Answer: No. They have a panel and design with fabrication and other procedures that have been established.

Comments: In their design, MDAC misinterpreted the Code to determine the thickness. They added a factor of 0.065 in. to the thickness. This factor is a threading factor that is only valid for pipes of nonferrous material. It is not valid for tubes. The value of thickness used is 0.115 in.

The formula for thickness for this case with  $e = 0$  can be written as:

$$t = \frac{PD}{2S+P} + 0.005D$$

If  $P = 1700$  psi and  $D = 0.5$  this reduces to

$$t = \frac{850}{2S + 1700} + 0.0025$$

In their review CE used 1260°F and  $S = 6900$  psi for Incoloy 800H material and got a thickness of 0.057. If one uses 1260°F and Incoloy 800 material the allowable stress

To: File  
Subject: 10-MWe Pilot Plant Receiver Design Evaluation

April 2, 1979  
Page 5

by interpolation is 3760 psi and the required thickness is 0.095. If the design temperature is 1100°F then the design stress is 13,000 psi. The required thickness is 0.033. There is a very great variation. Thus it is important to establish a valid design temperature. The value used in design by Rocketdyne by subtracting the 0.065 thread allowance was a thickness of 0.05 in. or less.

The question of thickness is very important because of its fatigue life implications as well as its weight, temperature, and flow aspects. This thickness can be reduced by some amount as shown above. If it is reduced on the inside, flow area is increased. If it is reduced on the outside, the area that sees the radiation is reduced, if the number of tubes is not increased.

Question: How are low-cycle creep fatigue considerations going to be incorporated into the design?

Answer: Use Code Case N-47 of the ASME Code (Subsequent letter of March 23rd meeting indicates that Rocketdyne is doing only fatigue analysis, i.e., no creep).

Comment: N-47 has various methods of meeting creep-fatigue requirements. It is difficult to tell without the Rocketdyne detailed conditions and calculations whether or not they meet the 30-year life as defined in N-47.

Code Case N-47 does not have fatigue curves for Incoloy 800. They do have curves for Incoloy 800H. The curve for an inelastic analysis with 800H is shown in Figure C and that for elastic analysis in Figure D. The curve for elastic analysis is to be used with an elastic analysis approach in N-47. This curve was developed to account for creep damage due to peak stress relaxation during hold times and slow strain rates. There are other special rules that must be followed but the general analysis is simpler. The results, however, should be much more conservative.

It would not be practical to develop such a curve for elastic analysis for Incoloy 800. Therefore, the curve for inelastic analysis should be developed. Such a curve was developed by Rocketdyne as shown in Figure E. This type of curve should be used if N-47 is to be followed with an inelastic analysis. It should now be reviewed in terms of all the data available since it has substantially higher allowable cycles than Incoloy 800H and for 304SS and 316SS (Figure F).

For example at 10,000 cycles and 1100°F the allowable strain range for Incoloy 800 is about 0.0045 from their curve. From T-1420-1C (Figure C) for 10,000 cycles for Incoloy 800H in the Code the allowable strain range would be 0.0021. The strain range of 0.0045 would only permit about 500 cycles. The values for stainless steel in the Code are in T-1420-1A (Figure F). The allowable strain range for 10,000 cycles is 0.0030.

In the proposed Interim Structural Design Standard for Solar Energy Applications, a number of possible simplifications to N-47 were indicated which would reduce the effort required for the creep-fatigue analysis.

- Creep-fatigue analysis would not be required for receiver components that are not directly exposed to the solar heat flux, as well as for some special cases.



To: File  
Subject: 10-MWe Pilot Plant Receiver Design Evaluation

April 2, 1979  
Page 6

- On page 4-11 in the Explanation Section of the Proposed Standard, it indicates that for the receiver components exposed to direct radiation "the computed strain range is approximately the same whether determined from an elastic analysis or inelastic analysis."

This statement is based on the assumption that the receiver components exposed to direct radiation would have deformation controlled strains or that the strains calculated elastically would be fairly close to the inelastic strains. Unfortunately, funds were not available in the development of the Interim Standard to run the calculations necessary to place this important assumption on a sound footing. It would be of value to run some typical cases both elastically and inelastically to evaluate whether or not elastic analysis can safely be used with the inelastic fatigue curves.

- It was assumed that for 304 and 316 stainless steel the maximum principal tensile stress rather than effective stress or stress intensity could be used for determination of creep damage. Unfortunately, this cannot be done even partially for Incoloy 800 because the initial indications are that the compressive hold times are more damaging than tensile hold times.
- The allowable time,  $T_d$ , in T-1411 of Code Case 1592 is determined from stress-to-rupture curves at a stress value equal to the effective stress divided by a factor  $K^1$ . For 304SS, 316SS, and Incoloy 800H this factor is taken as 0.9. This is a conservatism related to nuclear applications. The proposed Interim Structural Design Standard proposes a factor of 1.0. I believe that this should be used at MDAC.
- The proposed Interim Structural Design Standard permits the Creep Damage Calculation to be done either with elastic analysis or inelastic analysis. The inelastic analysis portion is not changed from Code Case N-47 for Incoloy 800 since the effective stress must be used. The elastic analysis, however, is quite different in that only the portion of the Elastic Analysis Rules for evaluating Creep Damage Due to Primary Plus Secondary Stresses is required. This should and will be modified to include peak stresses. This is done because peak stresses were considered in N-47 in their elastic fatigue damage evaluation. This whole elastic analysis approach is based upon the assumption that the stresses are mainly deformation controlled. It should apply to the MDAC design.
- The creep-fatigue damage allowable is not increased from D to 1 for elastic analysis in the proposed interim structural design standard. This is not done because the supposed added conservatism of the elastic analysis in the Nuclear Code is not included in the elastic analysis. Current data indicates that the value of D shown for Incoloy 800H in the Code (N-47) may be high. An appropriate value of Incoloy 800 should be determined.

Question: In what way is ratcheting going to be considered?

Answer: Thermal ratcheting will be evaluated by means of Section VIII-Division 2.

Comment: If thermal ratcheting is evaluated, it should be done with N-47. Section VIII-Division 2 is based on the Simple Bree chart that does not consider creep. However,

To: File  
Subject: 10-MWe Pilot Plant Receiver Design Evaluation

April 2, 1979  
Page 7

the thermal creep ratcheting evaluation does not seem necessary except perhaps in a very approximate form. The tubes of the receiver will be inspected in service so that any "swelling" would be detected.

Question: What material properties are going to be used and how are they obtained?

Answer: (From the MDAC letter of March 23, 1979). Data base being prepared from all available information will obtain low-cycle fatigue information and will use conservative values. No information is available on high-cycle fatigue properties of Incoloy 800 or Incoloy 800H. Brookhaven studies indicate that there is no endurance limit.

Comment: GE studied the DNB oscillation in terms of stress. They simply extended the design curves in Section III and N-47 for Incoloy 800H.

Question: Are any structural tests planned?

Answer: No.

Comment: There are various pieces of hardware that are available on which accelerated tests can be run. These include the five-tube panel and the full panel that will be tested at Sandia. Calculations on Creep Fatigue for increased loadings could be evaluated and would give strong support to the longer term calculations if the calculations are substantiated by experiment. The tests on the full panel would be extremely valuable and could be carried out after the flow tests are completed.

Question: Do you foresee any cyclic stress problems with longitudinal tube to the weld areas?

Answer: No. The tube-to-tube welds are on the back (cool) side of the tube. Small cracks in the weld that are light tight are not considered to be a problem. The weld materials for Incoloy 800 are limited in number.

Comment: The weld materials used have substantially different thermal expansion coefficients than Incoloy 800. Although there is no radiant heat directly on the welded side, there is an overall temperature cycle at least once a day.

Cracks even if they occur in the weld and are light tight, may help start a crack in the tube. In that sense they may be a problem.

Question: Why is the tube-to-manifold connection part way?

Answer: It meets requirements.

Comment: MDAC indicated that the overall manifold connection question is being studied and that they would like Foster Wheeler input.

To: File  
Subject: 10-MWe Pilot Plant Receiver Design Evaluation

April 2, 1979  
Page 8

CLOSURE

It is important that the work on this 10-MWe be reasonably consistent in terms of a reliability level and that the design basis have some clearly stated philosophy. In addition, it would be desirable to have the design be reasonably consistent with the ASME Solar Power Standard that should be in print sometime before the pilot plant is completed.

*Irwin Berman*  
I. Berman

IB/po/yla  
Enclosure

FIGURE A

Low-Cycle Fatigue of Incoloy 800 (HH9088A) at 1100°F

Test No.	Int. Press. (psi)	Hold Time (min)	Axial Strain Range		Dia. Strain Range (%)	Axial Stress		Average Hoop Stress (ksi)	Cycles to Failure	Mean Dia. Strain At Failure (%)
			Total (%)	Plastic (%)		Range (ksi)	Mean (ksi)			
1053*	0	0	0.5	0.20	0.19	64.8	1.6	0	33498	-
1057*	1100	0	0.5	0.19	0.20	68.1	0	6.0	9359	1.2
1061*	2000	0	0.51	0.18	0.23	72.8	-	10.9	9047	3.3
1062	0	1C	0.50	0.19	0.20	68.3	-	0	4700	-
1064	0	0	0.50	0.20	0.19	65.1			6640	
1066	0	1T	0.50	0.17	0.20	71.7			>8300- 11000	

B-9

\*These tests were run at axial strain rate =  $4 \times 10^{-3}$  / s. All others were run at  $10^{-3}$  / s.

CASE (continued)  
N-47  
(1592-10)

CASES OF ASME BOILER AND PRESSURE VESSEL CODE

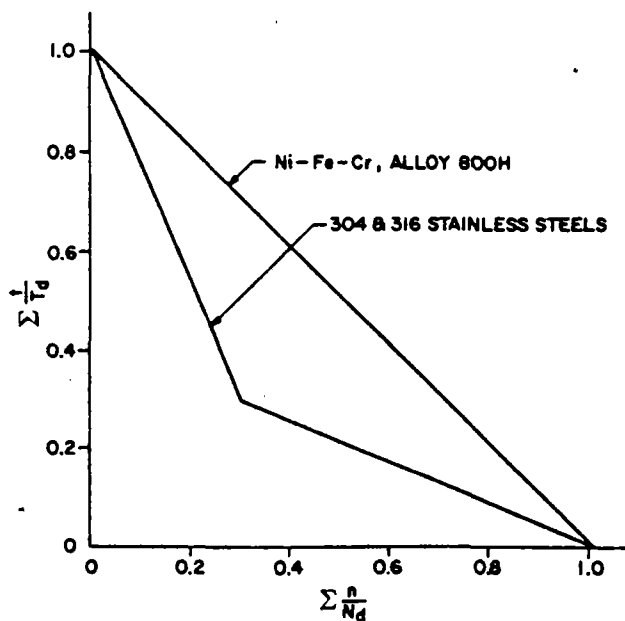


Fig. T-1420-2 Creep-fatigue damage envelope

FIGURE B

CASES OF ASME BOILER AND PRESSURE VESSEL CODE

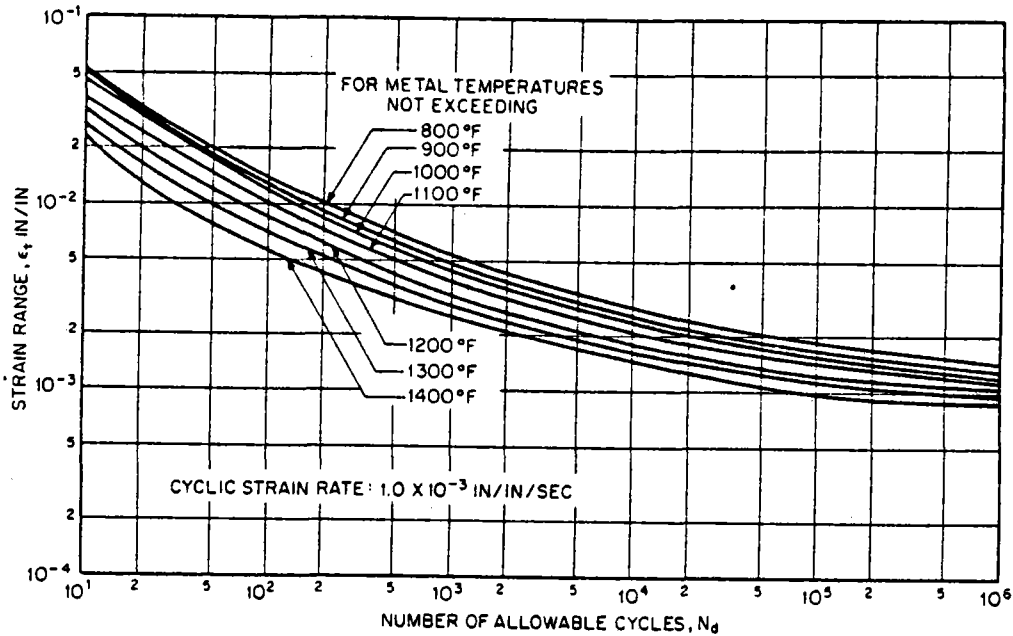


Fig. T-1420-1C Design fatigue strain range,  $\epsilon_f$ , for Ni-Fe-Cr Alloy 800H

Table T-1420-1C

Design Fatigue Strain Range,  $\epsilon_f$ , for Ni-Fe-Cr Alloy 800H

$N_d$ Number of Cycles*	$\epsilon_f$ , Strain Range (in./in.) at Temperature						
	800 F	900 F	1000 F	1100 F	1200 F	1300 F	1400 F
$10^1$	.0513	.0498	.0468	.0378	.0308	.0263	.0231
$2 \times 10^1$	.0328	.0313	.0298	.0243	.0198	.0168	.0129
$4 \times 10^1$	.0218	.0208	.0190	.0163	.0130	.0113	.00866
$10^2$	.0139	.0129	.0119	.01	.00823	.00725	.00566
$2 \times 10^2$	.0103	.00939	.00861	.00722	.00603	.00535	.00426
$4 \times 10^2$	.00777	.00699	.00641	.00542	.00463	.00405	.00331
$10^3$	.00537	.00489	.00441	.00392	.00328	.00285	.00254
$2 \times 10^3$	.00427	.00379	.00351	.00312	.00261	.0023	.00209
$4 \times 10^3$	.00347	.00314	.00291	.00259	.00213	.00195	.00176
$10^4$	.00277	.00249	.00233	.0021	.00174	.00159	.00143
$2 \times 10^4$	.00242	.00219	.00201	.00182	.00155	.00142	.00125
$4 \times 10^4$	.00215	.00193	.0018	.00162	.0014	.00127	.00109
$10^5$	.00187	.00164	.00151	.00139	.00122	.00115	.000959
$2 \times 10^5$	.00169	.00149	.00141	.00128	.00113	.00105	.000919
$4 \times 10^5$	.00157	.00139	.00129	.00121	.00108	.000987	.000889
$10^6$	.00139	.00129	.00119	.00112	.00103	.000937	.000869

\*Cyclic strain rate:  $1 \times 10^{-3}$  in./in./sec.

CASE (continued)  
 N-47  
 (1592-10)

CASES OF ASME BOILER AND PRESSURE VESSEL CODE

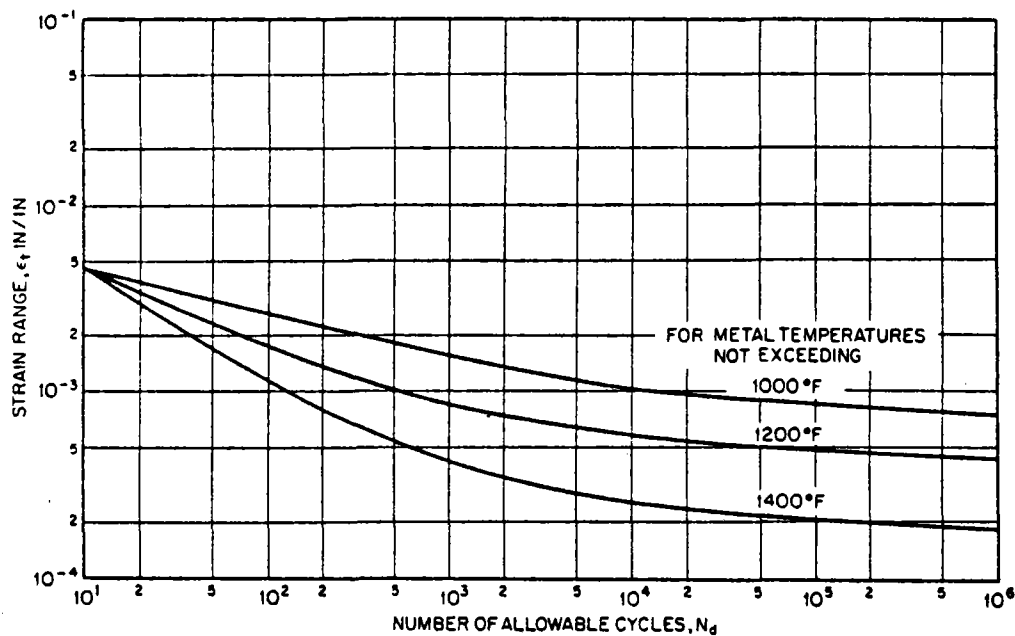
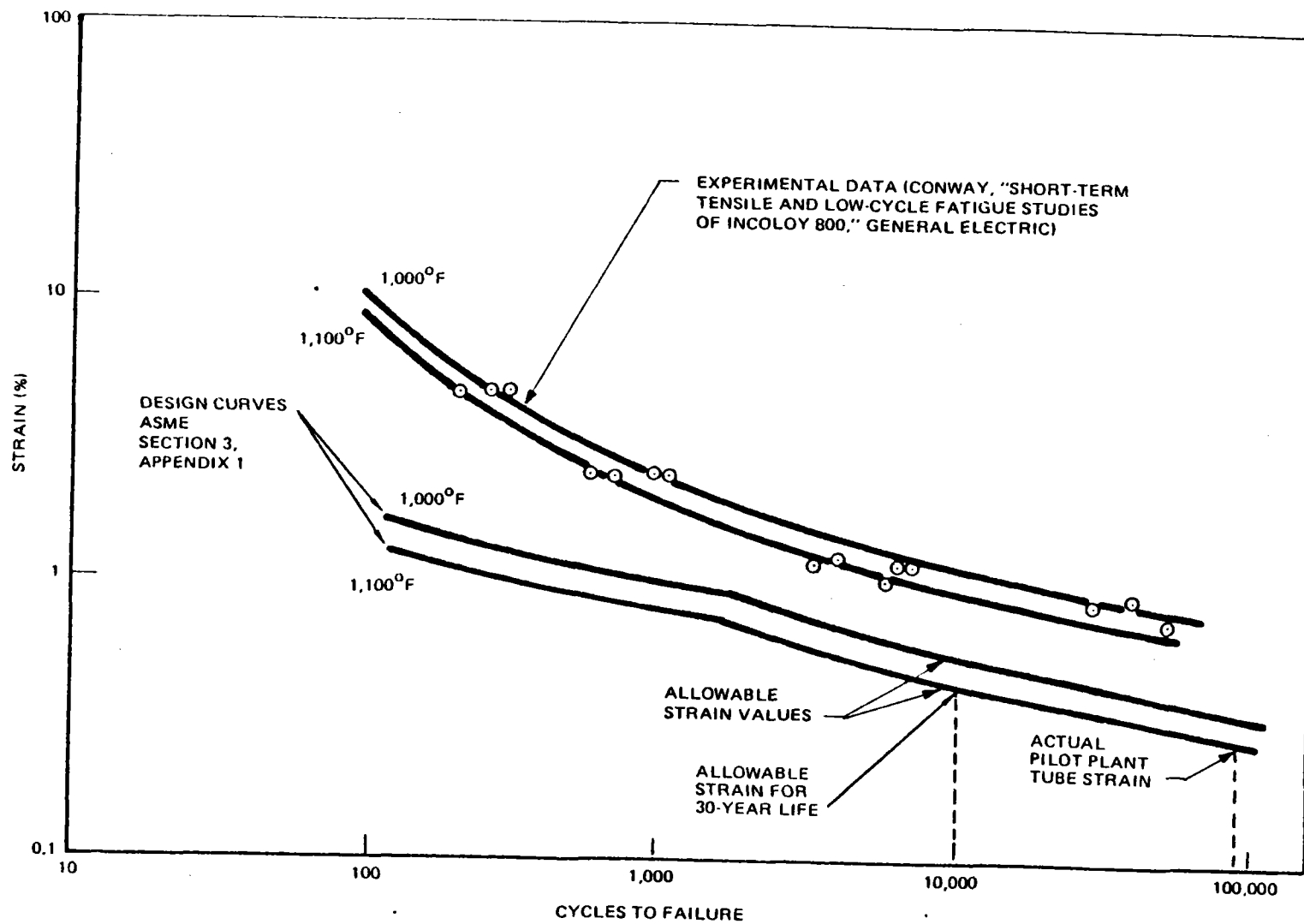


Fig. T-1430-1C Design fatigue strain range  $\epsilon_f$  for Ni-Fe-Cr (Alloy 800H) — elastic analysis

Table T-1430-1C  
 Design Fatigue Strain Range,  $\epsilon_f$ , for Ni-Fe-Cr Alloy 800H  
 (Elastic Analysis)

$N_d$ Number of Cycles	$\epsilon_f$ , Strain Range (in./in.) at Temperature		
	1000 F	1200 F	1400 F
$10^1$	.00453	.00458	.00462
$2 \times 10^1$	.00388	.00341	.00295
$4 \times 10^1$	.00318	.00253	.0019
$10^2$	.00253	.00173	.00114
$2 \times 10^2$	.00215	.00135	.000791
$4 \times 10^2$	.00183	.00109	.000581
$10^3$	.00148	.00085	.000411
$2 \times 10^3$	.00129	.00073	.000341
$4 \times 10^3$	.00116	.00065	.000291
$10^4$	.001	.00058	.000251
$2 \times 10^4$	.00091	.00053	.000231
$4 \times 10^4$	.00088	.00051	.000214
$10^5$	.00082	.00048	.000201
$2 \times 10^5$	.00078	.00046	.000192
$4 \times 10^5$	.000765	.00044	.000186
$10^6$	.00074	.00043	.000181

FIGURE D



B-13

FIGURE E



CASE (continued)

N-47-12

(1592-12)

CASES OF ASME BOILER AND PRESSURE VESSEL CODE

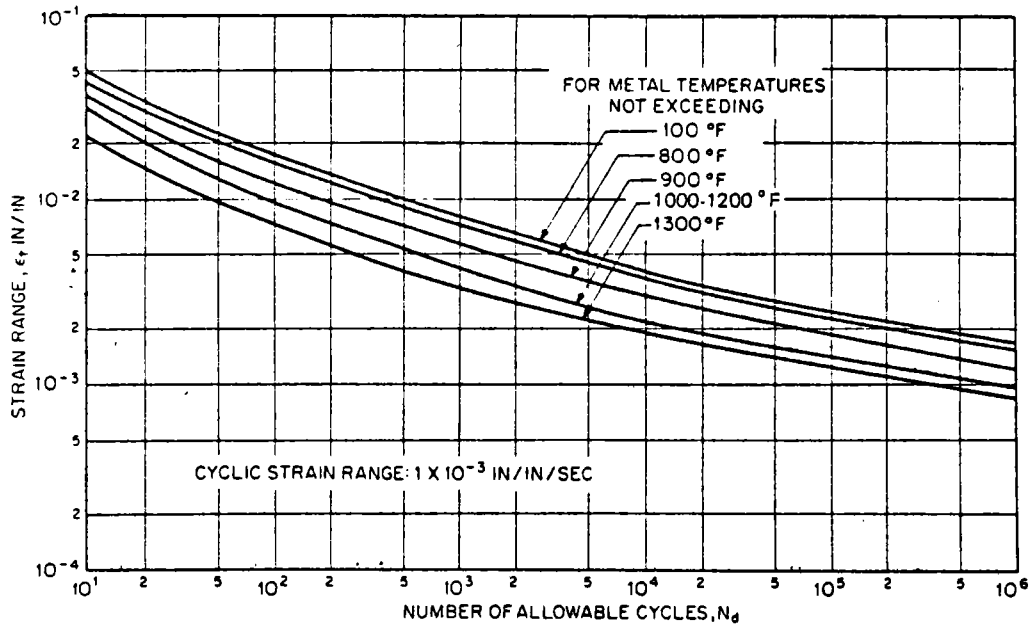


Fig. T-1420-1A, 1B Design fatigue strain range,  $\epsilon_f$ , for 304 SS and 316 SS

Table T-1420-1A, 1B

Design Fatigue Strain Range,  $\epsilon_f$ , for 304 SS and 316 SS

$N_d$ Number of Cycles*	$\epsilon_f$ , Strain Range (in./in.) at Temperature				
	100 F	800 F	900 F	1000-1200 F	1300 F
$10^1$	.0507	.0438	.0378	.0318	.0214
$2 \times 10^1$	.0357	.0318	.0251	.0208	.0149
$4 \times 10^1$	.026	.0233	.0181	.0148	.0105
$10^2$	.0177	.0159	.0123	.00974	.00711
$2 \times 10^2$	.0139	.0125	.00961	.00744	.00551
$4 \times 10^2$	.0110	.00956	.00761	.00574	.00431
$10^3$	.00818	.00716	.00571	.00424	.00328
$2 \times 10^3$	.00643	.00581	.00466	.00339	.00268
$4 \times 10^3$	.00518	.00476	.00381	.00279	.00226
$10^4$	.00403	.00376	.00301	.00221	.00186
$2 \times 10^4$	.00343	.00316	.00256	.00186	.00162
$4 \times 10^4$	.00293	.00273	.00221	.00161	.00144
$10^5$	.00245	.00226	.00182	.00136	.00121
$2 \times 10^5$	.00213	.00196	.00159	.00121	.00108
$4 \times 10^5$	.00188	.00173	.00139	.00109	.000954
$10^6$	.00163	.00151	.00118	.000963	.000834

\*Cyclic strain rate :  $1 \times 10^{-3}$  in./in./sec.

FIGURE F

Appendix C

COMMENTS ON RECEIVER SUBSYSTEM ANALYSIS PLAN FOR 10-MWe SOLAR THERMAL CENTRAL RECEIVER PILOT PLANT, PROPOSED REVISION, MARCH 16, 1979

By Dr. Irwin Berman, Foster Wheeler Development Corporation, May 11, 1979

This note is restricted to a brief discussion of the Structural Analysis of the pressure parts of the receiver subsystem. It is written without having read References 1, 2, and 3 of the Analysis Plan. However, a general idea of the content of those references can be inferred from the Analysis Plan.

The major approach of the Analysis Plan (especially before the proposed revisions) is to use the Nuclear Codes even though the code stamp is Section I. Detailed analytical approaches are indicated in some places.

There is an attempt in the revisions to revert to a Section I approach with a fatigue analysis addition. This does not, however, seem to be completely carried out. The philosophy is stated on Page 5 of the Analysis Plan and, as revised, seems satisfactory. Essentially this philosophy is based on:

- Design and Code Stamp - Section I
- Additional Analytical Criteria for receiver absorber panel fatigue analysis from Section III, Class 1; Code Case N-47 and/or Section VIII-Division 2.

The philosophy is important to consider because even though design has a great impact on reliability, there should be a consistent set of rules that include questions of material, fabrication, examination, and operation and maintenance practices. The simple imposition of upgraded design criteria without

related changes in the other aspects that affect reliability may not be of value. Our point of view is, therefore, that the 10-MWe Solar Thermal Central Receiver Power Plant be designed at a level of reliability consistent with fossil fuel plant practice. To do this, additions to the design requirements should only be made for those instances in which the loading conditions, operating conditions, etc. are substantially beyond those to be encountered in fossil fuel boilers and only for those parts affected. Consider various sections of the Analysis Plan:

#### 4.3.2 Complete Documentation and 4.3.3 Certified Analysis Report

The Complete Documentation includes the words design analyses. This would relate more to nuclear application. The idea of a certified analysis report is also more for nuclear than fossil. We believe that the explicit requirements to be reported for the pressure parts should be the thickness and the fatigue calculation. These should be spelled out.

#### 4.3.5 Verification of Computer Programs

This is also not in Section 1 but is probably worthwhile if not carried to excess.

#### 4.6.2 RS (Receiver Subsystem) Pressure Parts

The only "stress analysis" required is that for the fatigue evaluation. It is indicated on Insert A that the fatigue analysis criteria from Section III-Division 1 and Code Case N-47 should be used.

On the top of Page 30 the words design analysis are again used which indicates a nuclear type of analysis. If something else is meant by these words it should be spelled out.

The design parameters listed on Page 30 are again not explicitly considered by Section 1. Other than the fatigue aspect the others should mainly be considered in terms of loads or attachments and the effect on piping by means of building code rules.

#### 4.6.2.4 Definition of Design Criteria

Consider the fatigue criteria. It is indicated on Page 30 that the fatigue analytical criteria of Section III, Class 1, and Code Case N-47 be used for the life analysis of the receiver absorber panels. This is good because it defines the extent of the analysis. We assume that this means that the temperature of the absorber panel is sufficiently low (1080°F maximum?) for Incoloy 800 material, such that the contribution of the creep damage to reduction of expected life is negligible. If that is a correct assumption it should be so stated. However, this does not mean that at 1080°F, creep does not take place and affect an inelastic analysis. This subsequent statement about elastic versus inelastic methods should be clarified.

Code Case N-47 has a specific elastic method. This method is generally so restricting that it cannot be used. There have been approximations of inelastic behavior results by the use of elastic analysis. These must be used with care. One such approximation was used in the CE report (Reference 7 in the Analysis Plan). This was based on a Westinghouse report by Houtman. We assume that various analyses were done to compare this to some data base in order to show the validity of the method. It would be important to review the data base in terms of the conditions of the receiver panels.

There are other ways of carrying out an approximation. For Foster Wheeler's advanced nuclear work, we use a simple method to run a relatively inexpensive inelastic program in which we use a specific geometry.

The proposed Interim Solar Code Rules for ASME include an elastic analysis for the panel. The conditions of the panel are the basis of the use of this analysis. It is not yet sufficiently verified.

4.6.2.5.2 Fabrication Effects

We don't understand how this can be considered in an analysis. Section I considers this by design rules.

4.6.2.6 Piping System Structural Analyses

We believe that the indication of B31.1 with the possible addition of words on seismic analysis would be adequate.

APPENDIX D

Appendix D

REPORT ON REVIEW OF HEAT TRANSFER AND PRESSURE DROP CORRELATIONS  
USED BY ROCKETDYNE IN DESIGN OF PILOT PLANT RECEIVER

F. M. Talmud, Foster Wheeler Energy Corporation, April 18, 1979

The correlations used by Rocketdyne in the design of the pilot plant receiver, as reported in the CRSTPS Phase 1 Preliminary Design Report, were reviewed. Our comments follow.

PRESSURE DROP CORRELATIONS

SINGLE PHASE

Use of the Moody<sup>1</sup> friction factors for determining single phase, water or steam pressure drop is the generally accepted method and we have no comment on this selection.

TWO PHASE

The Martinelli-Nelson<sup>2</sup> correlation for determining pressure drops in two-phase flow was derived for adiabatic flows and its application to diabatic flow introduces uncertainty into the results. The practice of applying Martinelli-Nelson, or some modification of it, to adiabatic flow is quite common in the industry and we now have a good estimate of how much error, if any, is introduced.

## HEAT-TRANSFER CORRELATIONS

Determination of tube I.D. film conductance impacts the design of the receiver in that it permits calculation of the tube metal temperature. Tube metal temperature determines material selection and heat losses to ambient. Because the receiver is designed entirely of a single material, that material must be selected for the highest metal temperature at any location in the receiver. The highest metal temperature in the receiver can occur at one of two possible locations: the outlet of the boiler/superheater panels or the location where film boiling occurs. Consequently, the only heat-transfer correlations which have a significant impact on receiver design are those for film boiling and for superheated steam. If there is inaccuracy in the other correlations used it is of secondary importance because it will not affect the design of the receiver.

## WATER HEATING

The Dittus-Boelter<sup>3</sup> correlation for determination of film coefficients in subcooled water is very widely used and is reasonably accurate when applied to water below the saturation temperature.

## SUBCOOLED NUCLEATE BOILING

Rocketdyne has used Jens and Lottes<sup>4</sup> correlation published in 1951 for this heat-transfer regime. More recent investigations by Thom et al.<sup>5</sup> indicate that the Jens correlation yields consistently low values for the temperature difference between the inside tube wall surface and saturation temperature. Thom suggests a modified equation which fits the more recent data.



For the range of adsorption rates expected for the pilot plant receiver the difference in tube wall temperature between the Jens and Lottes and Thom correlations is less than five degrees Fahrenheit. This is because the sub-cooled boiling film coefficient is so high that a significant difference in film coefficient produces a very small change in temperature. Consequently, the use of the Jens and Lottes correlation should not introduce significant error for the pilot plant.

#### NUCLEATE BOILING

The same Jens and Lottes correlation used for nucleate boiling as for subcooled boiling. This is not strictly correct. For the reasons outlined above it is probably not critical which value is used. However, there are superior correlations available for this regime such as that of Chen.<sup>6</sup>

#### SUPERHEATED STEAM

Rocketdyne used the Dittus-Boelter<sup>3</sup> correlation for superheated steam. Foster Wheeler used this same correlation prior to 1965. At that time it was found that this correlation yielded excessively conservative (low) film coefficients. We reevaluated the available correlations and found that the Heineman<sup>6</sup> correlation was superior for the following reasons:

- It is based on more accurate steam properties and a wider range of data
- More recent work is in good agreement with the Heineman correlation.

The superheated steam film coefficient could have a significant effect on the selection of materials for the receiver tubing if it developed that the

peak metal temperature occurred at the boiler/superheater panel outlet. Reevaluation of material selection using a more accurate film conductance may be justified.

#### CRITICAL HEAT FLUX AND FILM BOILING

Rocketdyne reports that they have used their own experimental results for determination of the critical heat flux. They also are using experimental results for evaluating film boiling heat-transfer coefficients. We have been told in telephone conversation with John Carroll of Rocketdyne that they are using two-thirds of the saturated vapor film conductance as the minimum film conductance in film boiling. He asserts that the single panel tests substantiate this procedure.

Our comment on these areas is that care must be used in applying test results to be certain that the tests truly represent the full range of receiver operation. If the tests were properly designed and the number and range of the test points were sufficiently wide then these tests should provide an accurate guide for design of the receiver.

## REFERENCES TO APPENDIX D

1. L. F. Moody, "Friction Factors for Pipe Flow," Transactions of the ASME, Vol. 66, 1944.
2. R. C. Martinelli and D. B. Nelson, Prediction of Pressure Drops During Forced Circulation Boiling of Water," Transactions of the ASME, Vol. 70, p. 695, 1948.
3. F. W. Dittus and L. M. K. Boelter, "Heat Transfer in Automobile Radiators of the Tubular Type," University of California, Publications in Engineering, Vol. 2, No. 13, 1030, pp.443-461.
4. W. H. Jens and P. A. Lottes, Argonne National Laboratories, prepared for U.S. Atomic Energy Commission, Report No. 4627, May 1951.
5. J. R. S. Thom, et al., "Boiling in Subcooled Water During Flow Up Heated Tubes or Annuli," Proceedings of the Institute of Mechanical Engineers, Vol. 180, Pt. 3C, p. 226.
6. J. C. Chen, "A Correlation for Boiling Heat-Transfer to Saturated Fluids in Convective Flow," ASME Paper No. 63-HT-34.
7. J. B. Heineman, "An Experimental Investigation of Heat-Transfer to Superheated Steam in Round and Rectangular Channels," Argonne National Laboratories, Report No. 6213, 1960.

APPENDIX E

APPENDIX E  
MCDONNELL DOUGLAS PILOT PLANT  
RECEIVER PANEL STATIC STABILITY

INTRODUCTION

The McDonnell Douglas Astronautics Company (MDAC)/Rocketdyne solar receiver pilot plant preheater and boiler panels were analyzed to determine static stability and panel sensitivity to heat flux variations across the panel width. For the purpose of analysis the FWEC pressure drop computer program EQPRSDRP was used. The program incorporates the following:

- Moody friction factors for single phase flow.
- Martinelli-Nelson two-phase frictional multiplier  $\phi_{FO}^2$  evaluated at zone average conditions.
- Flow acceleration static pressure changes computed from zone inlet and outlet velocity head assuming no slip between phases.
- Computational capability for multiple circuits, zones, flows, and absorptions.

The general procedure followed for analysis (details of which are included under Discussion) was to compute and plot the static pressure difference between panel inlet and outlet headers as a function of mass flow rate for different heat absorption rates. These curves were analyzed to note whether negative sloping regions exist indicating static Ledinegg instability and also, to note flow increases or decreases as a function of heat absorption variations across the width of the panel.

Header configuration induced flow imbalances and the maximum boiler panel metal temperature were also investigated.

## CONCLUSIONS

Analysis of the preheater and boiler panel sensitivity to heat flux variations across the panel width revealed the following:

1. The upflow preheater panels are stable at the design, maximum and minimum load conditions, and no instability is expected due to heat flux variations.
2. The downflow preheater panels are unstable and will be subject to flow stagnation or reversal at the design and minimum load conditions. At the maximum load conditions, the pressure drop will be positive and the flow will be stable. However, the margin of safety is quite small.
3. The boiler panels are relatively stable at the design, minimum, and maximum loads for the expected heat flux variations. Flow variations are less than 5%. However, since the average enthalpy change from panel inlet to outlet is large (approximately 974 Btu/lb at the design load) relatively small percentage heat absorption increases combined with a small flow reduction can result in a large increase in final steam temperature and consequently metal temperature for that tube in the panel which receives the greatest heat absorption.
4. Of the boiler panel load conditions analyzed (design, maximum, and minimum) the worst steam side conditions, i.e., the highest leaving steam temperature, result in panel #18 at the design load. For a 9.1% incident heat flux variation, the absorbed heat flux increases 5.4%, the flow is reduced by 4.1%, and the leaving steam temperature is 1129F.

5. The highest boiler panel mean metal temperature (1242F) was computed at a location 38.5 ft. from the heated inlet of panel #18 at the design load.
  
6. No header configuration induced flow unbalances are expected for both the preheater and boiler panels over the operating load range.

## SECTION 1

### PREHEATER PANEL STATIC STABILITY

#### A. MODEL

A single tube model was developed based on panel arrangement information supplied by MDAC (see Figure 1-1). For the purpose of calculating pressure drop, the model was divided into an unheated inlet section, a vertical heated section, and an unheated outlet section. An internal tube surface roughness of 0.00003 in. was used. For the range of Reynold's numbers analyzed, the difference in friction factors computed from roughnesses of 0.00003 in. and 0.00006 in. is not significant.

#### B. OPERATING CONDITIONS

##### 1. Panel Absorption

During a meeting held on March 21, 1979, MDAC supplied FWEC with incident and absorbed power distribution data for the east, west, north, and south panels at different times on the best and worst days. These values were based on a heated length of 41 ft. In order to estimate heat absorption values for other than the aforementioned panels, the curves illustrated in Figure 1-2, 1-3, and 1-4 were plotted for the design load (2 PM winter day), the minimum load (4 PM winter day), and the maximum load (12 PM summer day). The preheater panels are the six (6) panels facing south (panels #22, #23, #24 - upflow, panels #1, #2, #3 - downflow).

Heat absorption variations across the entire preheater, the upflow panels, and the downflow panels are listed in Table 1-1. Maximum and minimum variations are relative to the average absorptions for the group of panels under consideration.



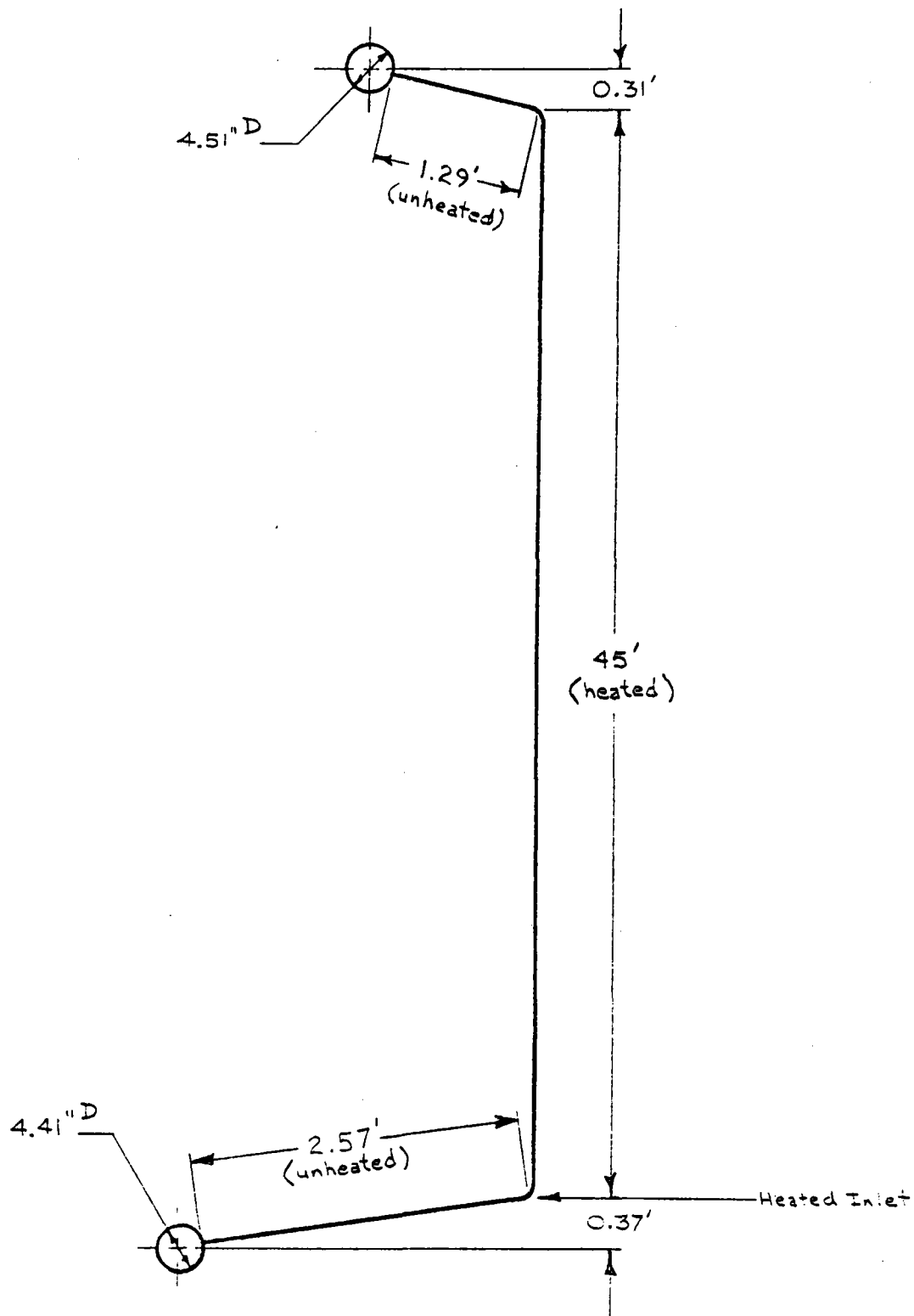


FIGURE 1-1. SINGLE TUBE MODEL.

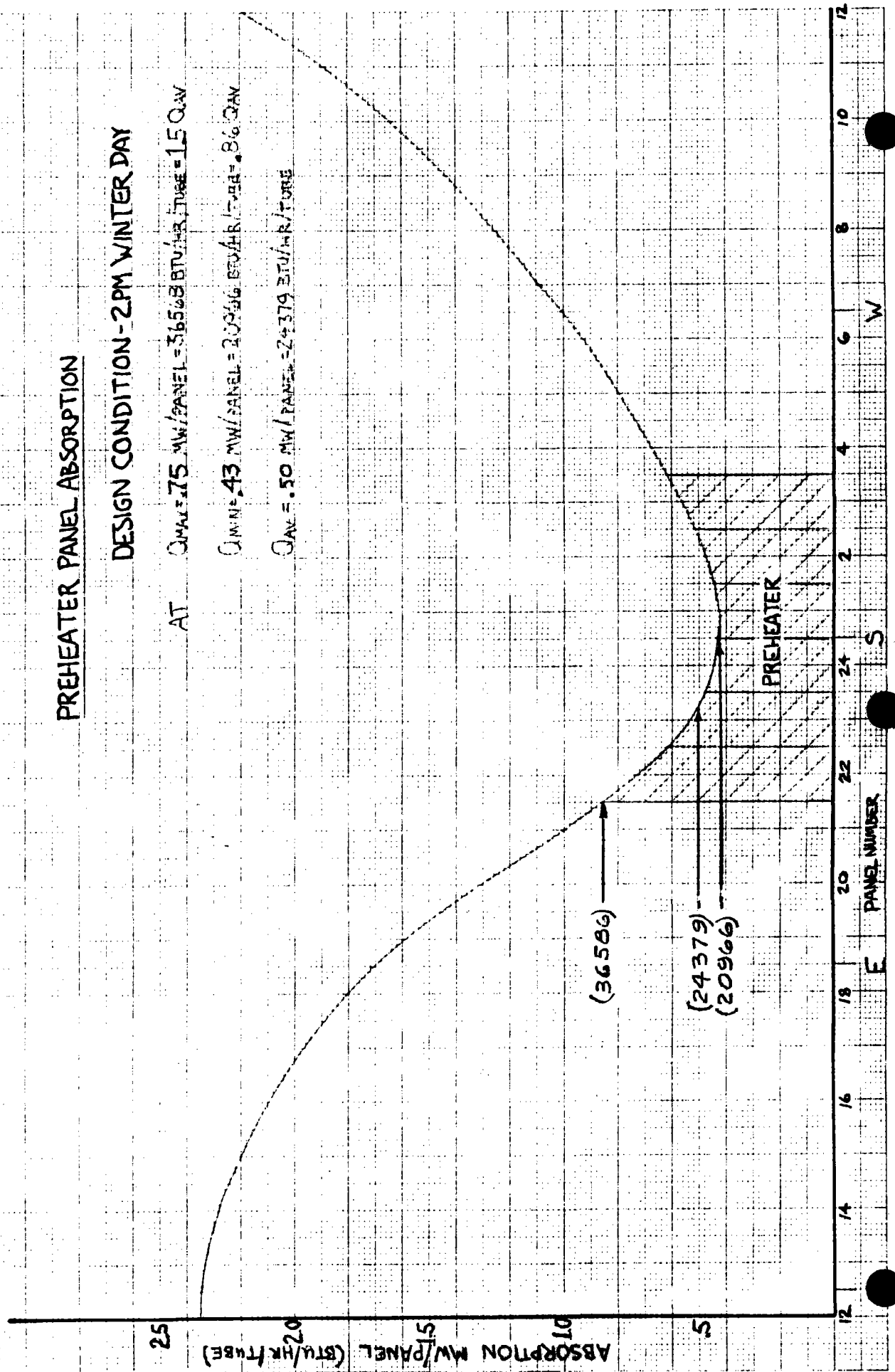
PREHEATER PANEL ABSORPTION

DESIGN CONDITION - 2 PM WINTER DAY

AT  $Q_{MW} = 75$  MW/PANEL =  $36568$  BTU/HR/TUBE =  $15$  QAW

$Q_{MIN} = 43$  MW/PANEL =  $20966$  BTU/HR/TUBE =  $8\frac{1}{2}$  QAW

$Q_{MAX} = 50$  MW/PANEL =  $24379$  BTU/HR/TUBE



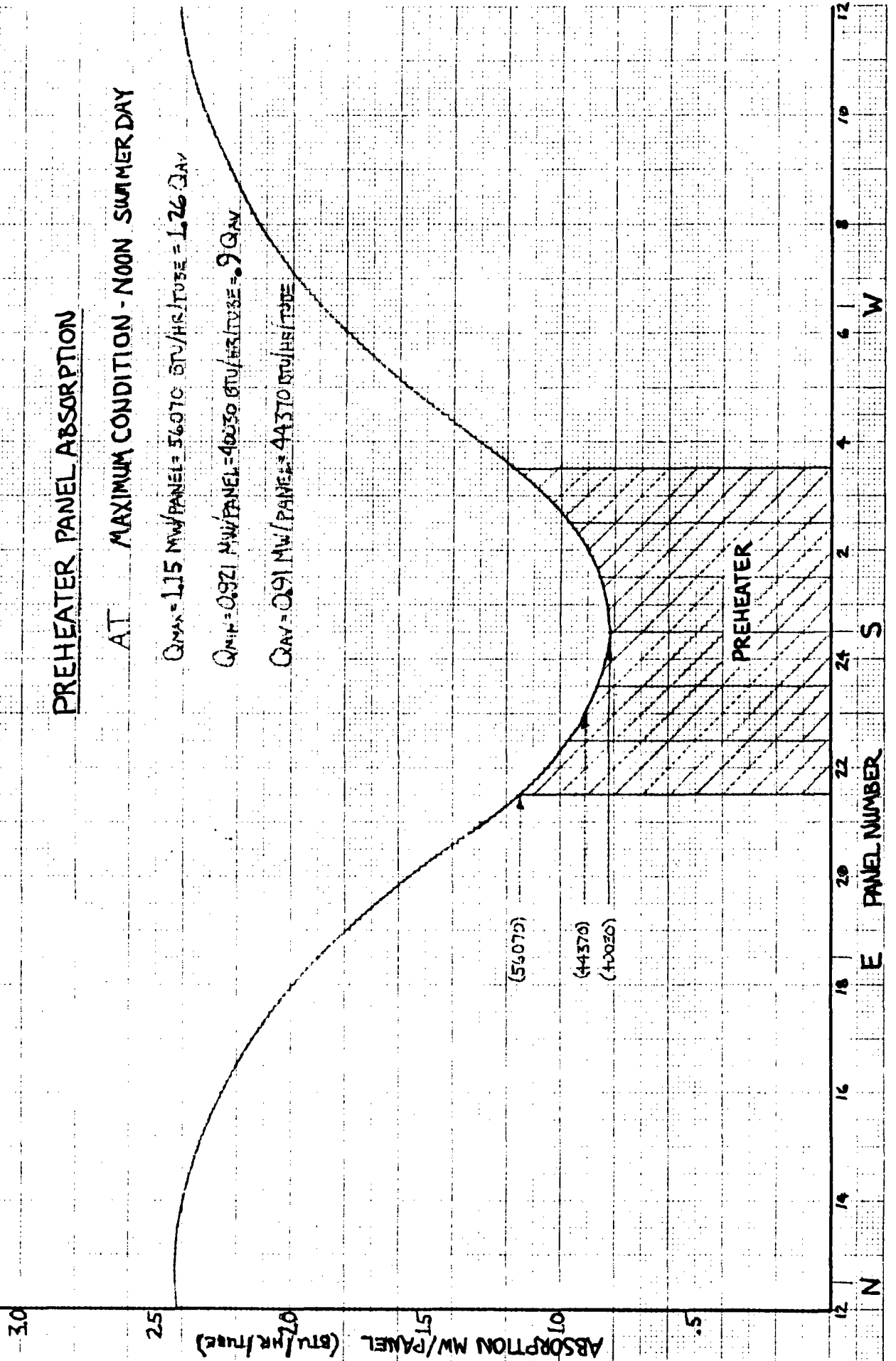
PREHEATER PANEL ABSORPTION

AT MAXIMUM CONDITION - NOON SUMMER DAY

$Q_{MAX} = 1.15 \text{ MW/PANEL} = 56070 \text{ BTU/HR/FT}^2 = 1.26 \text{ Q}_{AV}$

$Q_{MIN} = 0.921 \text{ MW/PANEL} = 40030 \text{ BTU/HR/FT}^2 = 0.9 \text{ Q}_{AV}$

$Q_{AV} = 0.91 \text{ MW/PANEL} = 44370 \text{ BTU/HR/FT}^2$



### PREHEATER PANEL ABSORPTION

AT MINIMUM CONDITION - 4 PM WINTER DAY

$$Q_{MAX} = 0.44 \text{ MW/PANEL} = 21453 \text{ BTU/HR/TUBE} = 2.1 \text{ QAV}$$

$$Q_{MIN} = 0.14 \text{ MW/PANEL} = 6826 \text{ BTU/HR/TUBE} = 0.67 \text{ QAV}$$

$$Q_{AV} = 0.21 \text{ MW/PANEL} = 10157 \text{ BTU/HR/TUBE}$$

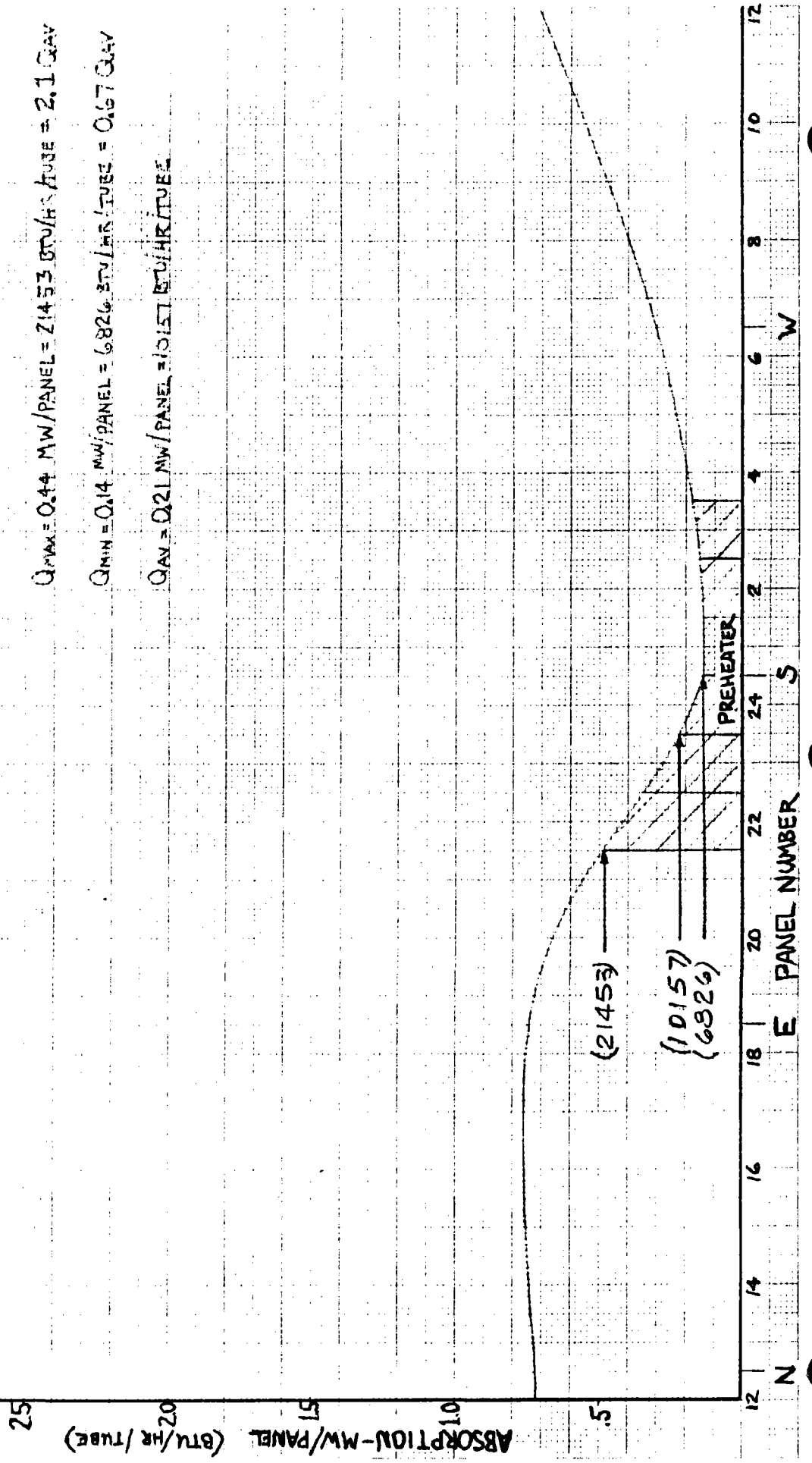


FIGURE 1-4

THIS PAGE INTENTIONALLY LEFT BLANK

TABLE 1-1  
PREHEATER PANEL ABSORPTION VARIATION

<u>Panels</u>	<u>Load</u>	<u>Heat Absorption Variation (%)</u>	
		<u>Minimum</u>	<u>Maximum</u>
Entire Preheater	Minimum	-33	110
	Design	-14	50
	Maximum	-10	26
Upflow	Minimum	-50	75
	Design	-20	59
	Maximum	- 9	30
Downflow	Minimum	0	29
	Design	- 9	32
	Maximum	- 9	30

Variations in heat absorption along the length of the tube were not considered.

## 2. Inlet Conditions

The following preheater panel inlet conditions were used:

<u>Load</u>	<u>Design</u>	<u>Minimum</u>	<u>Maximum</u>
Total feedwater flow (lbm/hr)	102,400	35,300	130,500
Ave. feedwater flow/tube (lbm/hr)	488	168	621
Inlet pressure (psia)	2,000	1,950	2,050
Inlet temperature (F)	401	315	414

Inlet temperature and pressure were obtained from Reference 1 while flow rate was computed from the specified receiver total power absorption data from which Figures 1-2, 1-3, and 1-4 were plotted.

## C. CALCULATION PROCEDURE

Static pressure difference was computed between inlet and outlet headers for positive flow (upflow in upflow panels and downflow in downflow panels) and between outlet header and inlet header for negative flow (recirculated downflow in upflow panels and recirculated upflow in downflow panels). The average fluid conditions in the outlet header were used for the negative flow inlet conditions.

Total pressure difference between headers was plotted as a function of mass flow rate for different heat absorption rates. For low flow rates below which calculations were not made, the pressure drop curves were extrapolated to the origin by dashed lines. Absorption rate variations plotted for both the upflow and downflow panels were those for the entire preheater as listed in Table 1-1. The expected variations, based on the absorption rate curves plotted in Figures 1-2, 1-3, and 1-4, would be those listed in Table 1-1 for

the appropriate set of panels (either upflow or downflow).

The pressure drop curves were then analyzed to note the following:

- Negatively sloping regions indicating static Ledinegg flow instability.
- Variation in flow rate as a function of heat absorption variation.
- Possibility of reverse flow for the operating pressure drop between headers.

#### D. CALCULATION RESULTS

##### 1. Upflow Panels

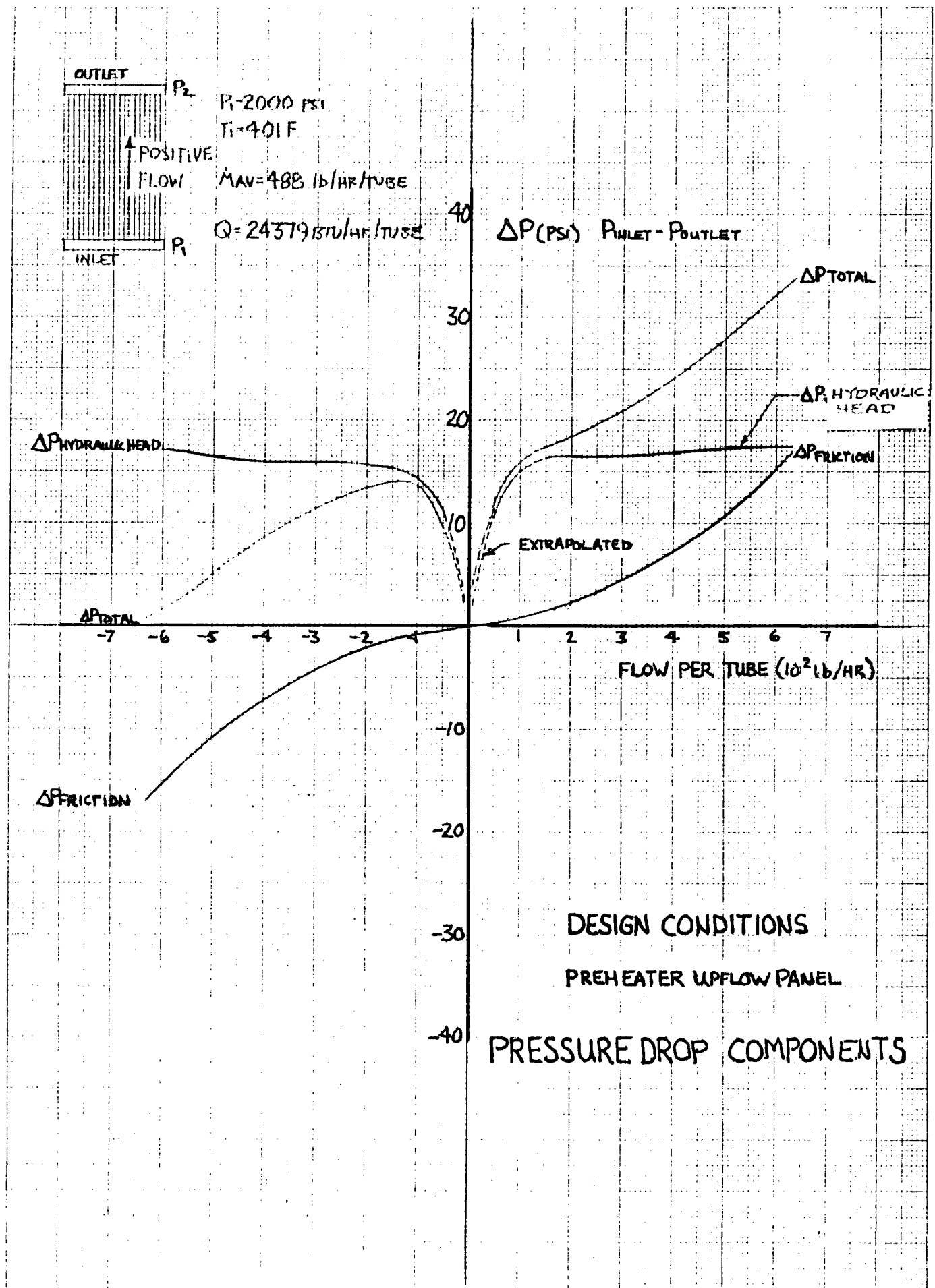
In the upflow direction, the frictional pressure drop and gravity head both work towards increasing the pressure drop with increasing flow. Figure 1-5 shows the components of pressure drop for the upflow panel operating at design conditions. At the design condition (Figure 1-6), the frictional losses begin to dominate above 25% of the average flow and the flow is stable. At the design absorption rate, flow reversal should not occur at flows greater than 15% of the average flow. At the average flow (488 lb/hr/tube), the sensitivity of flow to expected absorption variations is small. The same holds true for the maximum operating conditions (Figure 1-7). At the design and maximum conditions, the upflow panel is stable.

At the minimum operating conditions (Figure 1-8), the lower flow dictates lower frictional losses and gravity head dominates the pressure drop. This decreases the margin between positive and reverse flow. The panel

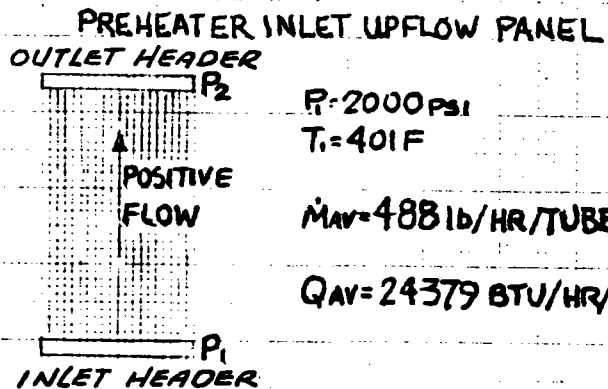


46 1517

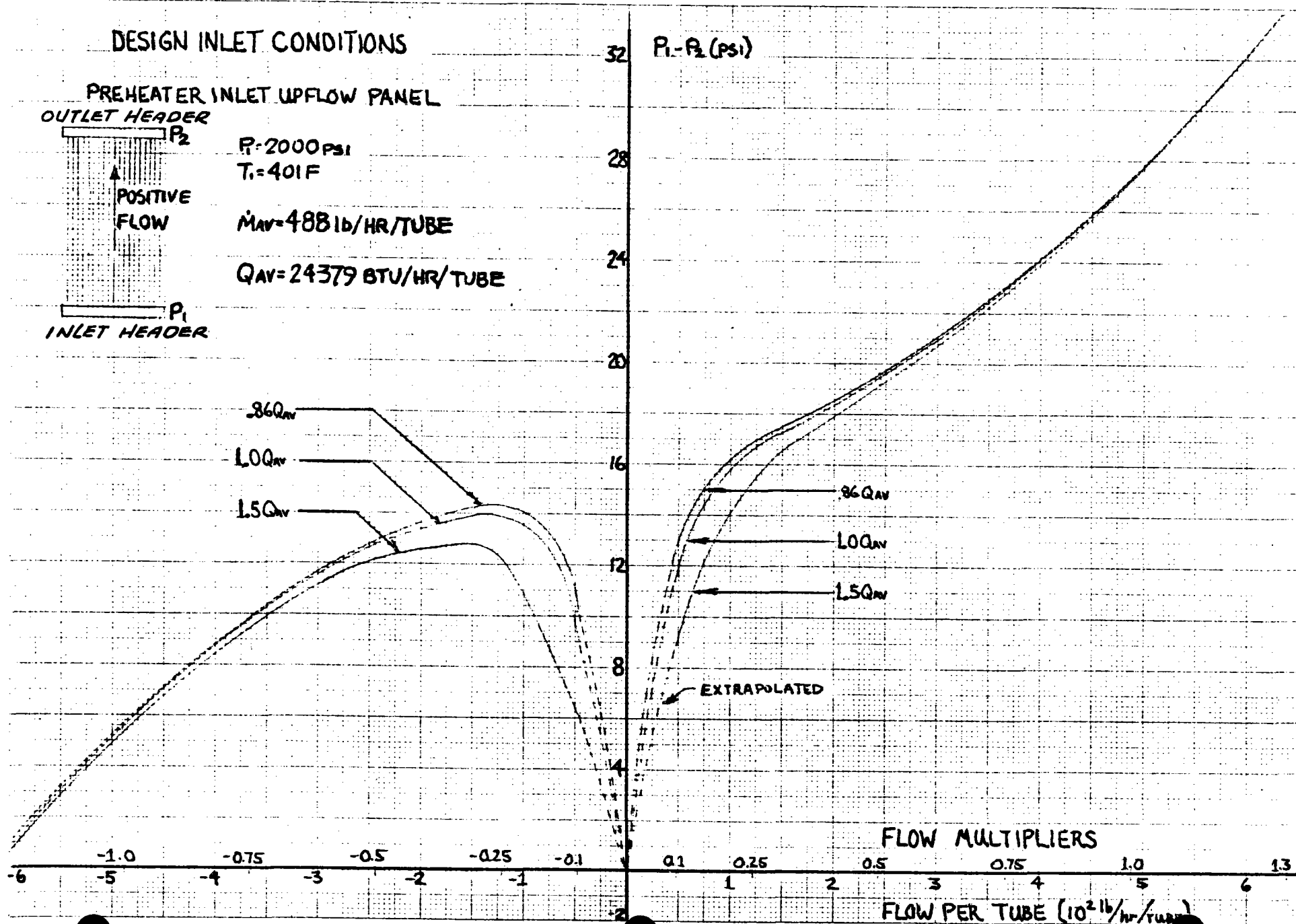
TYPE 10 TO THE CENTIMETER  
KEMPFL & ESSER CO. MADE IN U.S.A.



DESIGN INLET CONDITIONS



$P = 2000 \text{ PSI}$   
 $T_i = 401 \text{ F}$   
 $\dot{M}_{AV} = 488 \text{ lb/HR/TUBE}$   
 $Q_{AV} = 24379 \text{ BTU/HR/TUBE}$



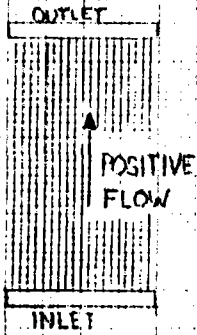
E-14

FIGURE 1-6

46 1517

### MAXIMUM INLET CONDITIONS

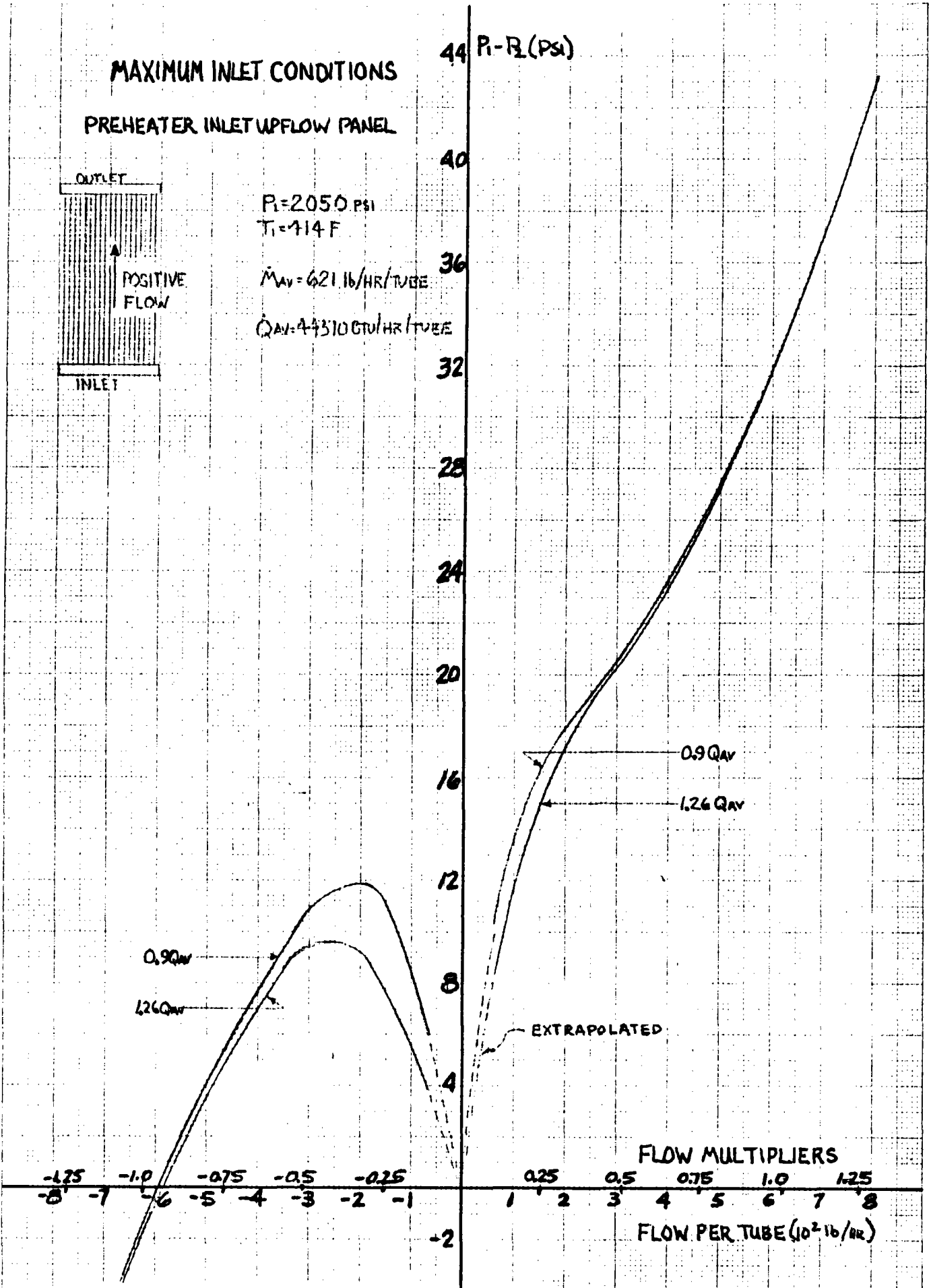
### PREHEATER INLET UPFLOW PANEL



$P_i = 2050 \text{ PSI}$   
 $T_i = 714 \text{ F}$

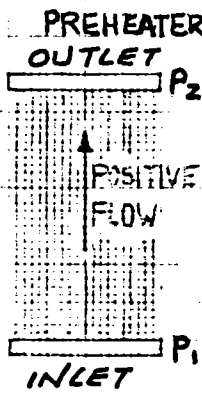
$\dot{M}_{AV} = 621 \text{ lb/HR/TUBE}$

$\dot{Q}_{AV} = 44310 \text{ BTU/HR/TUBE}$



INSTRUMENTS TO FIFTY CENTIMETER  
HUFFEL & ESSER CO. MADE IN U.S.A.

MINIMUM INLET CONDITIONS



$P_1 = 950 \text{ PSI}$   
 $T_1 = 315 \text{ F}$   
 $\dot{M}_{AV} = 168 \text{ LB/HR/TUBE}$   
 $\dot{Q}_{AV} = 10157 \text{ BTU/HR/TUBE}$

28  
24  
20  
16  
12  
8  
4

$P_1 - P_2 \text{ (Psi)}$

0.67  $\dot{Q}_{AV}$   
 1.0  $\dot{Q}_{AV}$   
 2.1  $\dot{Q}_{AV}$

0.67  $\dot{Q}_{AV}$   
 1.0  $\dot{Q}_{AV}$   
 2.1  $\dot{Q}_{AV}$

EXTRAPOLATED

-1.0 -0.8 -0.6 -0.4 -0.2      0.2 0.4 0.6 0.8 1.0 1.2 1.4 1.6 1.8 2.0  
 -2.0 -1.8 -1.6 -1.4 -1.2 -1.0 -0.8 -0.6 -0.4 -0.2      0.2 0.4 0.6 0.8 1.0 1.2 1.4 1.6 1.8 2.0  
 FLOW MULTIPLIERS  
 FLOW PER TUBE ( $10^{21} \text{ lb/hr}$ )

B-16

FIGURE 1-8

is more sensitive to heat flux variations, but at the actual minimum flow and absorption, the panel appears stable although the margin is small.

## 2. Downflow Panels

All heated down flow sections pass through a potentially unstable condition at low flows. Any time the frictional pressure drop is less than the gravity head (such as low flow), flow stagnation or reversal can occur. In the downflow panels, gravity head acts to decrease the pressure drop while frictional pressure drop increases it. The components of pressure drop at design conditions for the downflow panel are shown in Figure 1-9.

At the design operating conditions (Figure 1-10), gravity head dominates the total pressure drop resulting in a net negative pressure drop. As flow decreases a negative sloping region of the curve exists such that at the expected pressure drop, the circuit is unstable and could go to reverse flow.

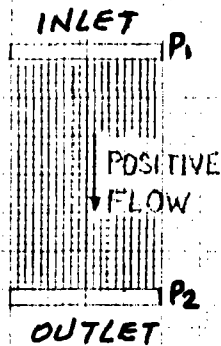
As the mass flow is increased, the frictional pressure drop increases sufficiently to yield a positive  $\Delta P$ . This occurs at the maximum operating conditions (Figure 1-11). Operating with sufficient mass flow to insure a positive  $\Delta P$  puts the panel into a stable condition.

At the minimum design conditions, gravity head dominates the total pressure drop and the panel is unstable at all flows and absorption rates as shown in Figure 1-12.

Variations in the heat flux change the mass flow per tube. Tubes receiving lower heat fluxes will have lower flows and be nearer to the unstable zone. The expected variations in heat flux will not be enough to put the downflow tubes into a stable area or positive pressure drop situation.

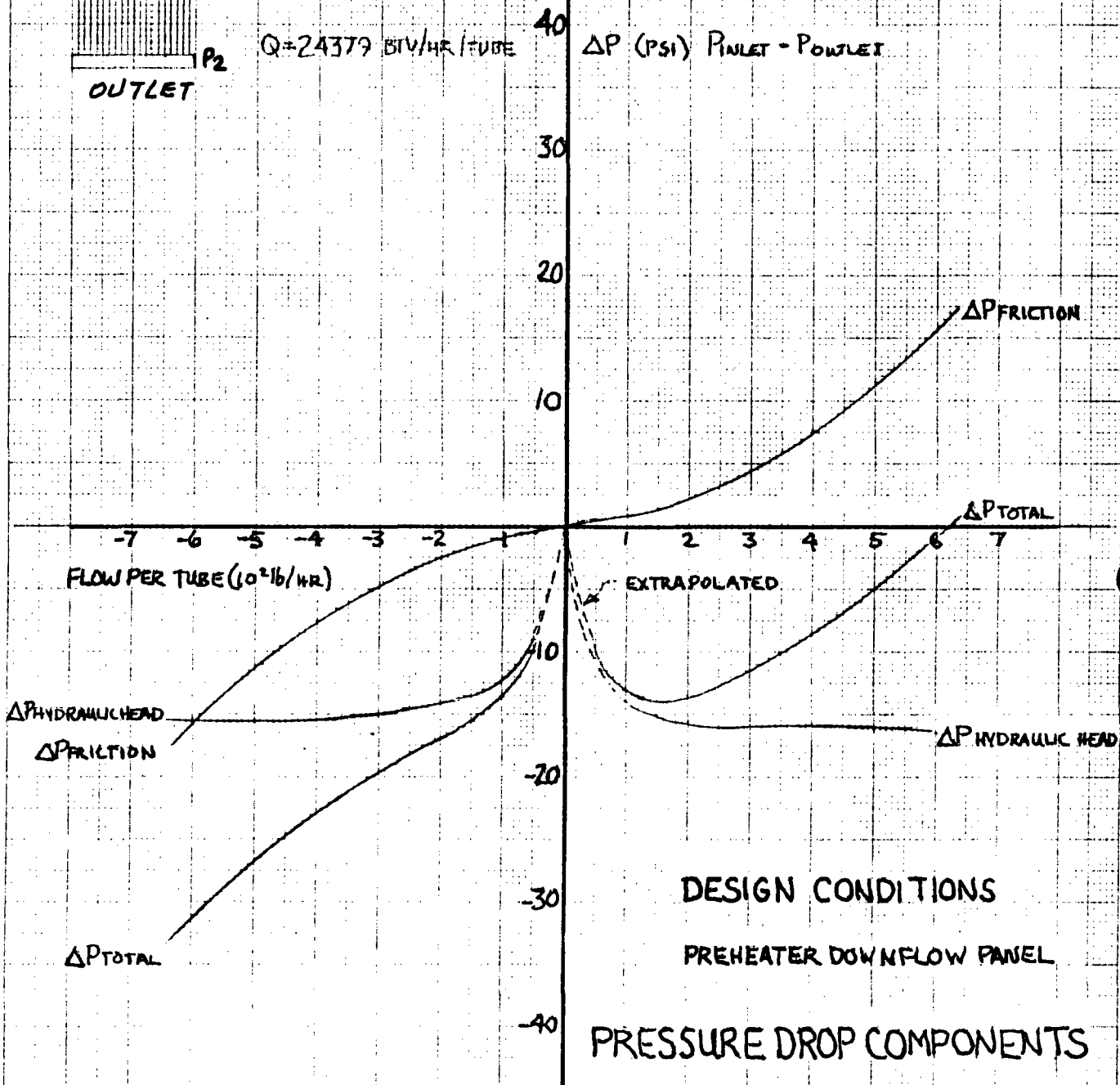
46 1517

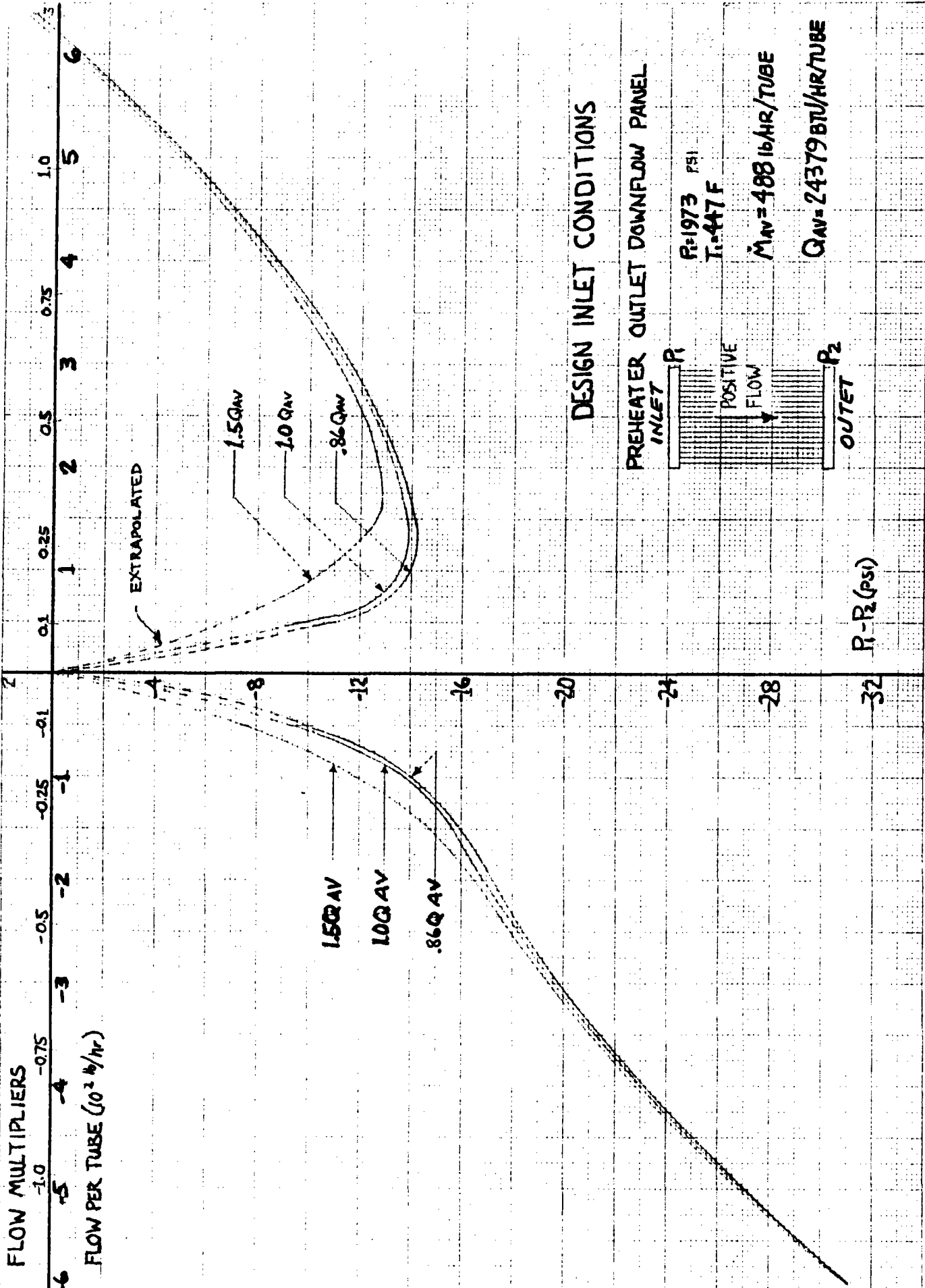
SEE PAGE 10 TO THIS CENTER FOLDER FOR KEUFFEL & ESSER CO. MODEL 501

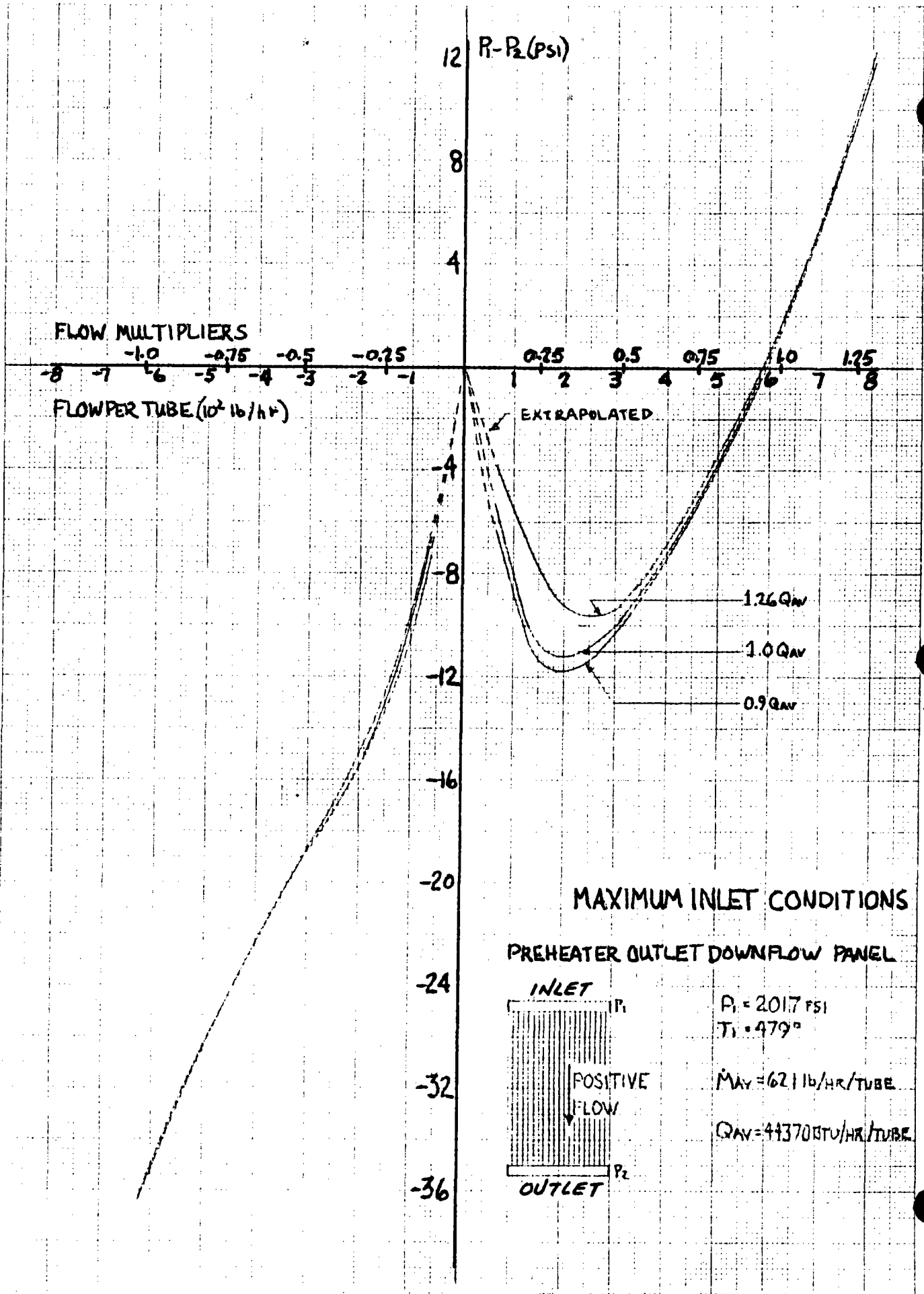


$P_1 = 1973 \text{ PSI}$   
 $T_1 = 447 \text{ F}$   
 $\dot{M}_{AV} = 488 \text{ LB/HR/TUBE}$

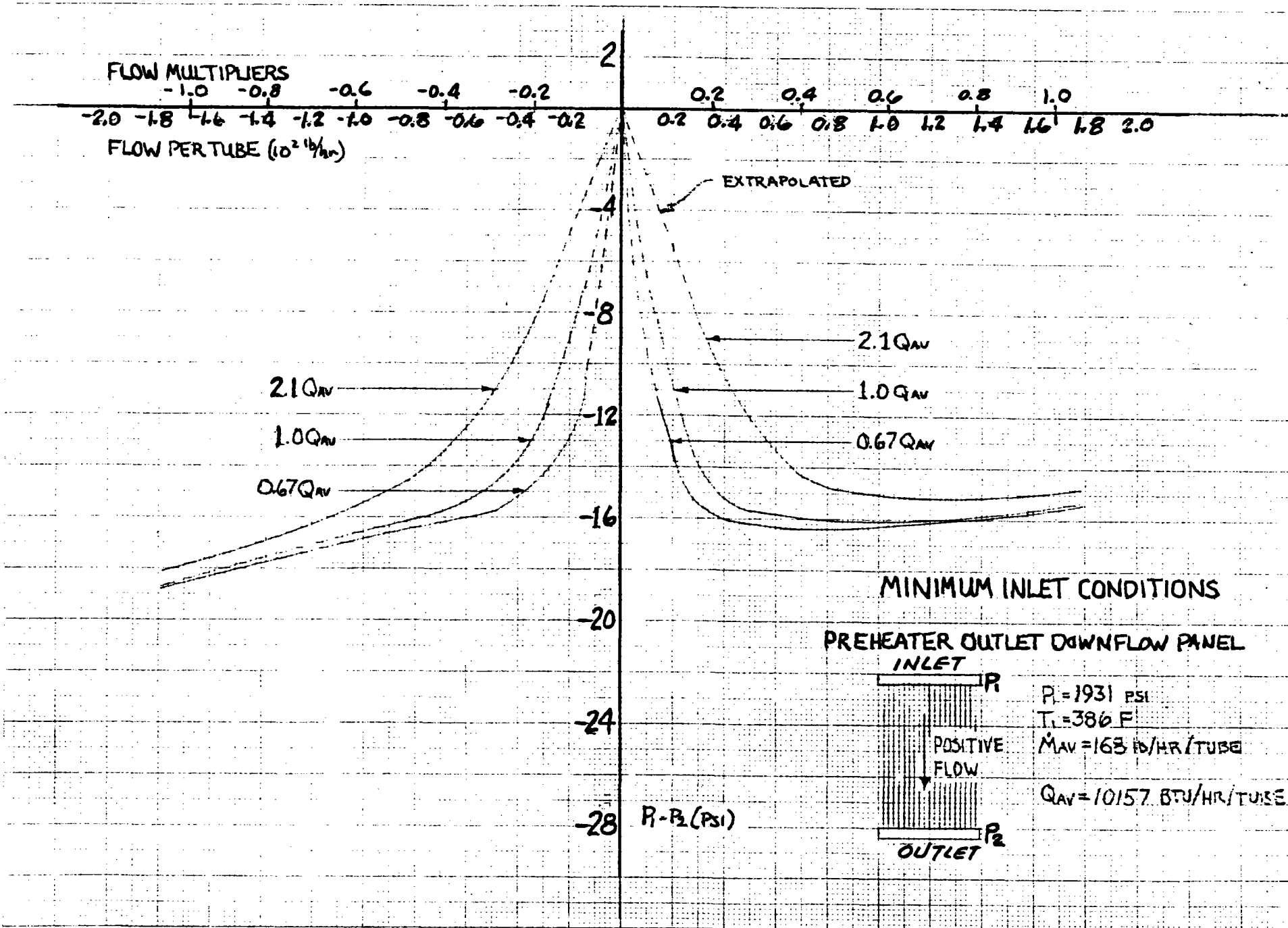
$Q = 24379 \text{ BTU/HR/TUBE}$











E-21

FIGURE 1-12

### 3. Header Unbalance

Piping connections into each preheater panel inlet header (4.41 in. ID) and out of each preheater panel outlet header (4.51 in. ID) are centrally located. Based on this configuration, and the range of preheater panel and header pressure drops, no significant flow imbalances should result because of header size or arrangement.

## SECTION 2

### BOILER PANEL STATIC STABILITY

#### A. MODEL

The single tube model described in Section 1 was used to analyze the boiler panels. However, instead of a single heated zone 45 ft. long, the heated portion of the tube was divided into nine (9) 5 ft. zones. A roughness of 0.00006 in. was used.

#### B. CALCULATION PROCEDURE

Static pressure difference was computed from inlet header to outlet header. Heat absorbed in each of the nine (9) 5 ft. heated zones was assumed equal to a fixed percentage of the total heat absorbed. Percentage absorbed was estimated from the absorbed heat flux curve included in Figure 1 of Reference 2 (see Figure 2-1).

Total pressure difference between headers was plotted as a function of mass flow rate for different heat absorption rates. Flow rate was represented by flow multipliers i.e., a flow multiplier of 1.0 corresponds to the average flow rate per tube required to maintain a leaving steam temperature of 960F for the average panel heat absorption rate. Assuming\* the pressure difference between headers is equal to that resulting from the average flow and average

---

\*NOTE: For a given heat flux variation across a panel the pressure drop between headers is not necessarily the pressure drop determined from the average flow and average heat absorption tube. Pressure drop curves for each tube within the panel should be determined so that a total flow characteristic curve can be generated from which the header to header pressure drop can be determined (see Figure 2-2). However, in general the total pressure drop determined from the average flow tube is not significantly different from that determined by analyzing each individual tube.

E-24

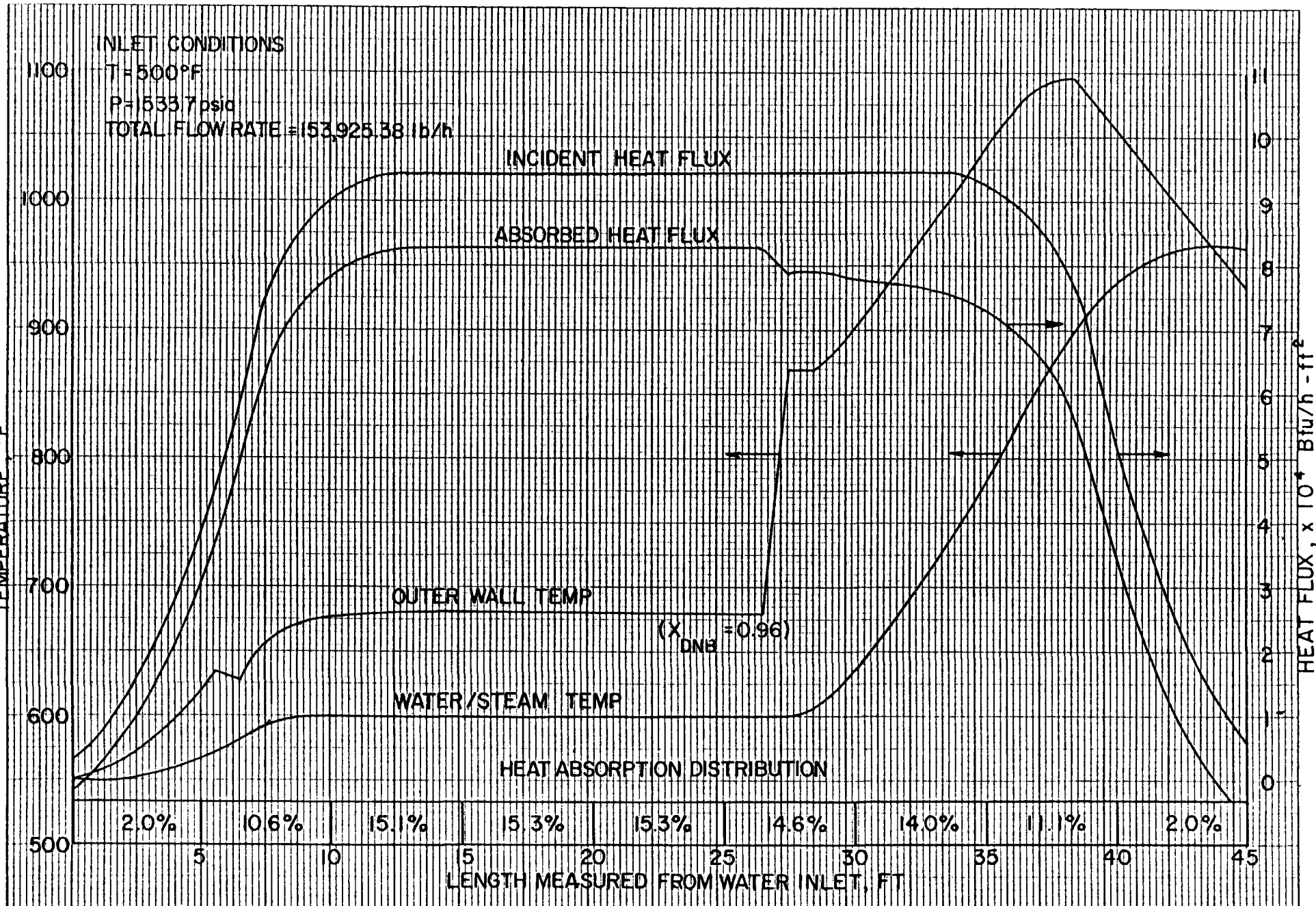


Figure 2-1 THERMAL PERFORMANCE OF PANEL 13 (W. FWEC. CORR)

TOTAL PRESSURE DROP

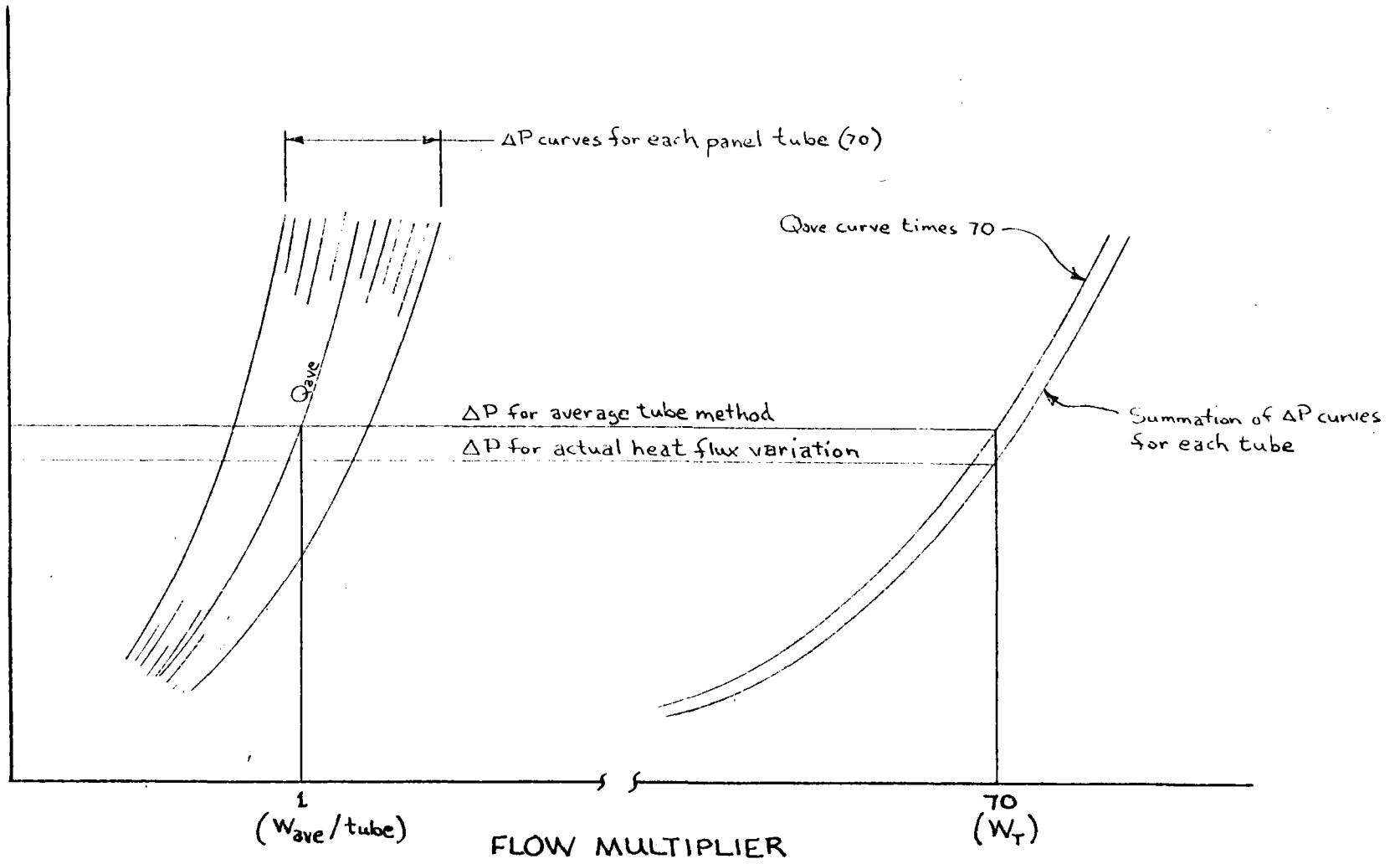


FIGURE 2-2

heat absorption condition, the flow rate in the tubes with heat absorption different from the average were determined. From these results, flow rate change versus heat absorption variation and final steam temperature versus heat absorption variation curves were plotted for each load condition.

## C. CALCULATION RESULTS

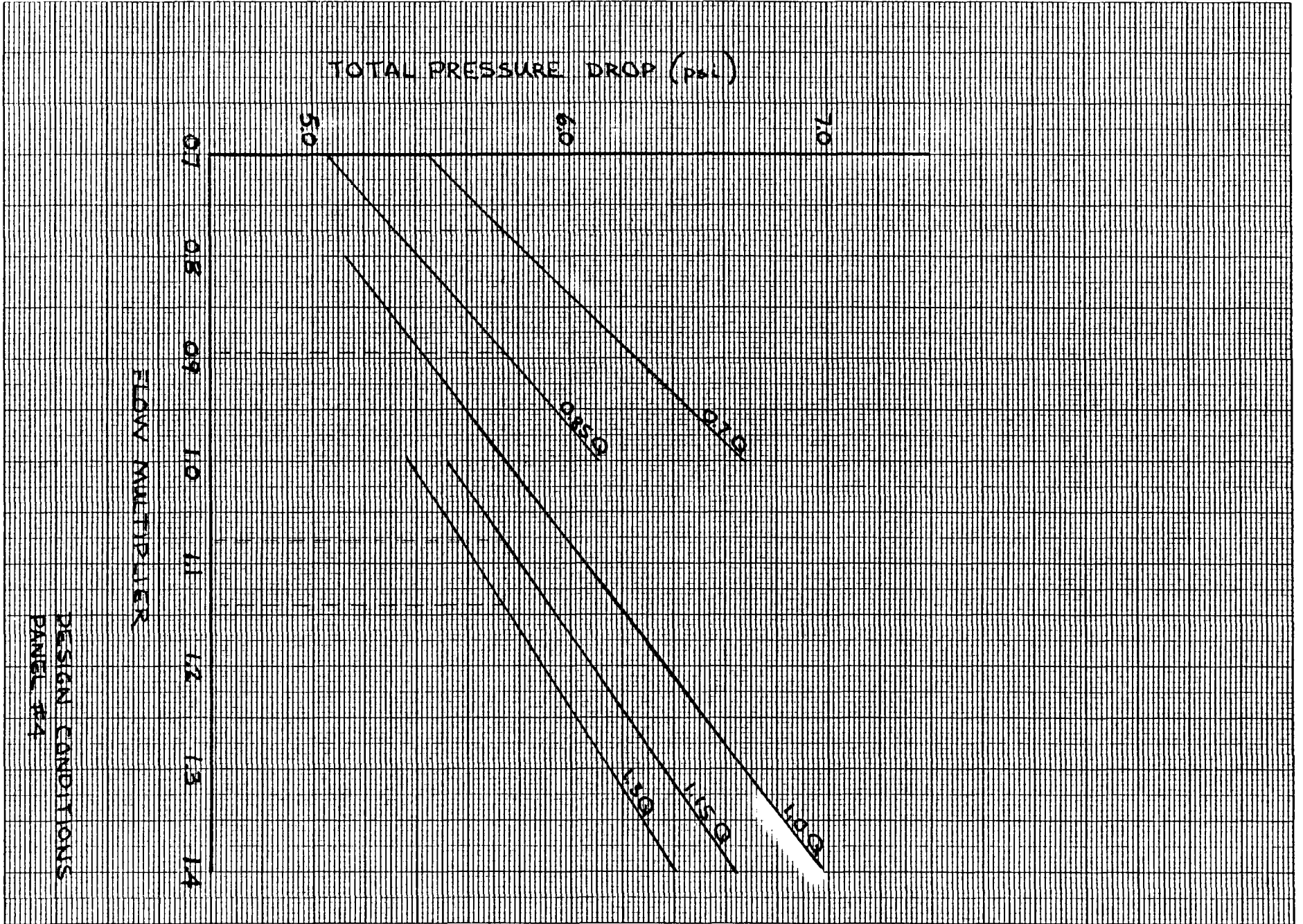
### 1. Flow Sensitivity Calculations

Initial calculations were based on the heat absorption curves plotted in Figures 1-2, 1-3, and 1-4 for the design, minimum, and maximum load conditions, respectively. Boiler panel inlet enthalpy for each load condition was determined from the preheater panel heat absorption computed from Figures 1-2, 1-3, and 1-4, and the preheater inlet conditions specified in Section 1. The boiler panel inlet pressure was estimated so that the leaving pressure would be approximately 1520 psia.

Maximum (panel #13), intermediate (panel #8), and minimum (#4) flow panels for each load condition were analyzed. Total pressure drop versus flow multiplier curves for each of these panels at the aforementioned load conditions are included in Figures 2-3 through 2-11. The flow variations determined from these curves were used to plot the final steam temperature change versus absorption rate variation curves and the flow rate variation versus absorption rate change curves illustrated in Figures 2-12 through 2-17. The absorption rate variation for each of the panels analyzed was estimated from Figures 1-2, 1-3, and 1-4, and plotted on Figures 2-12, 2-14, and 2-16.

Items of special note include the following:

- The minimum flow panel (#4) for the minimum and design loads and the intermediate flow panel (#18) for the minimum load are gravity head



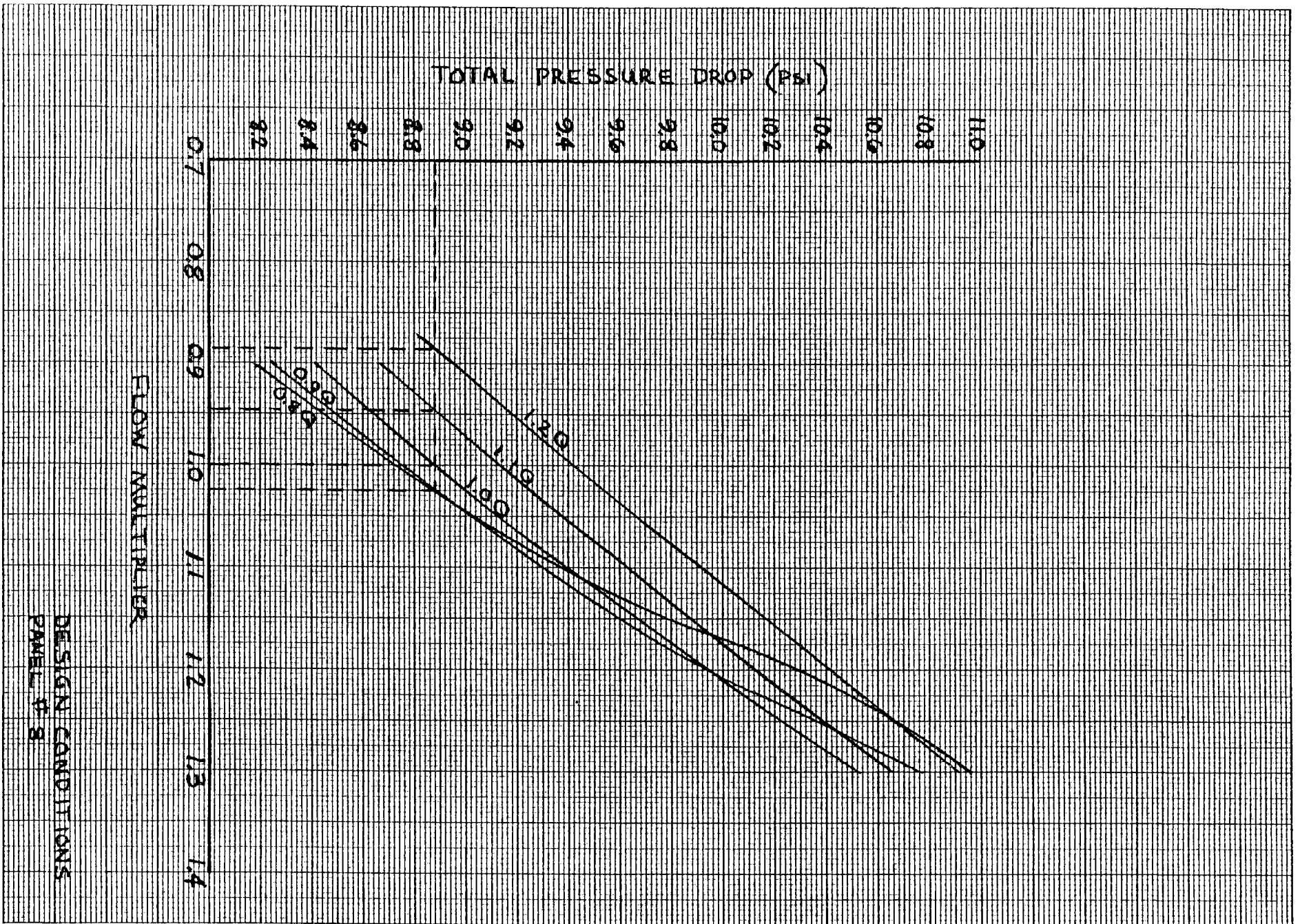


FIGURE 2-4



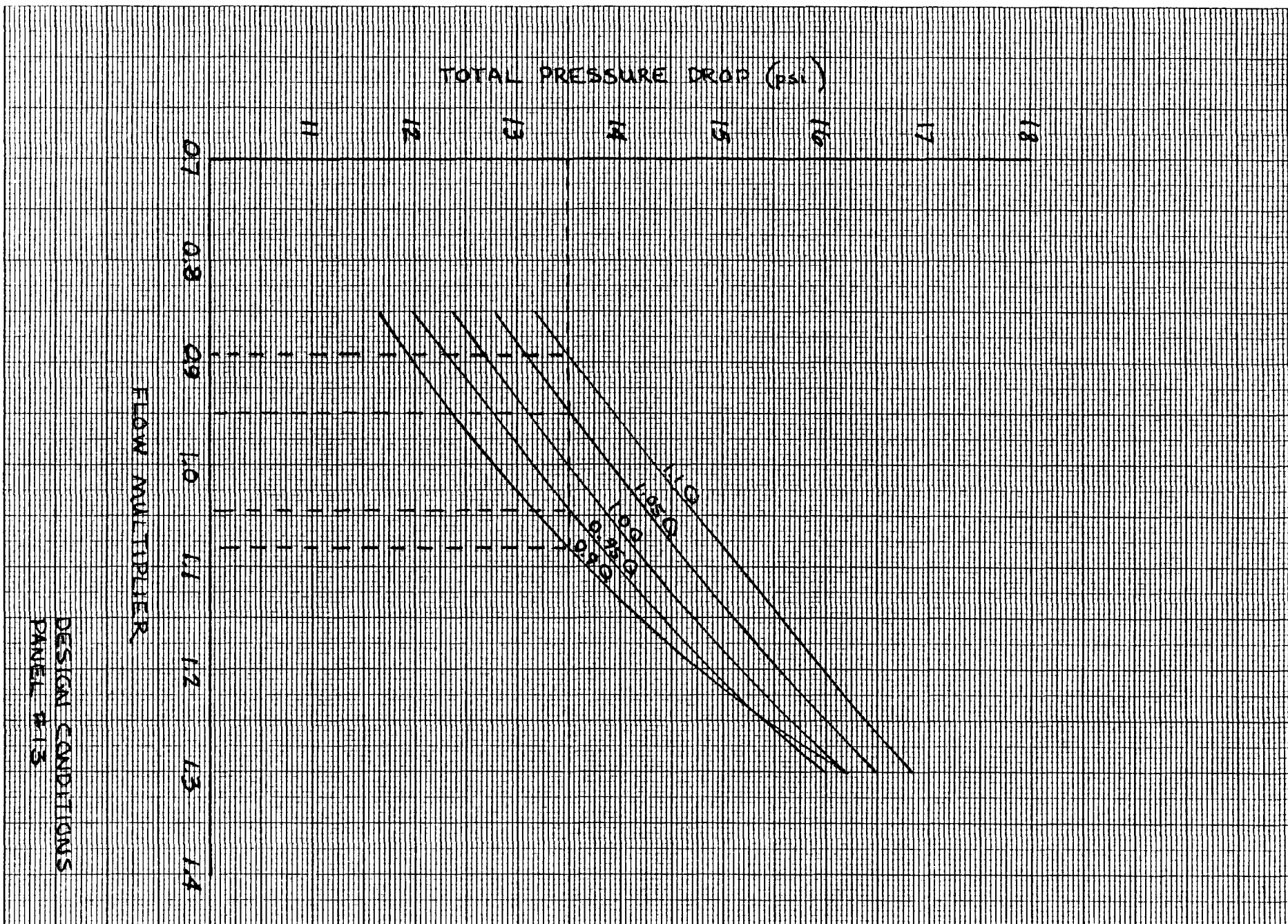
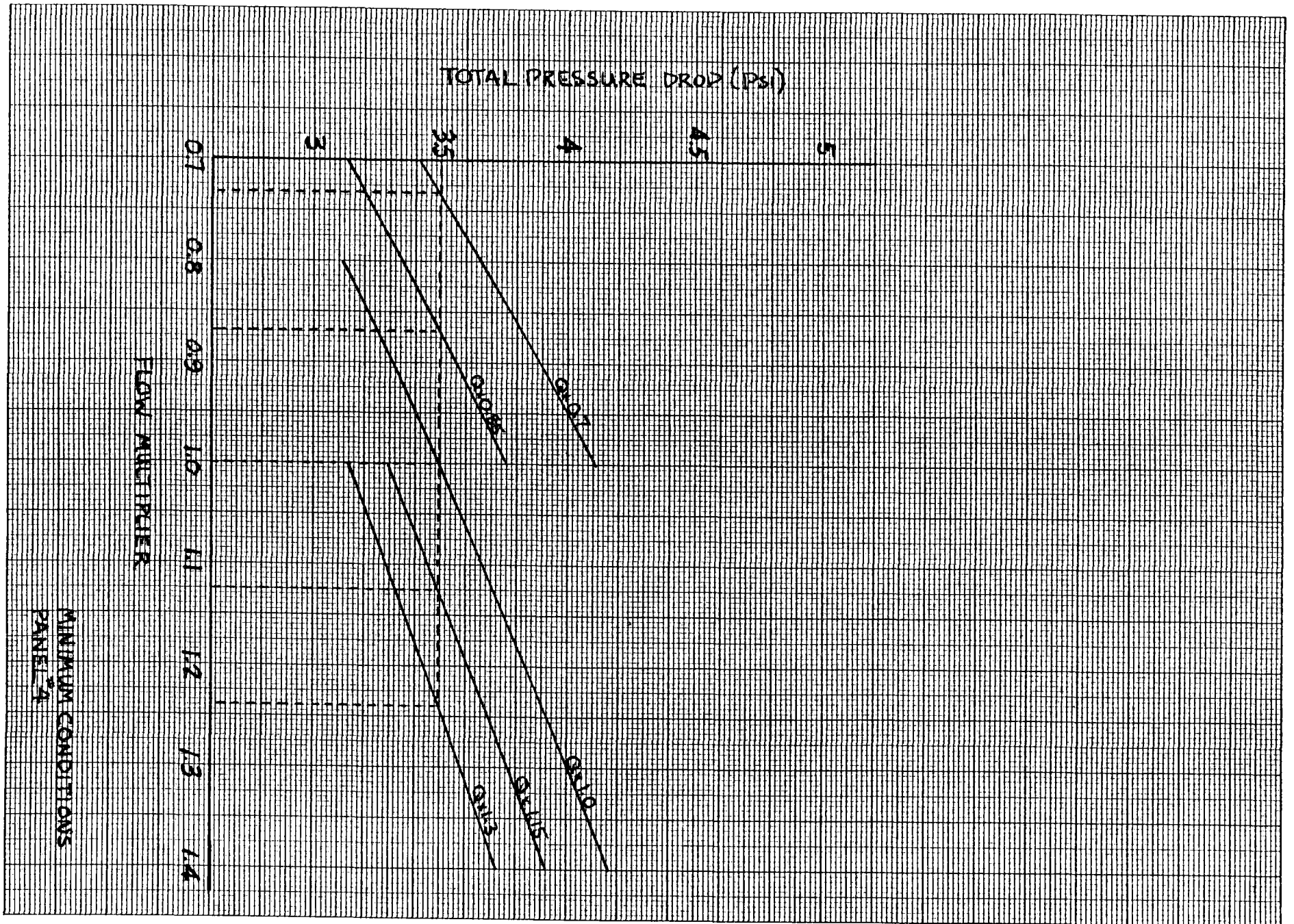
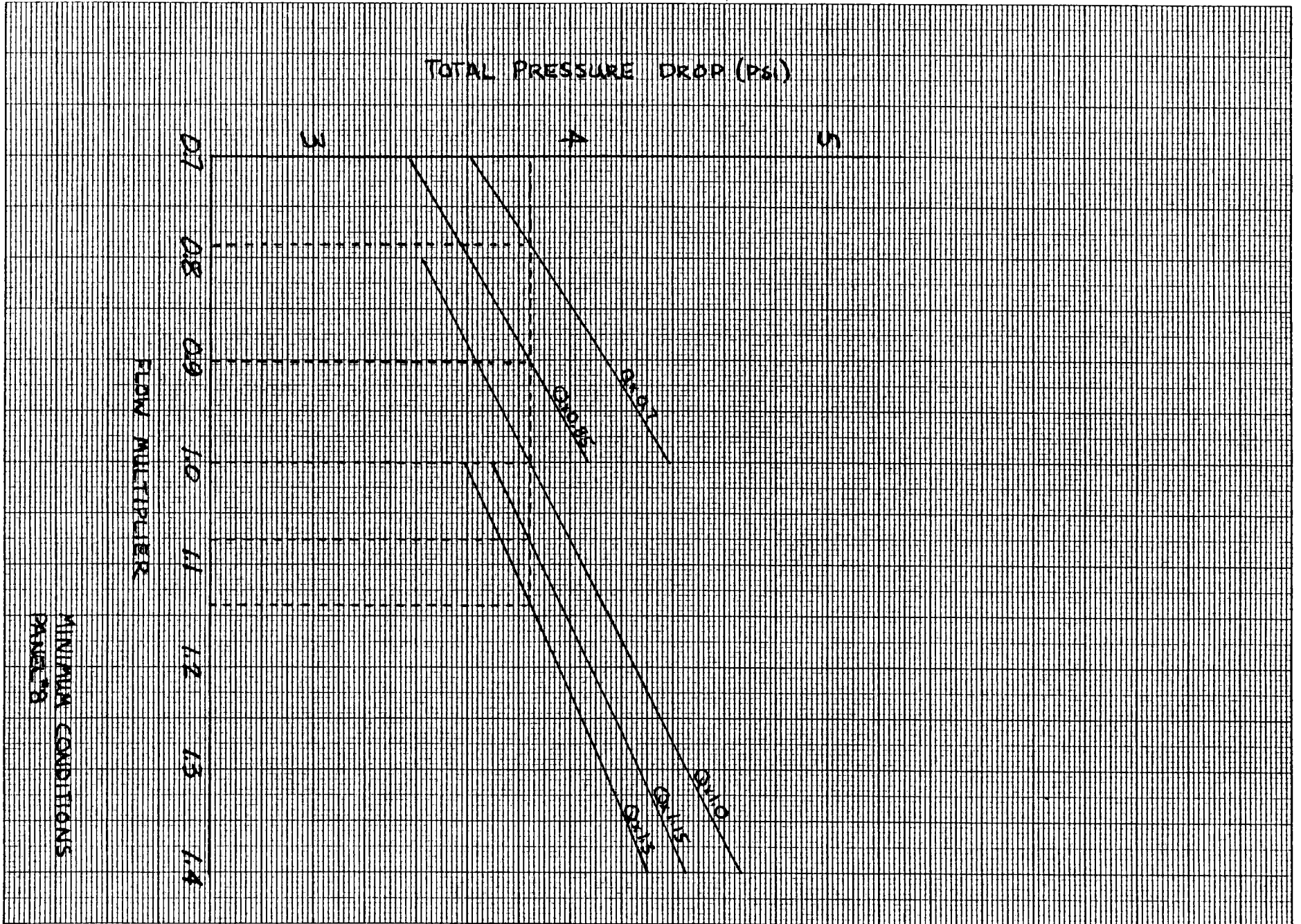


FIGURE 2-5



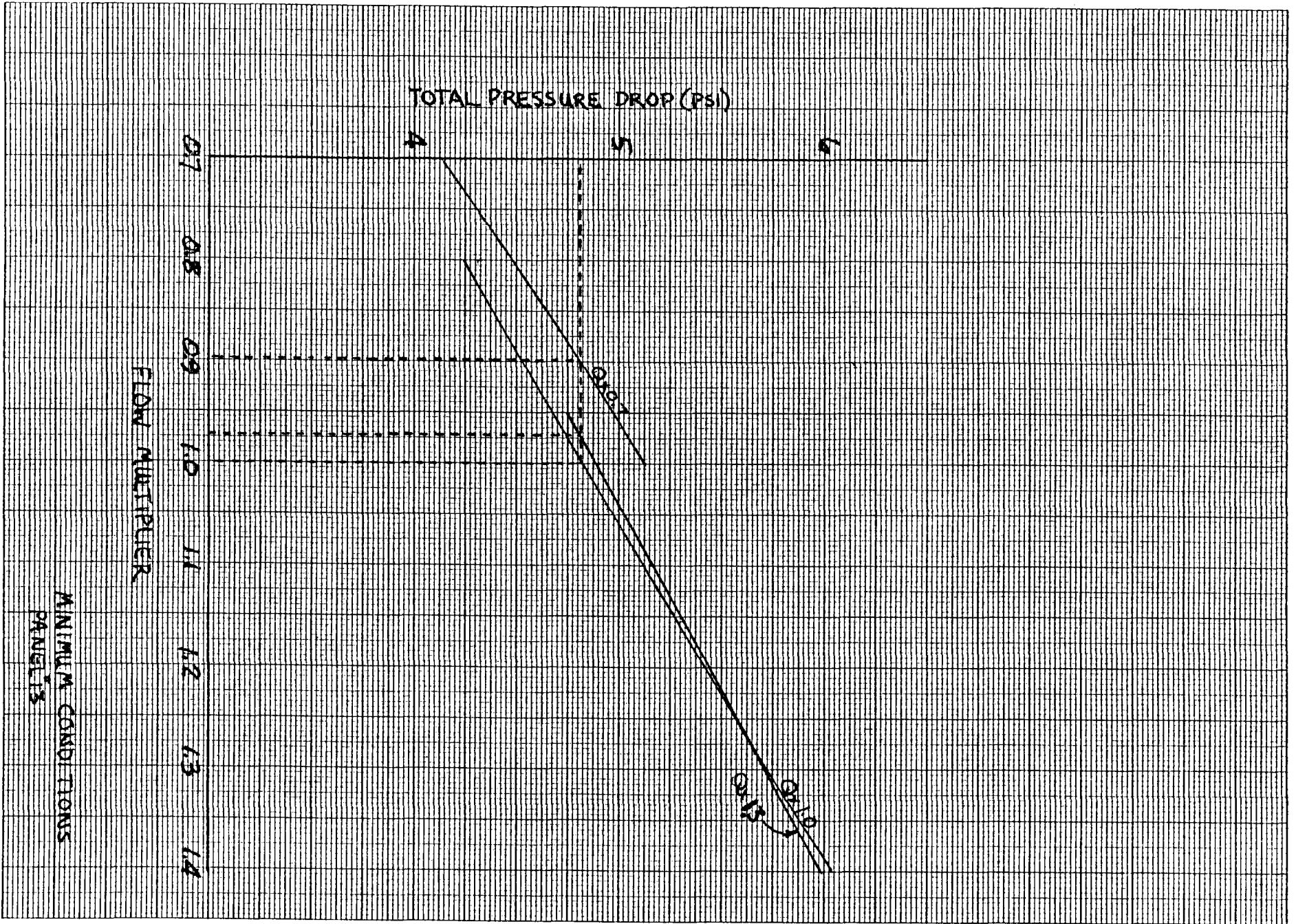
E-30

FIGURE 2-6



E-31

FIGURE 2-7



E-32

FIGURE 2-8

MINIMUM CONDITIONS  
PANELS

FLOW MULTIPLIER

TOTAL PRESSURE DROP (psi)

A

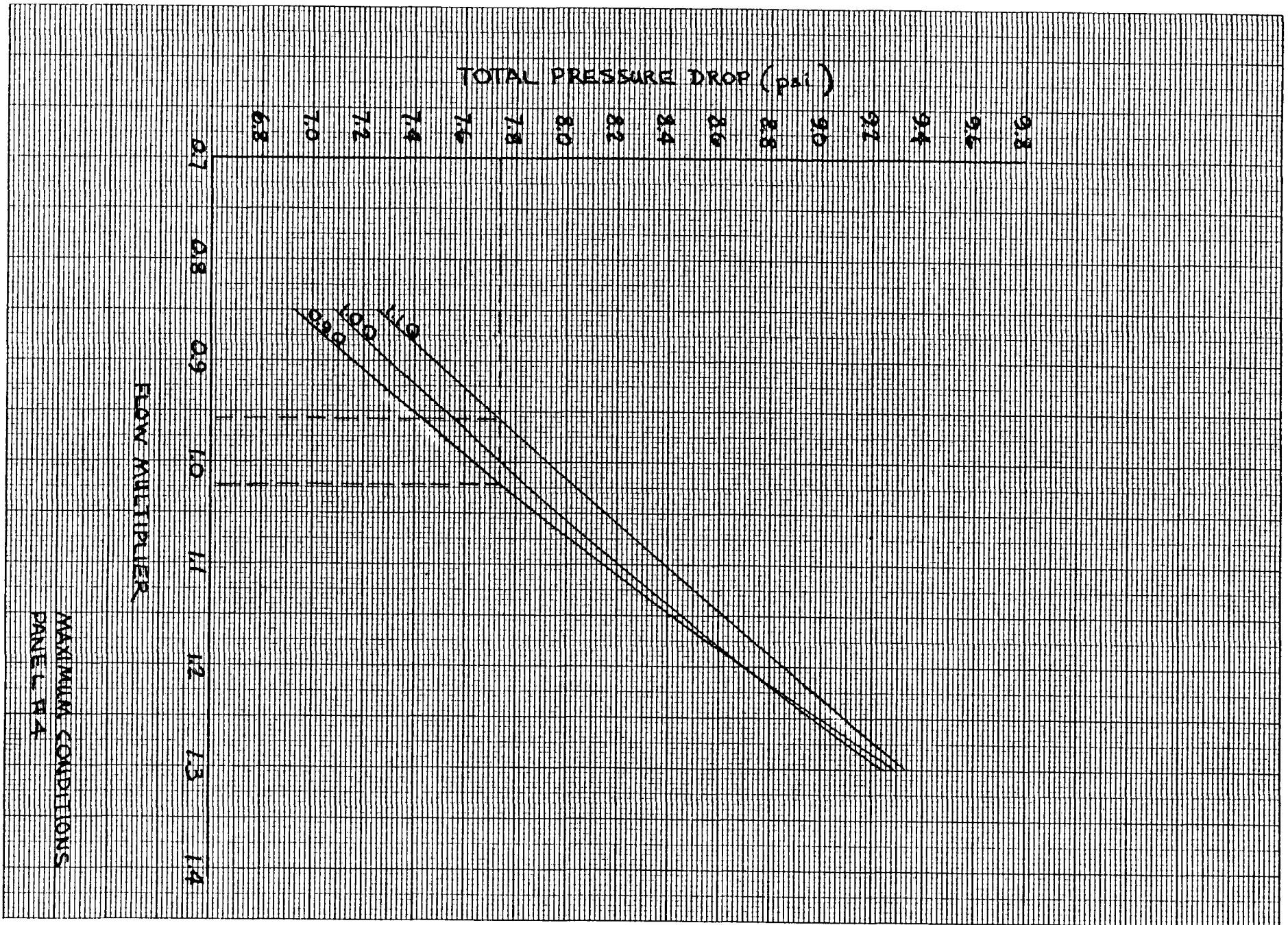
B

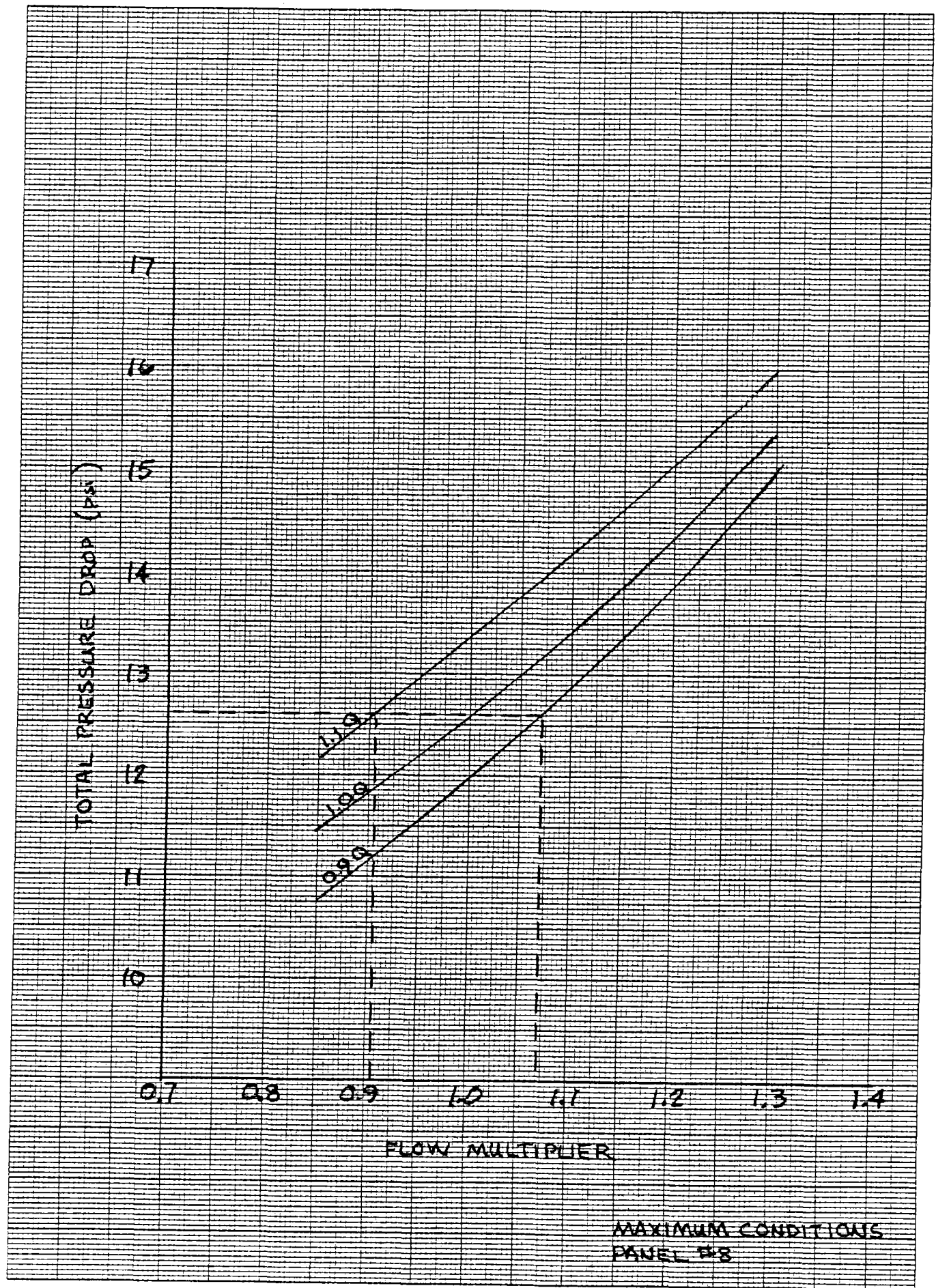
C

MINIMUM  
CONDITIONS  
STAYS

MINIMUM  
CONDITIONS  
STAYS

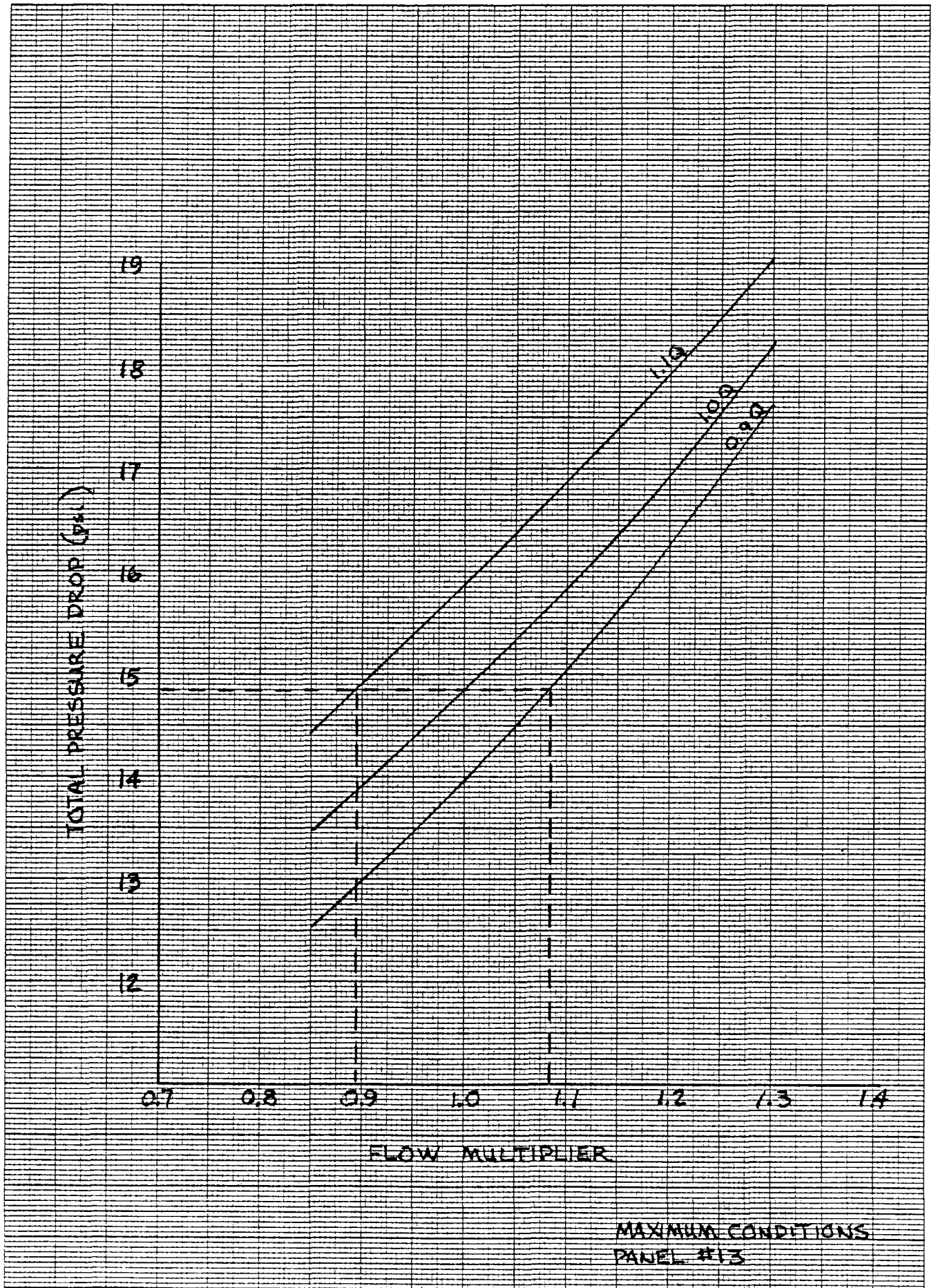






MAXIMUM CONDITIONS  
PANEL #8

FIGURE 2-10



MAXIMUM CONDITIONS  
PANEL #13

FIGURE 2-11

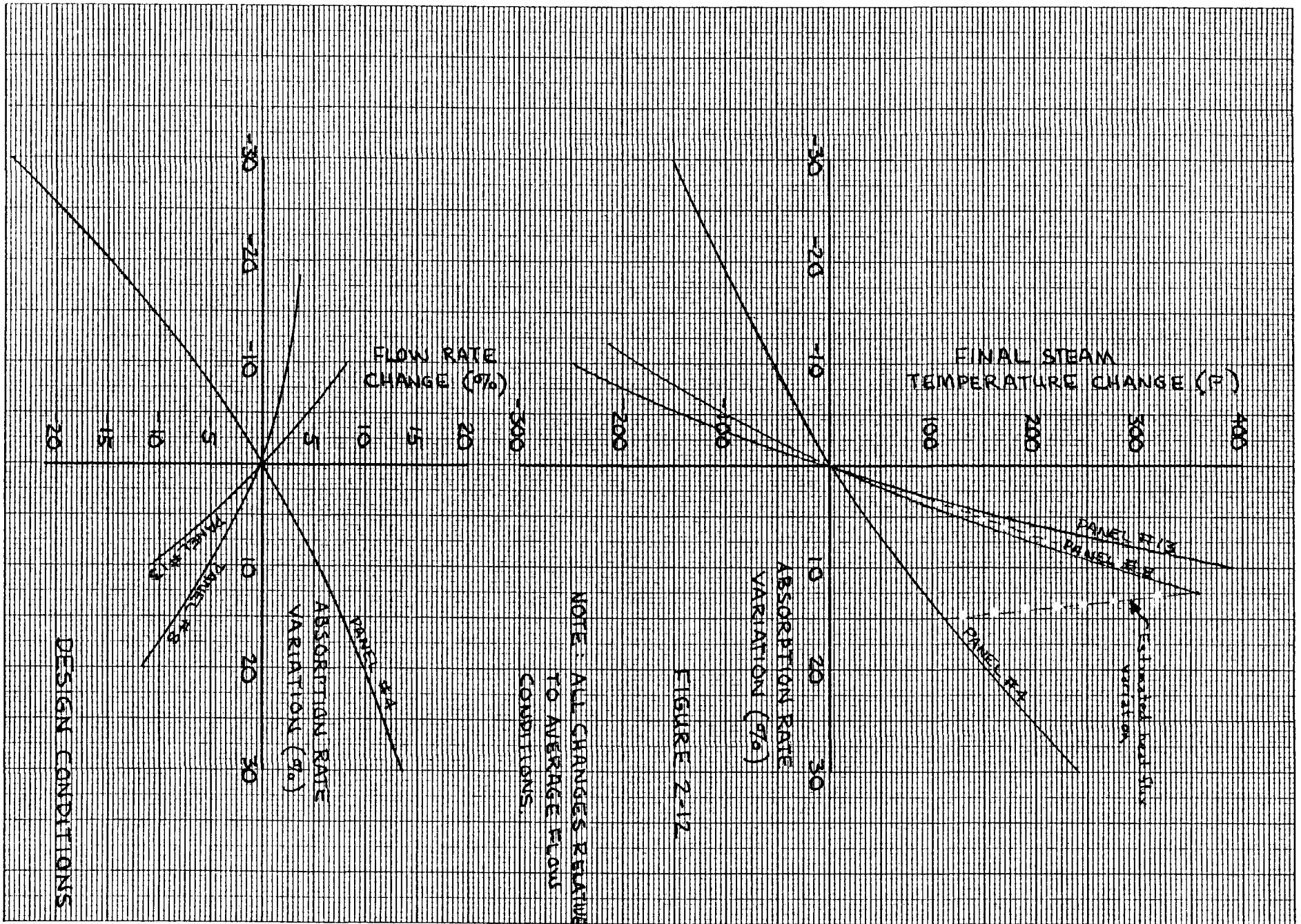
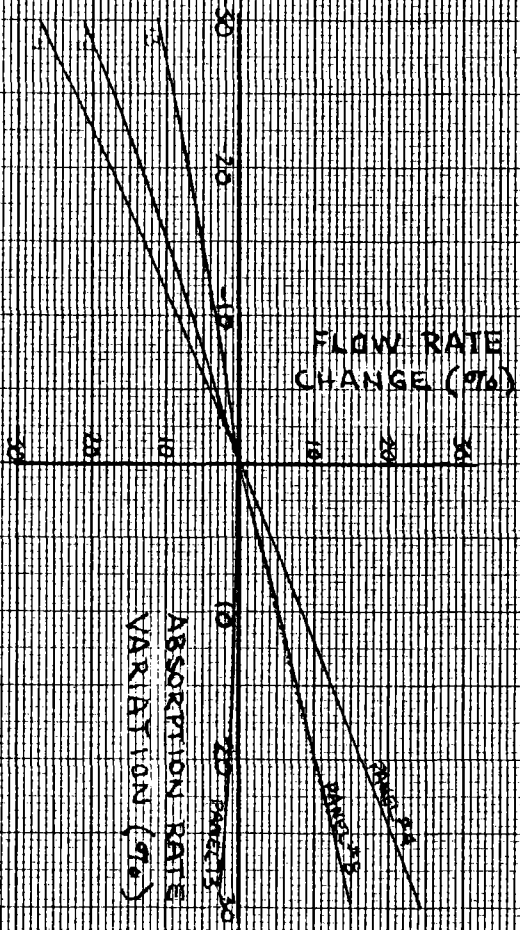


FIGURE 2-12

FIGURE 2-13





MINIMUM CONDITIONS

FIGURE 2-15

E-37

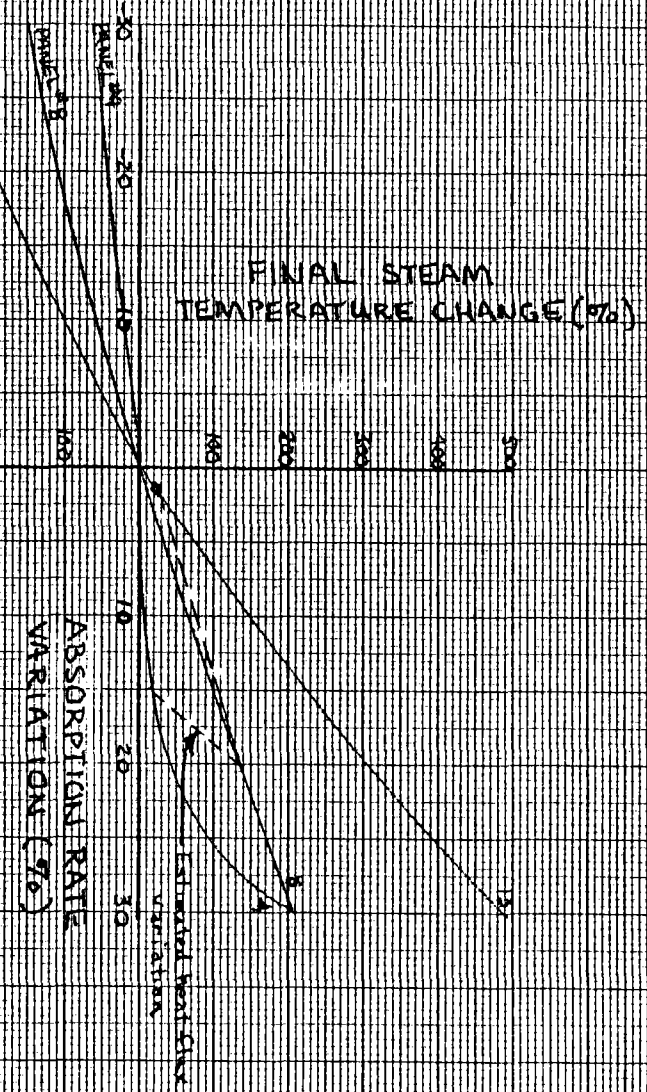


FIGURE 2-14

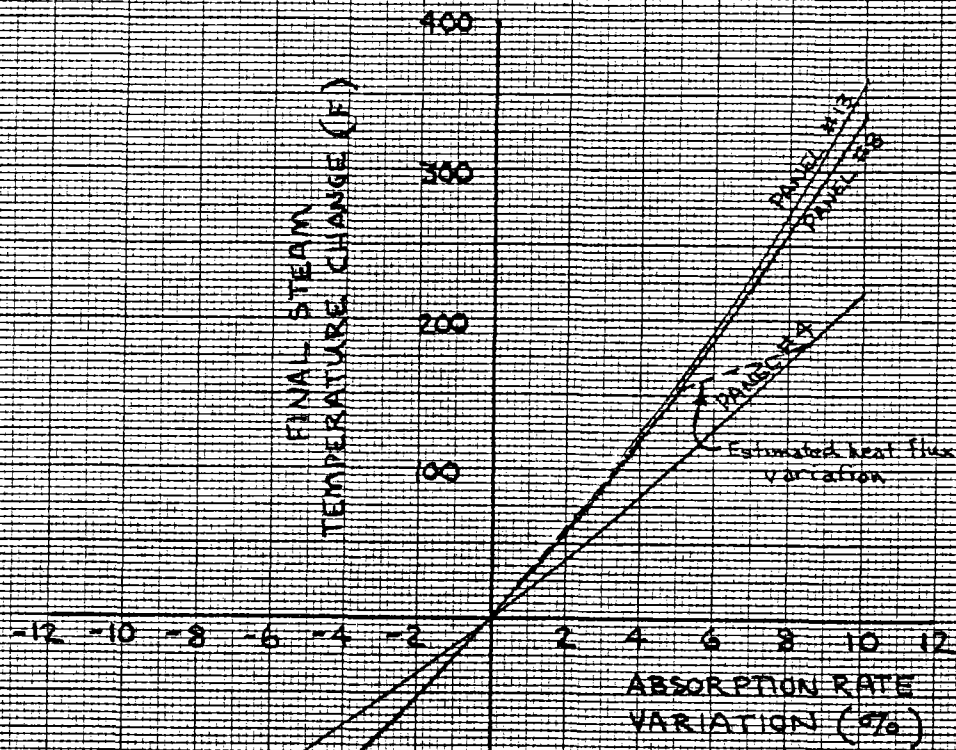
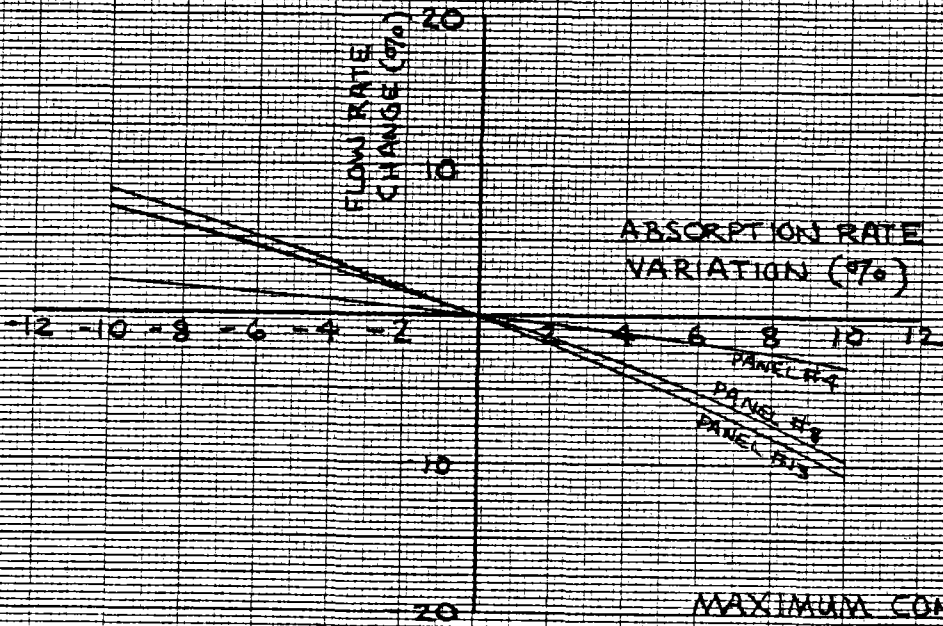


FIGURE 2-16



MAXIMUM CONDITIONS

FIGURE 2-17

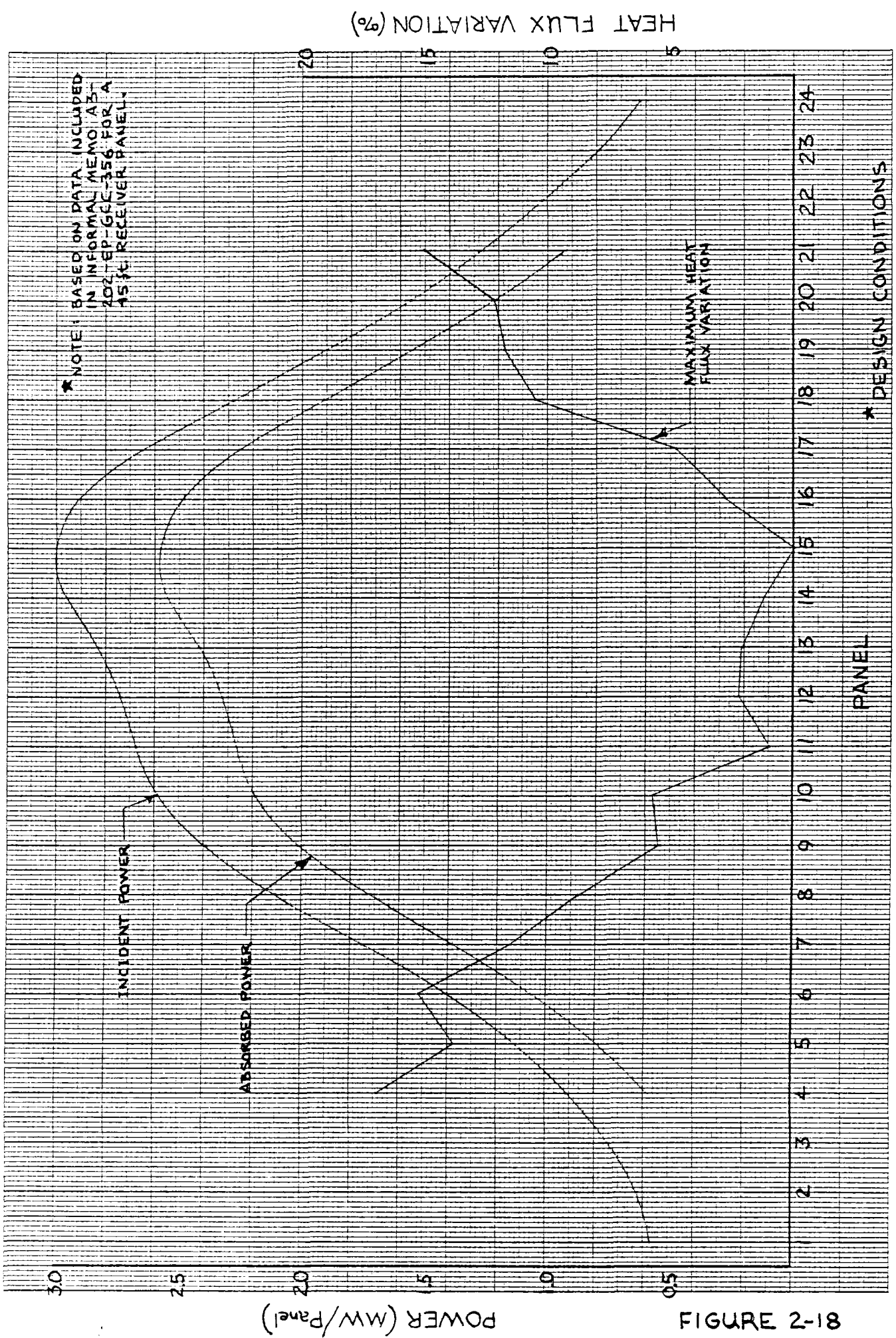
dominated, i.e., as absorption rate increases, flow rate increases. The remaining panels and load conditions analyzed are frictional pressure drop dominated, i.e., as absorption rate increases, flow rate decreases.

- No pressure drop versus mass flow rate curve plotted has a negative sloping region. Consequently, static Ledinegg instability should not result.
- The highest final steam temperature change (+340F) occurs in the intermediate flow panel (#8) for the design load condition.

After completing the preceding analysis FWEC received incident power data from MDAC revised for a 45 ft. receiver panel heat length (Informal Memo A3-202-EP-GCC-356). The data included integrated average incident power for each receiver panel at numerous load conditions.

Based on the results of the initial boiler panel analysis, the worst steam side conditions occur in the intermediate flow panels at the design load. Consequently, the revised data was used to determine which of the intermediate flow panels results in the worst steam side conditions at the design load.

Incident power was plotted as illustrated in Figure 2-18. In order to estimate absorbed power, a 5% reflected loss and a fixed convection and radiation loss to ambient was subtracted from the incident power. The fixed convection and radiation loss to ambient was estimated from incident and absorbed power values described in Section 1. These values are not exact since they were based on a 41 ft. receiver panel heated length, and as tube wall temperature varies with absorbed heat flux,



81-2 ERNFIG

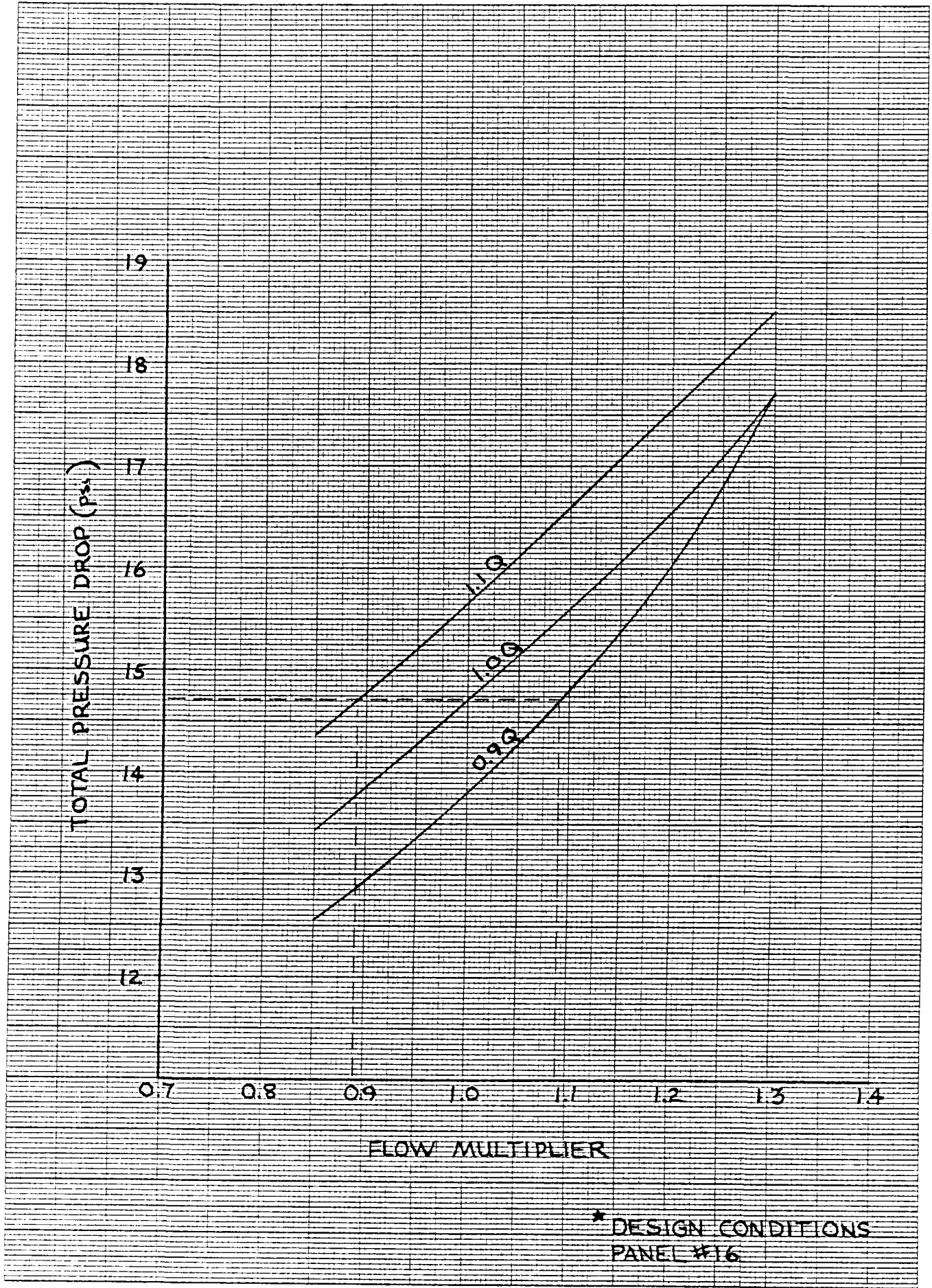
the losses to ambient will not remain constant. Also plotted in Figure 2-18 are the maximum absorbed heat flux variations for each boiler panel determined from the estimated absorbed power curve.

Based on the maximum absorbed heat flux variation curve plotted in Figure 2-18, intermediate flow panels #16, #17, #18, and #19 were selected for analysis since the corresponding panels on the opposite side of the receiver, i.e., panels with the same absorbed power, have lower heat flux variations. Total pressure drop versus flow multiplier curves for these panels are included in Figures 2-19, 2-20, 2-21 and 2-22. Figures 2-23 and 2-24 illustrate the final steam temperature change and flow rate variation as a function of absorption rate variation for each of the panels analyzed, respectively. Plotted on the final steam temperature change curves are the absorption rate variations obtained from Figure 2-18.

Worst steam side conditions occur in panel #18 with a final steam temperature of 1305F resulting from an absorption rate variation of +10.5% which reduces the flow rate in the worst tube by 7%. Since this high final steam temperature will result in high tube wall temperatures, increasing the heat loss to ambient, the estimated absorbed heat flux variation curve plotted in Figure 2-18 does not apply. Consequently, the analysis described in the following section was conducted to determine the expected absorbed heat flux variation for a given incident heat flux variation and also to determine the maximum tube wall temperature for panel #18.

## 2. Maximum Tube Metal Temperature

The analysis described in the preceding subsection assumed that heat losses to ambient due to convection and radiation are constant. This assumption is valid if the tube wall temperature does not vary greatly. However, as the



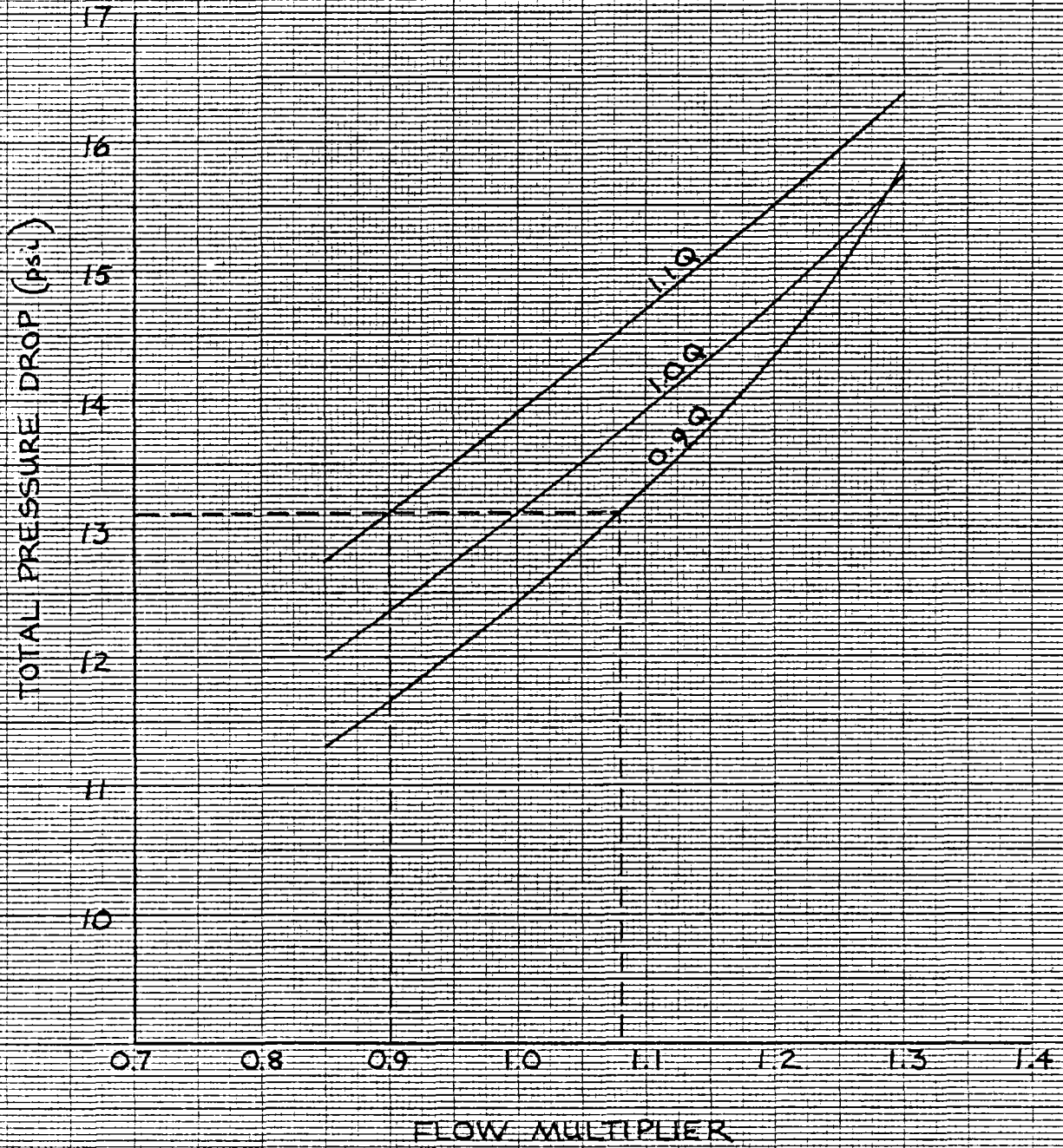
\* DESIGN CONDITIONS  
PANEL #16

FIGURE 2-19



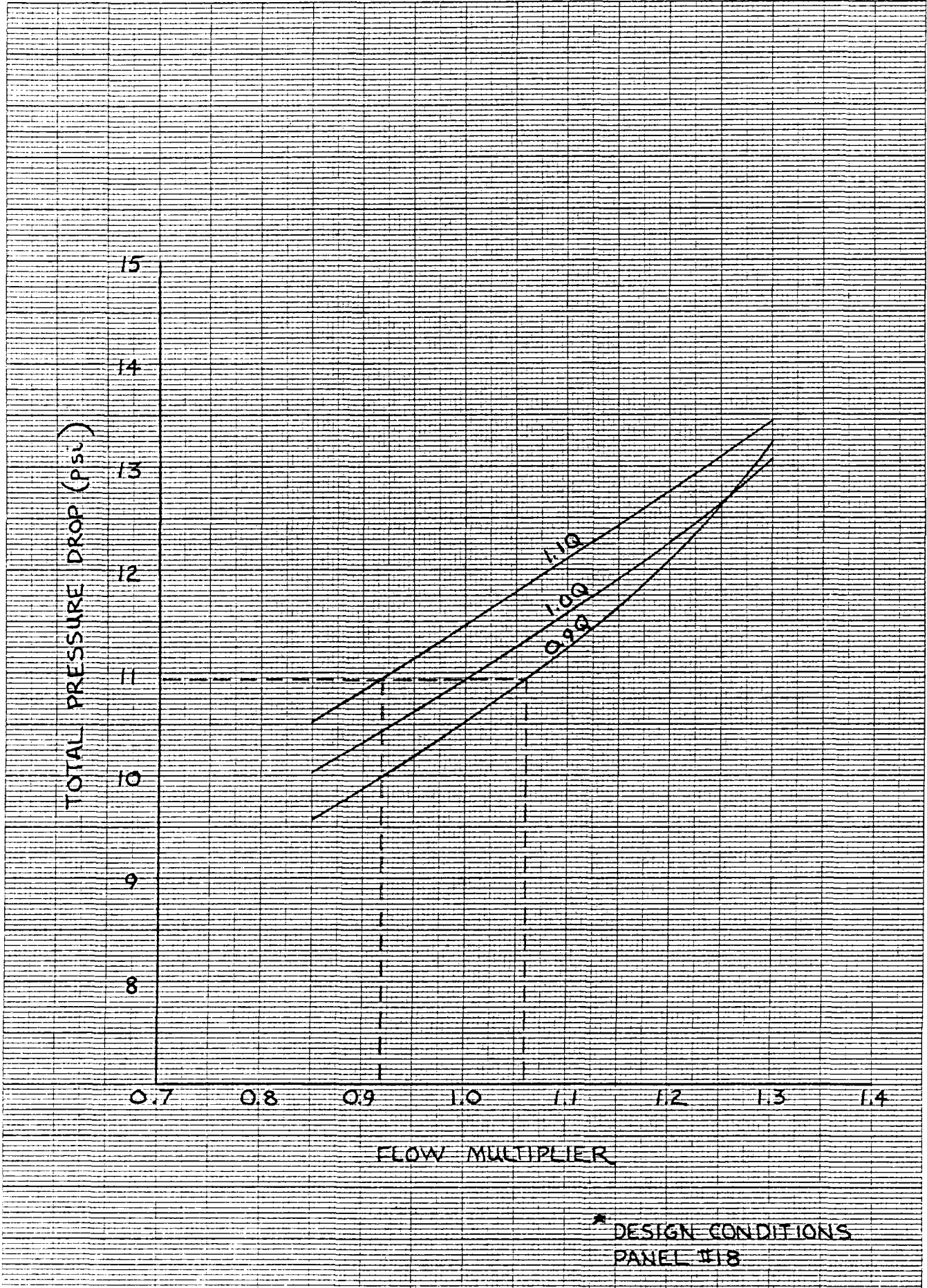
461510

1010 ENT  
REIFFEL & ESSER CO. MADE IN U.S.A.



\* DESIGN CONDITIONS  
PANEL #17

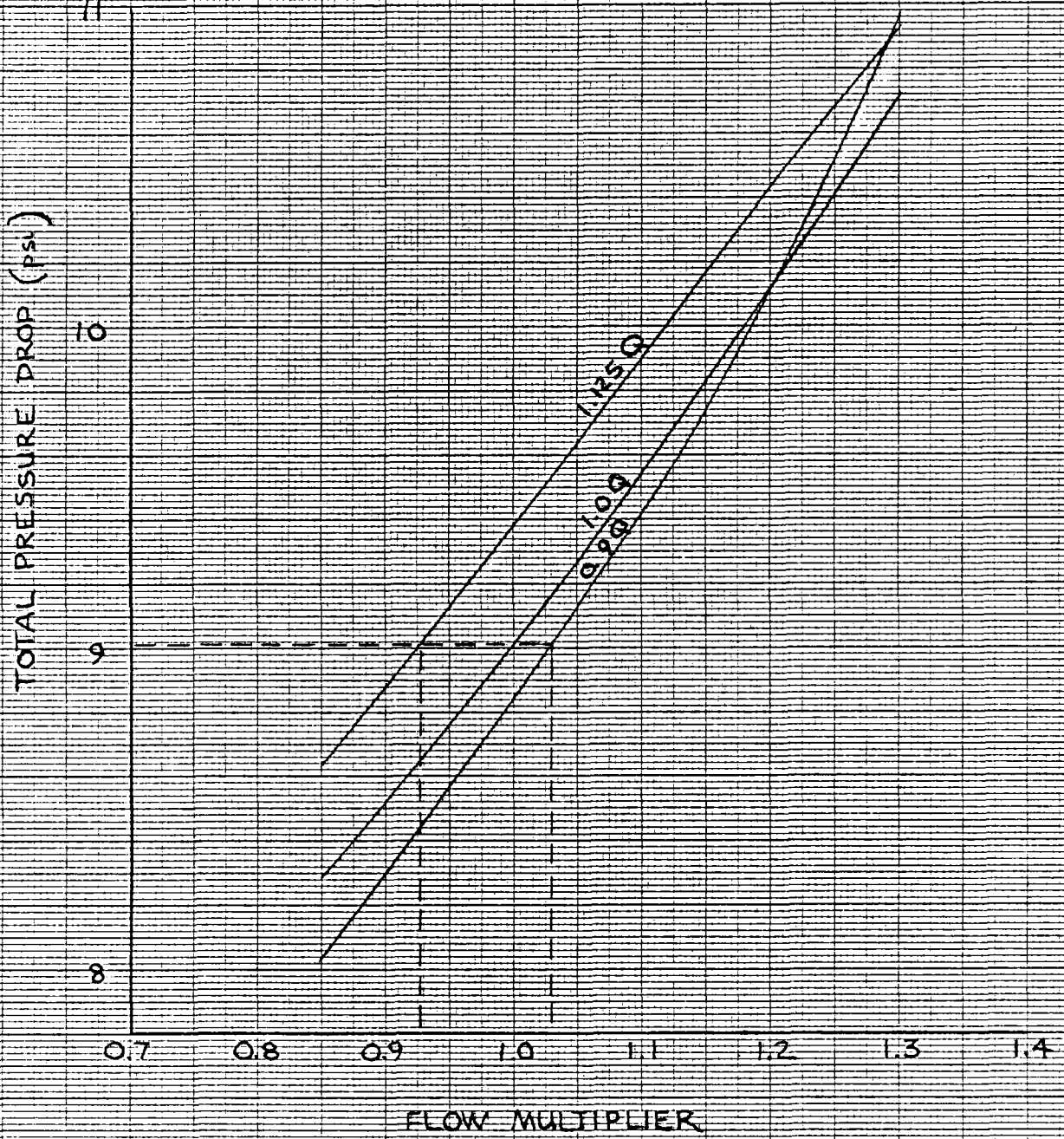
FIGURE 2-20



DESIGN CONDITIONS  
PANEL #18

FIGURE 2-21





\* DESIGN CONDITIONS  
PANEL #19

FIGURE 2-22

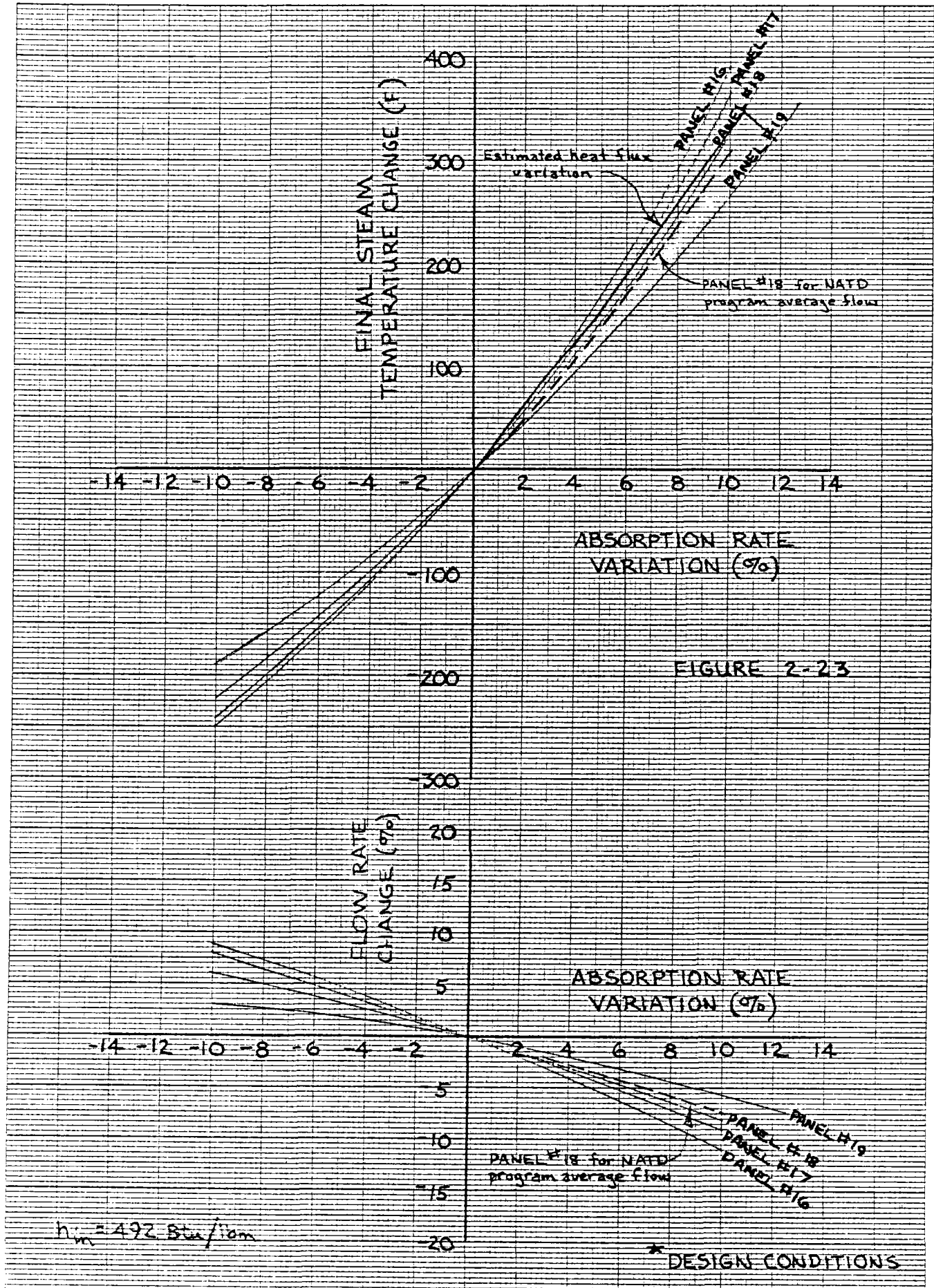


FIGURE 2-23

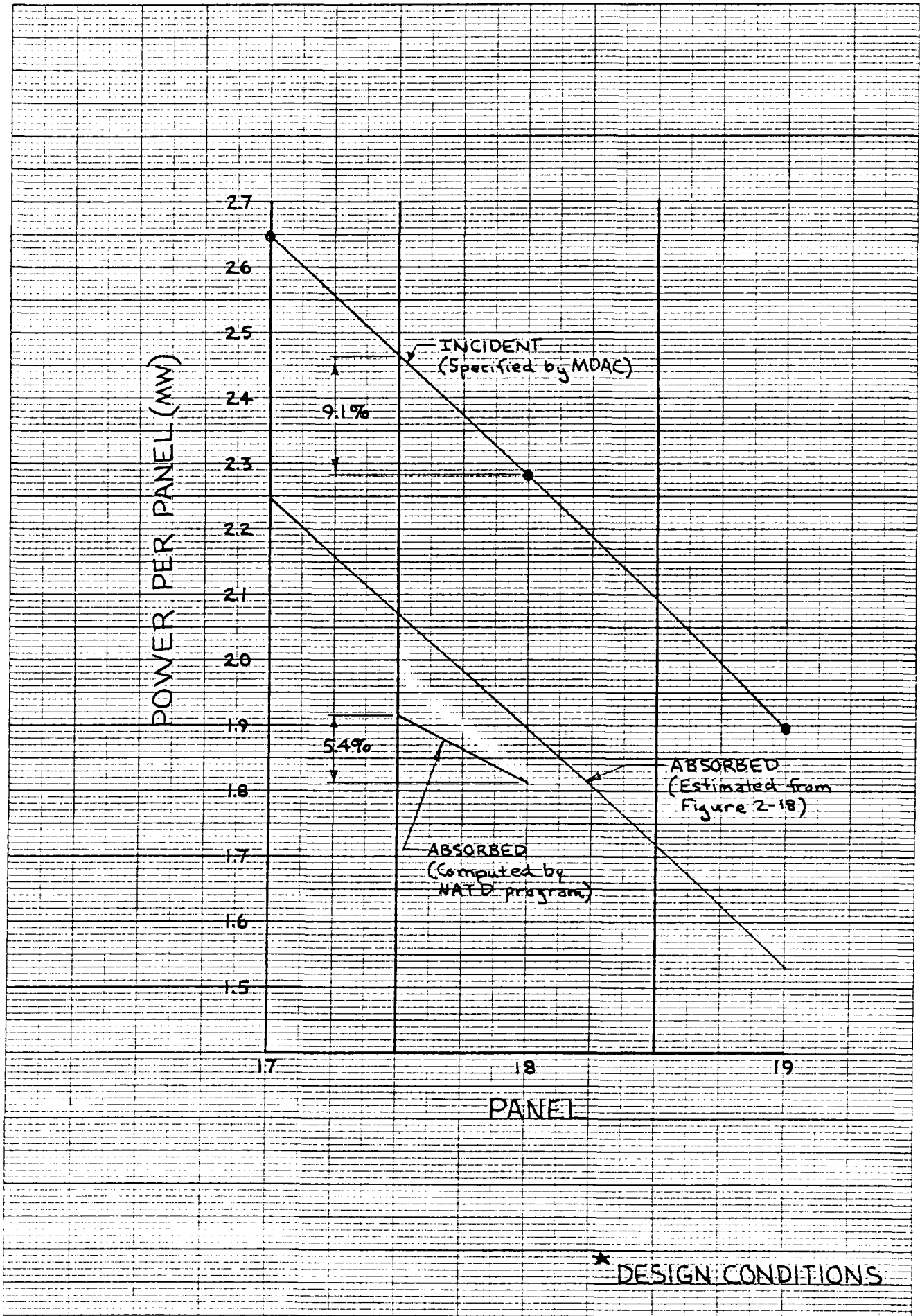
FIGURE 2-24

heat flux across a panel varies, flow variations result which, when combined with increased heat absorption, result in high steam temperatures and therefore, high tube wall temperatures. Consequently, heat losses to ambient increase.

The FWEC Nuclear and Advanced Technology Department (NATD) Thermal/Hydraulic and System Engineering Section has developed a computer program that determines absorbed power and resultant tube wall temperature distributions for a given incident heat flux distribution. Heat losses are computed using a reflectivity of 0.05, a tube surface emissivity of 0.88, and a convection film coefficient of 4.6 Btu/hr-ft<sup>2</sup>-F (see Reference 3 for program details).

Initially the NATD program was run to determine panel #18 average absorbed power for the average incident power specified in Informal Memo A3-202-EP-GCC-356. The incident heat flux distribution was determined by proportioning the incident heat flux distribution curve illustrated in Figure 2-1 of Reference 1 adjusted for a receiver panel heated length of 45 ft.

Figure 2-25 indicates the specified incident power, the previously estimated absorbed power, and the absorbed power for panel #18 computed from the NATD program. As can be seen the absorbed power computed by the NATD program is approximately 4% lower than that previously estimated. The NATD program average absorbed power corresponds to an average panel flow rate which falls between that previously used for panel #18 and panel #19. Consequently, a final steam temperature change curve and a flow rate change curve was drawn for the NATD program panel #18 average flow conditions (see Figures 2-23 and 2-24).



With the flow sensitivity curve established for the NATD program panel #18 average flow conditions, the NATD program was run with the incident power variation (+9.1%) determined from Figure 2-25. The program was run a number of times until the absorbed power variation and flow rate change matched values on the flow rate change curve plotted in Figure 2-23.

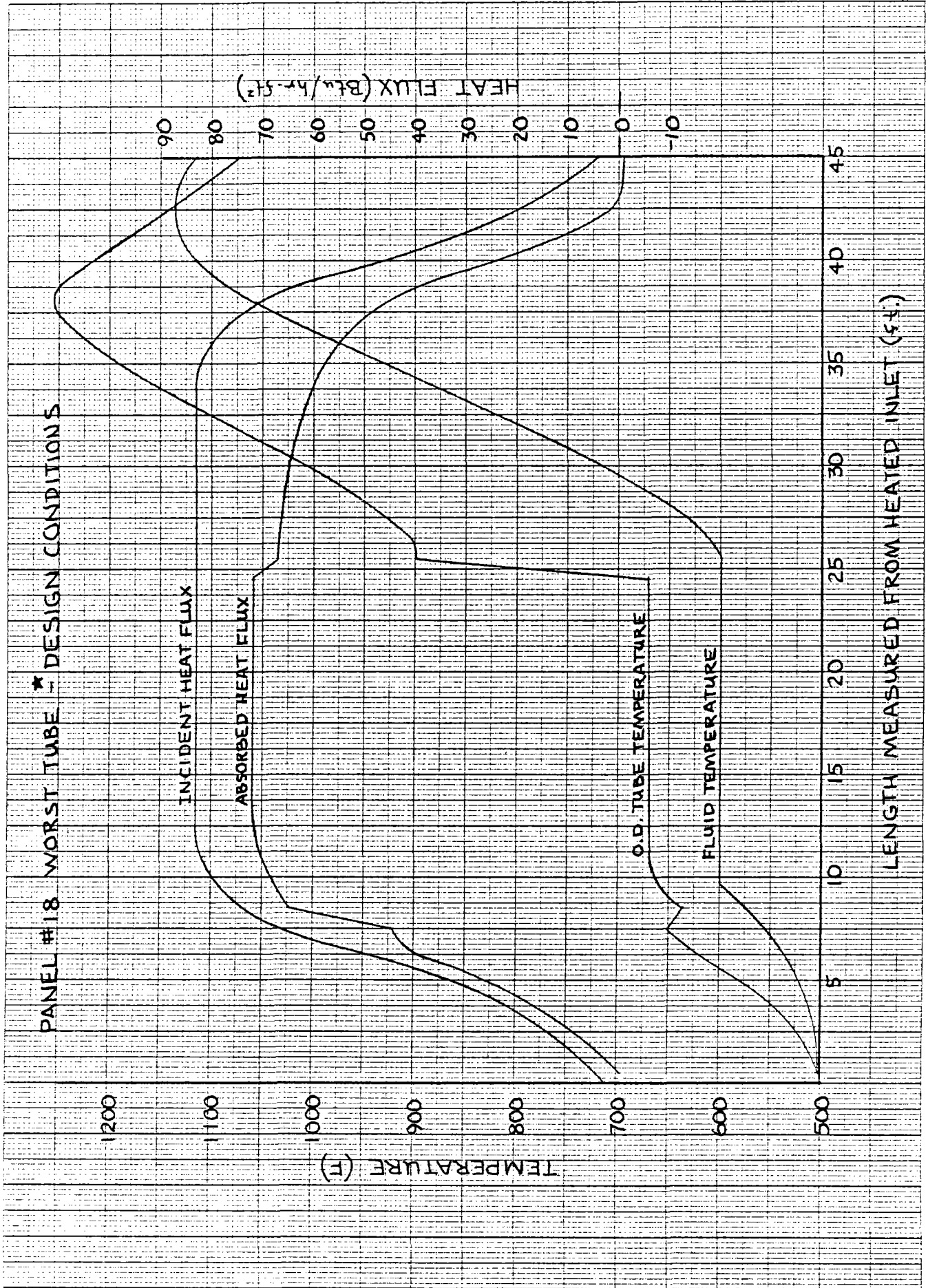
The final results for the panel #18 worst tube are:

Incident heat flux variation (%)	9.1
Absorbed heat flux variation (%)	5.4
Flow rate change (%)	-4.1
Final steam temperature (F)	1129
Maximum OD tube temperature (F)	1253
Maximum mean metal temperature (F)	1242

The maximum metal temperature is located 38.5 ft. from the heated inlet of panel #18 (see Figure 2-26).

Although a large flow reduction does not result, the final steam temperature in the worst tube increases by 169F. This occurs because the average enthalpy change is very large (974 Btu/lbm) and a relatively small increase in absorption (5.4%) combined with a reduction in flow significantly increases the final steam temperature.

Of the panels and load conditions analyzed, panel #18 at the design load results in the worst steam side conditions. Operation at a load slightly higher or lower than the design load may result in worse conditions. However, determination of the operating load during which the worst conditions will result would require extensive calculations which are beyond the scope of this study.



3. Header Unbalance

The header size and arrangement for the boiler panels is identical to that for the preheater panels. No header configuration induced flow unbalances are expected for the boiler panels over the operating load range.

REFERENCES TO APPENDIX E

1. R. W. Hallet, Jr., and R. L. Gervais, "Central Receiver Solar Thermal Power System, Phase 1, CDRL Item 2, Pilot Plant Preliminary Design Report," Volume IV, McDonnell Douglas Astronautics Company, MDC G6776, October 1977.
2. Letter from S. M. Cho to R. J. Zoschak, "MDAC Pilot Plant Receiver Evaluation-Monthly Progress Report," May 4, 1979.
3. S. Cho, T. Kao, and H. L. Chou, "Summary Report on Pilot Plant Receiver Evaporator/Superheater Panel Dynamic Stability Analysis, Foster Wheeler Energy Corporation, June 7, 1979.



APPENDIX F

## Appendix F

### Summary Report on Pilot Plant Receiver Evaporator/Superheater Panel Dynamic Stability Analysis

By S. Cho, T. Kao and H. L. Chou  
Foster Wheeler Energy Corporation  
June 7, 1979

#### INTRODUCTION

The solar receiver boiler panels for 10 Mwt pilot plant proposed by McDonnell Douglas Astronautics Company and Rocketdyne were analyzed to evaluate the overall thermal performance and the tube-side pressure drop. The thermal/hydraulic conditions obtained were then used to establish the static and dynamic stability characteristics of the tube-side boiling flow.

#### ANALYSIS CONDITIONS

The receiver boiler panel is a straight, once-through unit consisting of 0.5-in.-O.D. 0.269-in. I.D. Incoloy 800 tubes. Each boiler panel has 70 tubes with an active heated length of 45 ft. Subcooled water enters the bottom headers, flows upward, and exits at the top as superheated steam at 960°F and 1520 lb/in<sup>2</sup>a.

The analyses were performed at three levels of total incident thermal power per panel to examine the thermal performance and flow stability of the boiler panels under various conditions.

- Panel 13 at 3.218 Mwt
- Panel 21 at 1.758 Mwt
- Panel 21 at 0.625 Mwt

The absorptivity and emissivity associated with the Pyromark coating are set equal to 0.95 and 0.88 respectively. The ambient convective heat-transfer coefficient is  $4.6 \text{ Btu/ft}^2 \cdot \text{h} \cdot ^\circ\text{F}$ , and the ambient temperature is  $60 \text{ }^\circ\text{F}$ .<sup>1</sup>

#### STEADY-STATE THERMAL PERFORMANCE ANALYSIS

The overall thermal performance of the boiler panels were examined using an existing FWEC solar boiler performance computer code, which had been modified to accommodate the MDAC/Rocketdyne boiler configuration and thermal/hydraulic conditions. In the analysis, the entire 45 ft active tube length was divided into 45 elements. For each element under consideration, the energy balance equation was first solved using an iterative procedure to calculate the outside tube-wall temperature and the fluid enthalpy at the exit of the element. The thermal resistance of the tube and convection inside the tube were calculated based on the local conditions of the element. The tube-side pressure drop through the element was also computed simultaneously.

A review was made of available correlations for the calculations of heat transfer and pressure drop. The following correlations were utilized in the thermal performance computer code.

#### Heat-Transfer Correlations

Liquid heat transfer	Dittus-Boelter equation <sup>2</sup>
Subcooled nucleate boiling	Thom correlation <sup>3</sup>
Nucleate boiling	Chen correlation <sup>4</sup>
CHF/DNB correlation	Macbeth correlation <sup>5</sup>
Film boiling	Bishop-Sandberg-Tong correlation <sup>6</sup>
Superheated steam	Heineman correlation <sup>7</sup>

### Pressure Drop Correlations

Single-phase flow  
Two-phase flow

Moody diagram equivalent  
Modified Martinelli-Nelson<sup>8</sup>  
correlation

To establish the thermal/hydraulic conditions of the boiler panel under various incident thermal power levels, the outlet steam conditions were held constant at 960°F and 1520 lb/in<sup>2</sup>a. The water flow rate was, therefore, adjusted so that the outlet steam achieved the specified conditions and the inlet water subcooling was about 50°F. The results of the thermal performance are plotted in Figures 1 to 3. The figures show the incident and absorbed heat flux, and water/steam and outer tube wall temperatures as a function of the active heated tube length. It may be noted that the steam outlet temperature for panel 21 with 0.625 Mwt incident thermal power was 935°F instead of the specified value of 960°F. This was the maximum outlet temperature achievable by adjusting the water flow rate.

The outer tube-wall temperatures shown in the figures were the circumferentially averaged temperatures for the half of the tube circumference exposed to solar radiation. For panel 13 in Figure 1, the wall temperature increase at the CHF/DNB point was about 190°F on the average. However, at the location of the tube circumference where solar incidence was normal to the tube wall, the CHF - induced temperature increase was even greater and was estimated to be 260°F. This value may be considered as a potential  $\Delta T$  for transient boiling thermal oscillation in the tube wall. The thermal performance results were then used in static and dynamic stability analyses described in the following sections.

HEAT FLUX,  $\times 10^4$  Btu/HR-FT<sup>2</sup>

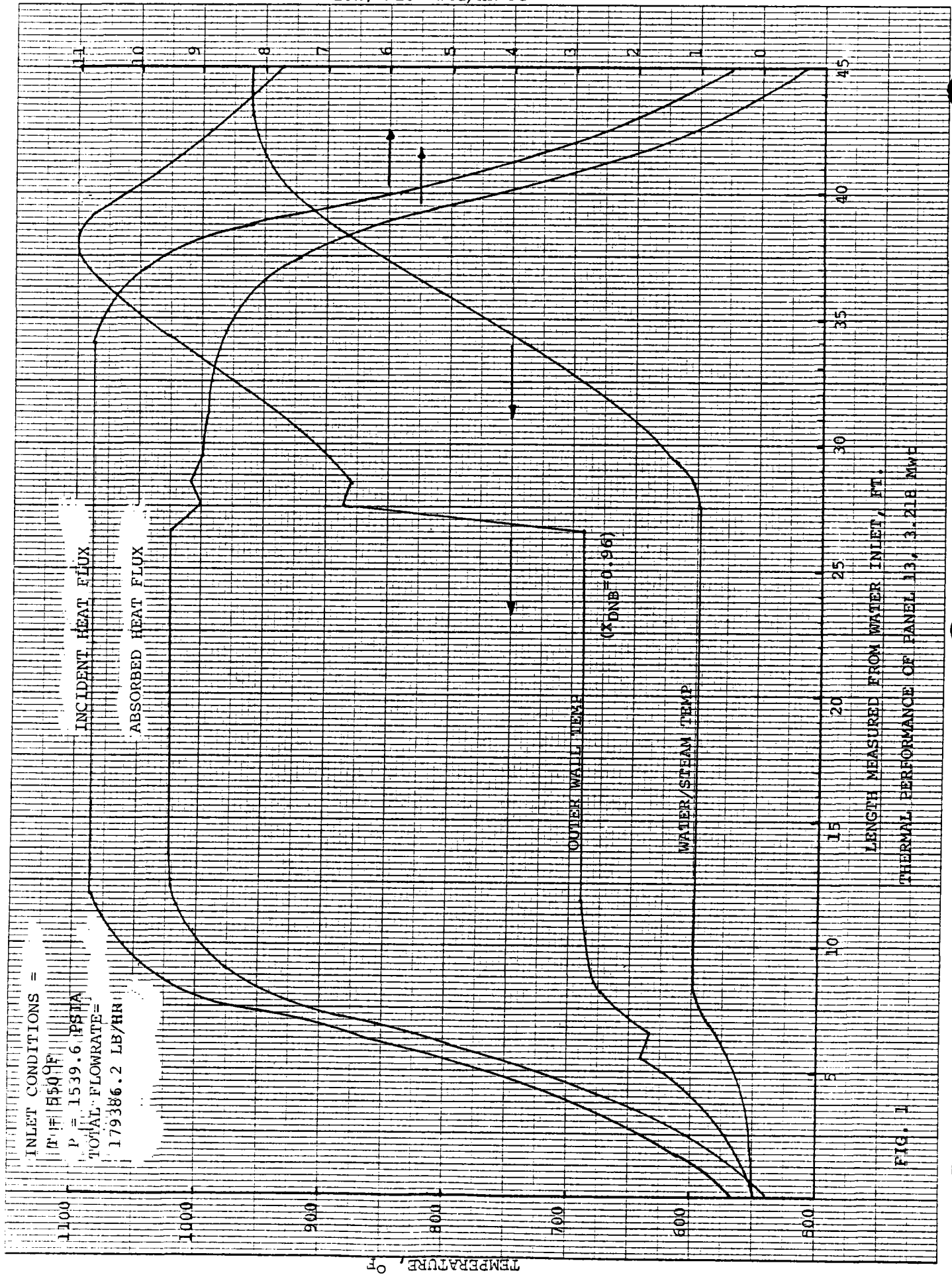


FIG. 1

THERMAL PERFORMANCE OF PANEL 13, 3.218 MWE

HEAT FLUX,  $\times 10^4$  Btu/HR-FT<sup>2</sup>

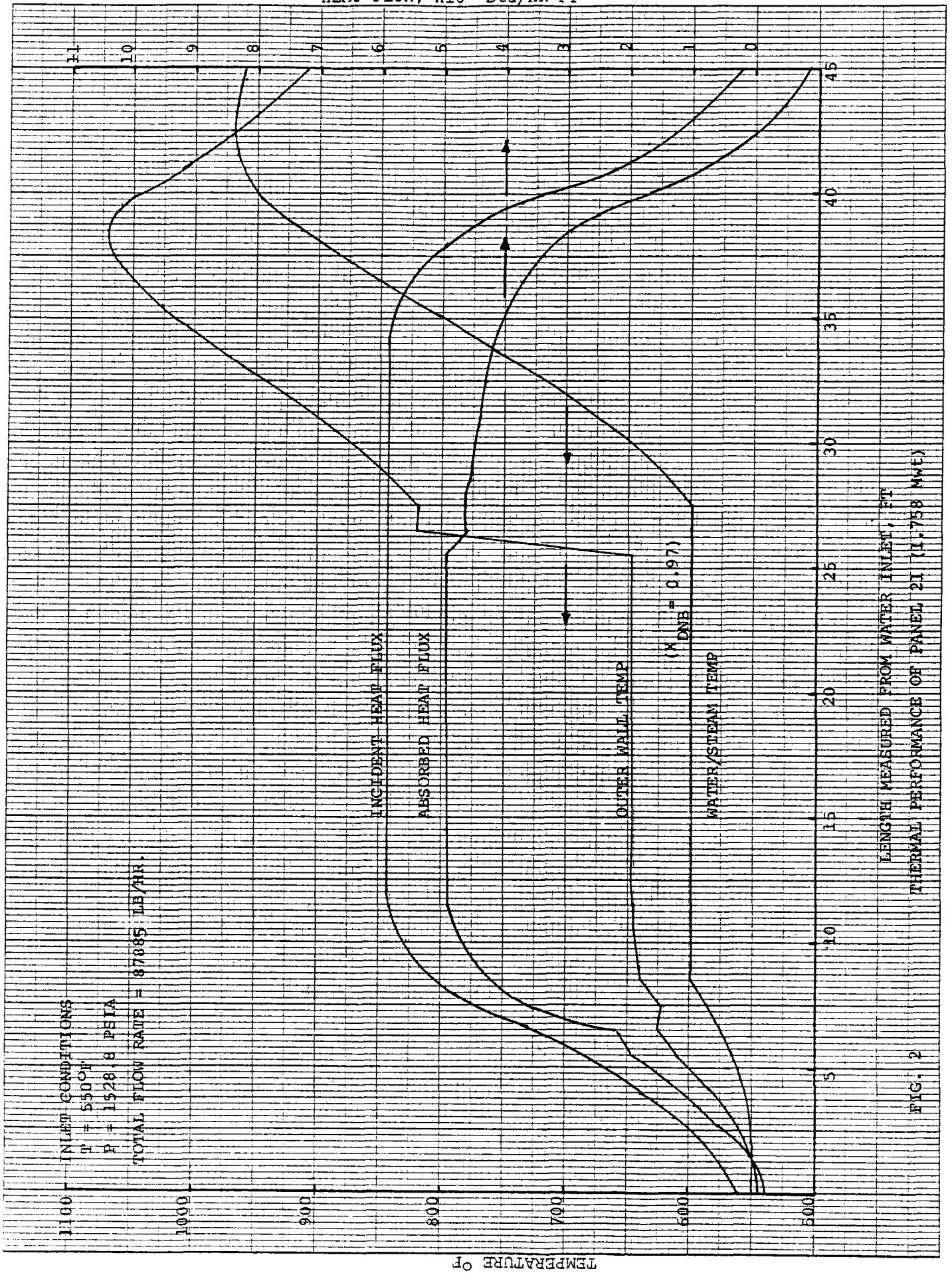


FIG. 2  
THERMAL PERFORMANCE OF PANEL 21 (1.758 MWE)

10 X 10 TO 1/2 INCH \* 7/2 X 10 INCHES  
NEUFEL & ESSER CO. MADE IN U.S.A.

46 1472

HEAT FLUX,  $\times 10^4$  Btu/HR-FT<sup>2</sup>

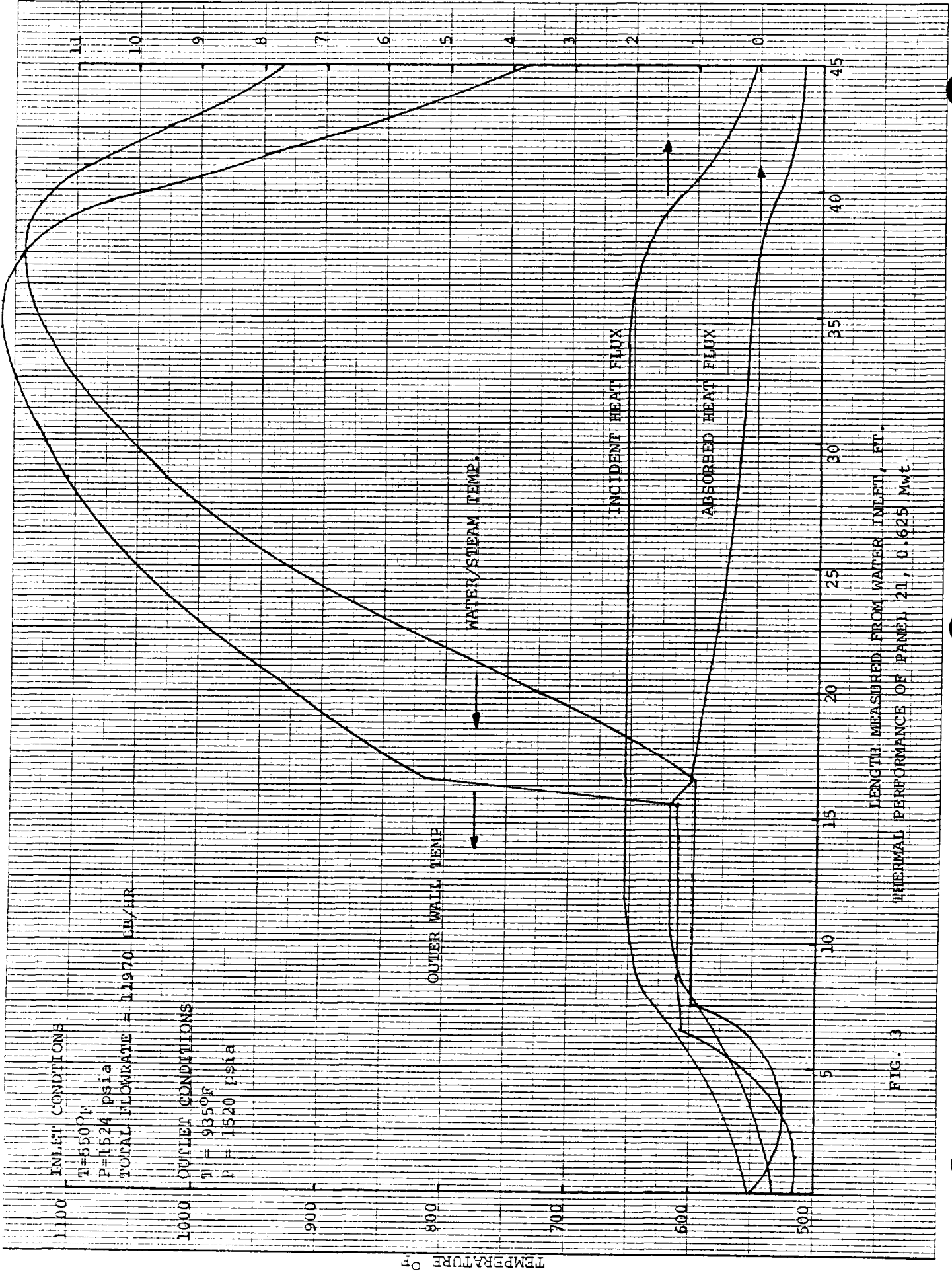


FIG. 3  
THERMAL PERFORMANCE OF PANEL 21, 0.625 MwT

## STATIC STABILITY

The static instability of primary design importance is the excursive instability of the Ledinegg type. A flow is subject to a static instability if the flow condition, when changed by a small perturbation, does not return to its original steady-state condition.

A one-tube model was analyzed for the conditions of panel 13 with 3.218 Mwt incident power. A positive slope of the pressure drop/flow rate curve was sought to ensure a statically stable boiling channel. The results of the analysis are shown in Figure 4 for the water/steam pressure drop versus the normalized water/steam flow rate. This curve has a positive slope throughout the flow-rate range, and therefore the boiler panel is statically stable under a given circumferentially uniform heat flux condition. The effect of circumferential non-uniformity of incident heat flux should be examined.

## DYNAMIC STABILITY

Dynamic flow instability is defined as sustained (or growing) oscillation of flow variables such as pressure drop, flow rate, fluid density, etc., within a tube.

In this analysis a density-wave type of dynamic instability was investigated. This type of instability is due to the feedback and interaction between the various pressure drop components and is caused specifically by the lag introduced through the density head term caused by the finite speed of propagation of density waves.



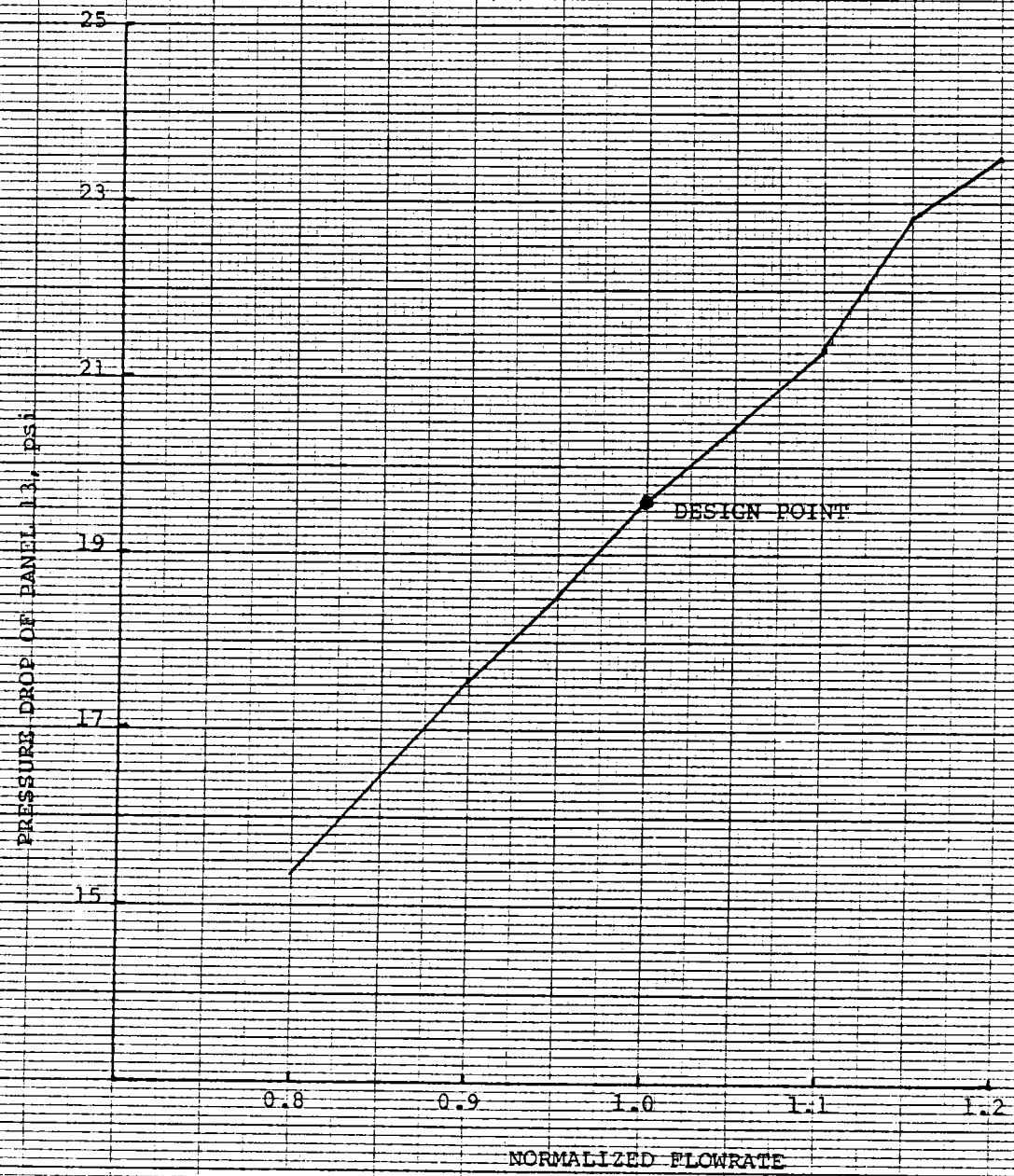


FIG. 4  
STATIC STABILITY DIAGRAM

Consider an oscillatory subcooled flow entering a heated channel. The inlet flow fluctuations create propagating enthalpy perturbations in the single-phase region. The boiling boundary defined as the instantaneous location of the point where the bulk fluid temperature reaches saturation oscillates because of these enthalpy perturbations. Changes in flow and the length of the single-phase liquid region result in an oscillatory single-phase pressure drop. At the boiling boundary, the enthalpy perturbations are transformed into quality (or void fraction) perturbations that travel up the heated channel with the flow. The combined effects of flow and void fraction perturbations and variations of the two-phase length create a two-phase pressure drop (and consequently superheat pressure drop) perturbation. However, the total pressure drop across the boiling channel from the inlet to outlet plenums is maintained constant. Thus, the two-phase and superheat pressure drop perturbation produces a feedback perturbation of the opposite sign in the single-phase liquid region which can either enforce or accentuate the imposed oscillation.

The density wave oscillation can be analyzed by the conventional linear feedback theory in the frequency domain. For this study, two computer codes, DYNAM<sup>9</sup> and NUFREQ<sup>10</sup> were used to calculate dynamic stability.

In DYNAM, the equations governing the conservation of mass, momentum and energy were first linearized about the normal operating condition. The dynamic analysis solved the linearized partial differential conservation equations using Laplace transformation of the temporal terms and integration of the spatial variations. The resulting equations represented the transfer function for each spatial node. The computer code was then written in complex

variable notation and employed frequency response techniques to develop the system transfer function.

NUFREQ is an FWEC updated and extended version of the NUFREQ-2 computer code developed by GE for the investigation of density-wave type of dynamic instability in a heated two-phase channel (boiling water reactor applications). FWEC has modified the GE version to include the superheated region to permit applications to once-through steam generators. The model for the superheated region includes both the heated region and an adiabatic riser.

For DYNAM and NUFREQ, the Nyquist stability criteria, used in control system theory, were applied to determine if the boiling channel was stable. Nyquist's theorem can be phrased as follows: "necessary condition for a linear system to be unstable is that the complex locus of the open-loop transfer function passes through or encircles in a clockwise manner the unity point on the negative real axis".

Panel 13 with 3.218 Mwt incident power and panel 21 with 1.758 Mwt incident power were analyzed using both DYNAM and NUFREQ. The resulting Nyquist diagrams are shown in Figures 5 to 8. Figure 9 shows the Nyquist diagram of panel 21 with 0.625 Mwt incident power obtained from using NUFREQ. From observing all these figures, we concluded that the boiler panels are dynamically unstable.

The unstable boiling flow is usually made stable by introducing flow orifices at tube inlets. Both DYNAM and NUFREQ were further run to

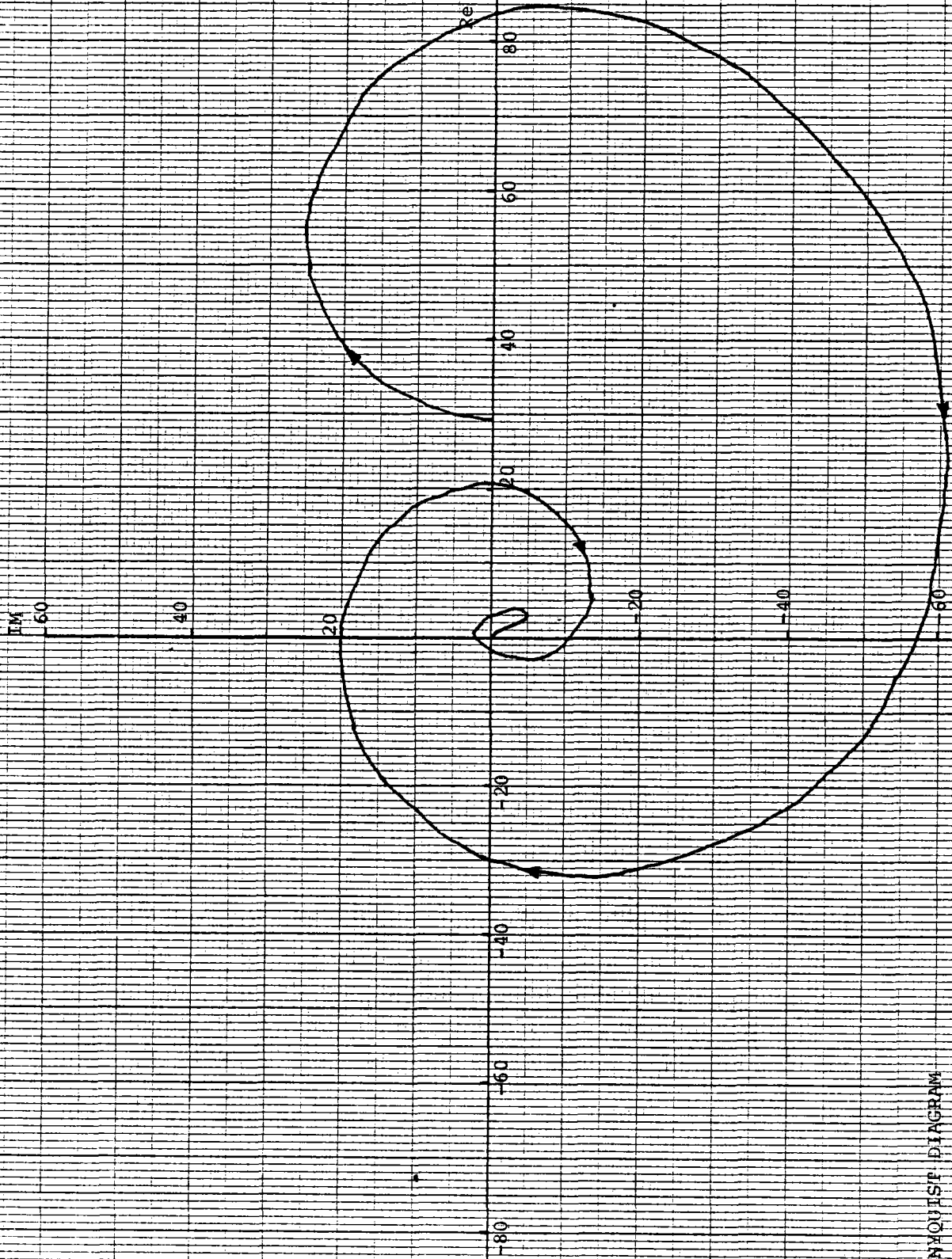


FIG. 5 NYQUIST DIAGRAM  
PANEL 13, 3,218 MWt  
DYNAM

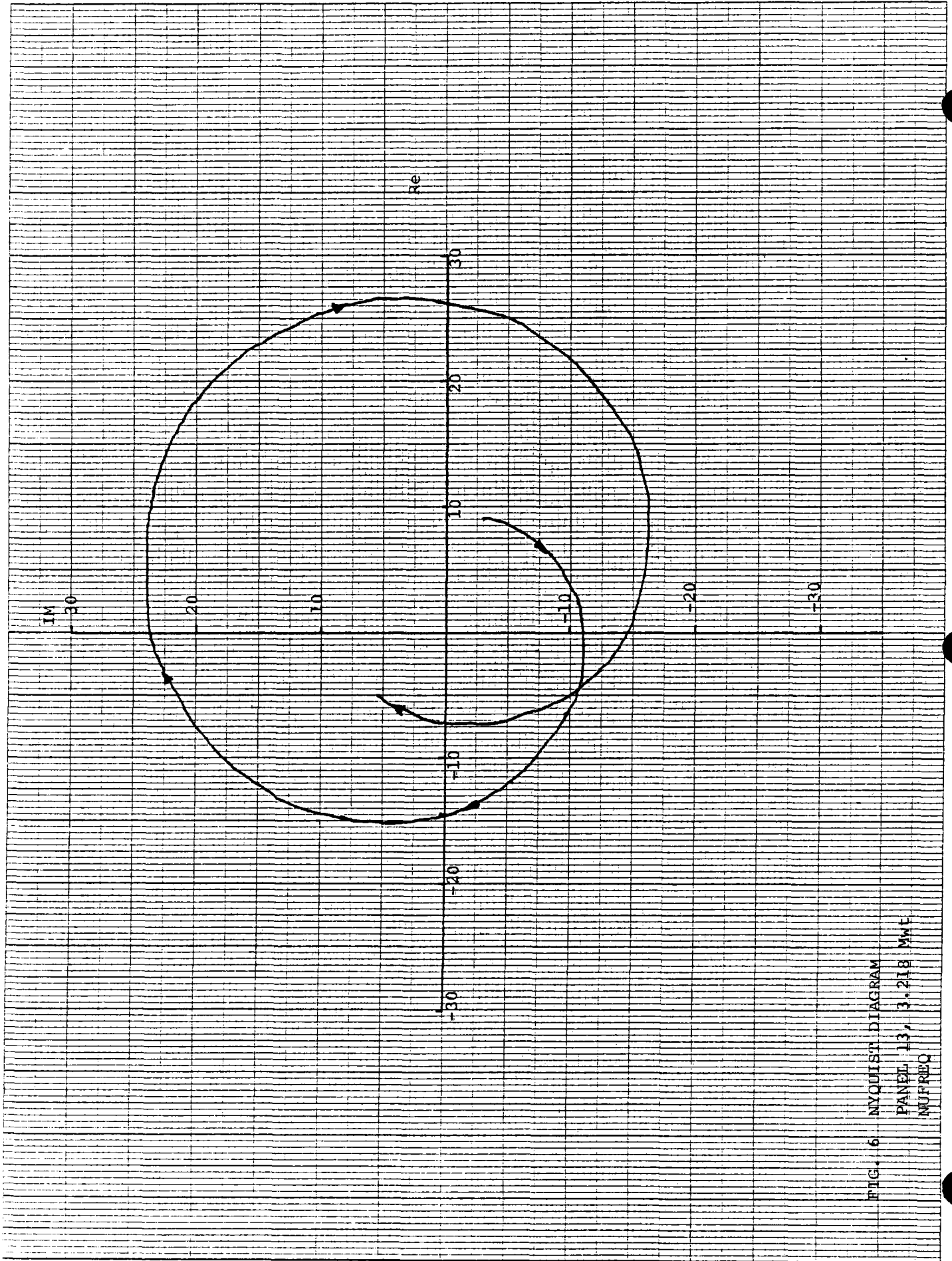


FIG. 6 NYQUIST DIAGRAM  
PANEL 13, 3.218 MWT  
MUFREQ

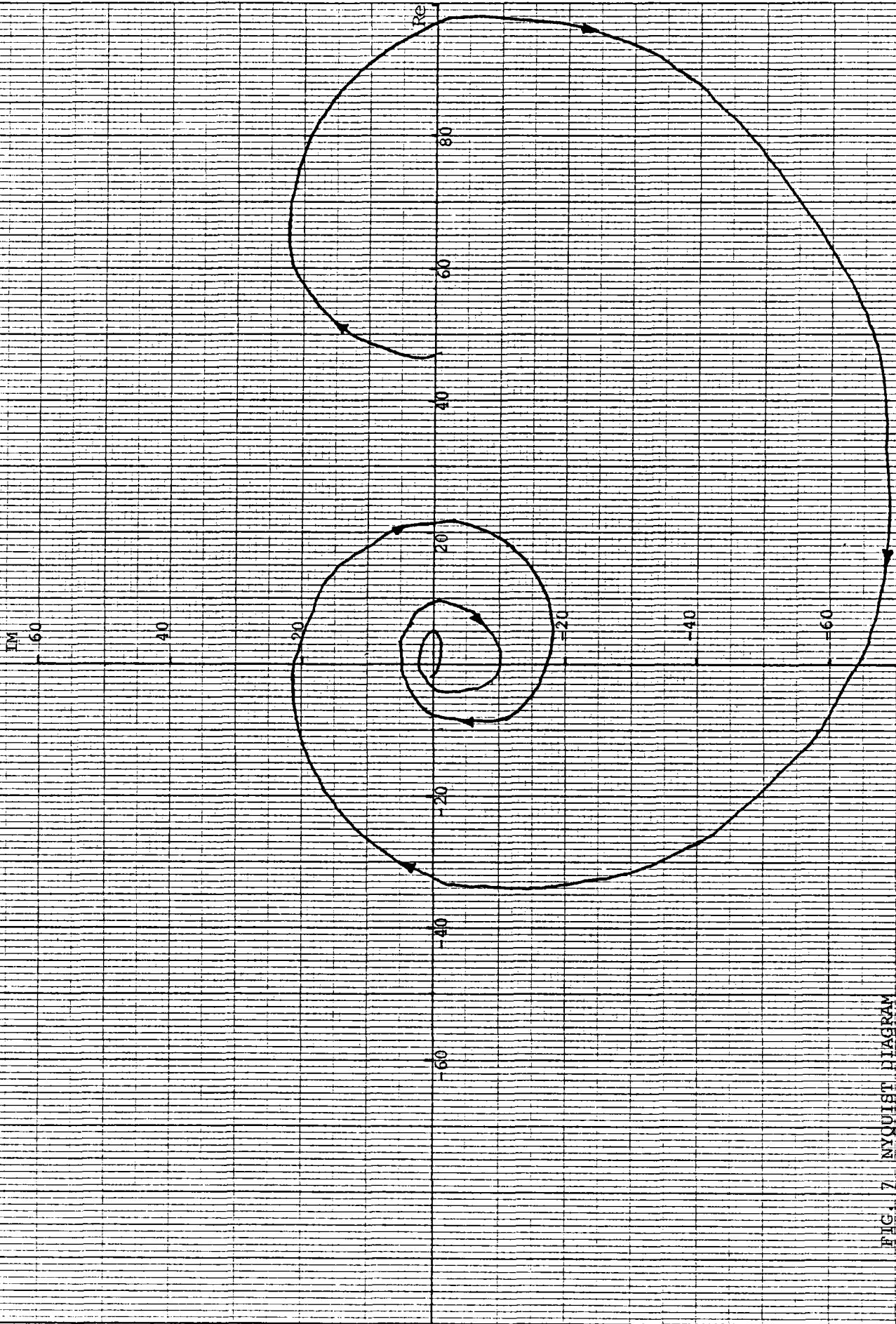


FIG. 7 NYQUIST DIAGRAM  
PANEL 21, 1.758 MWt  
DYNAM

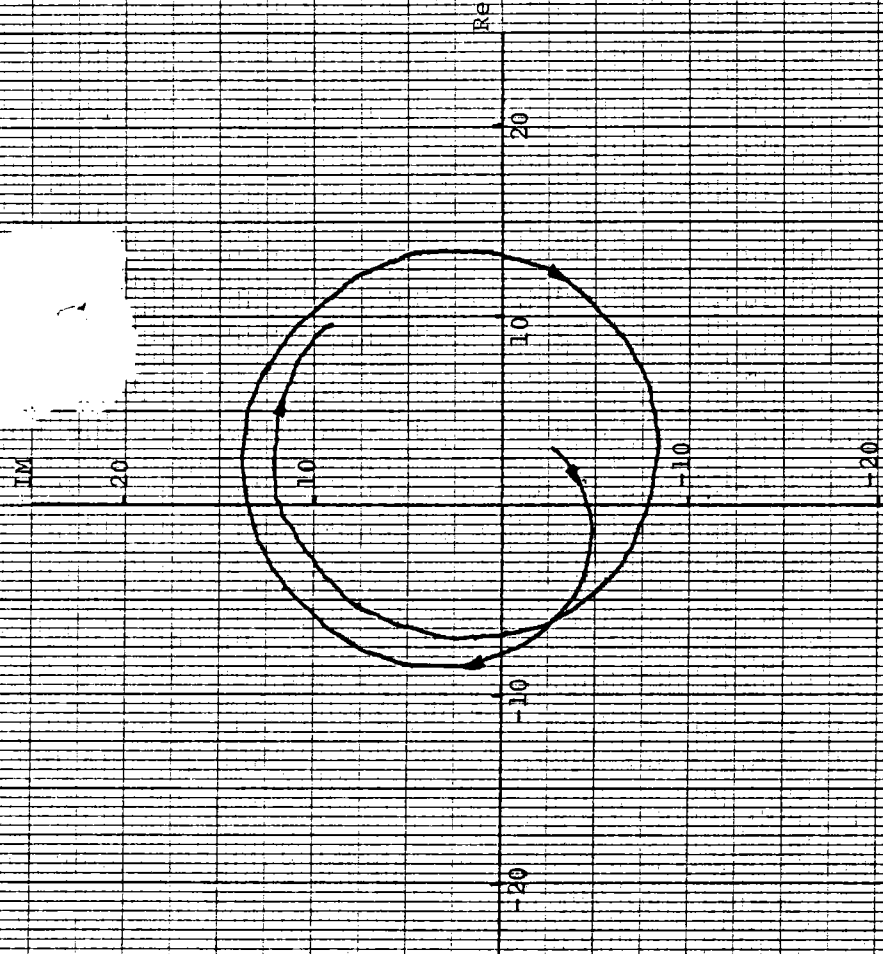


FIG. 8 NYQUIST DIAGRAM  
PANEL 21, 1.758 MWE  
NUPREQ

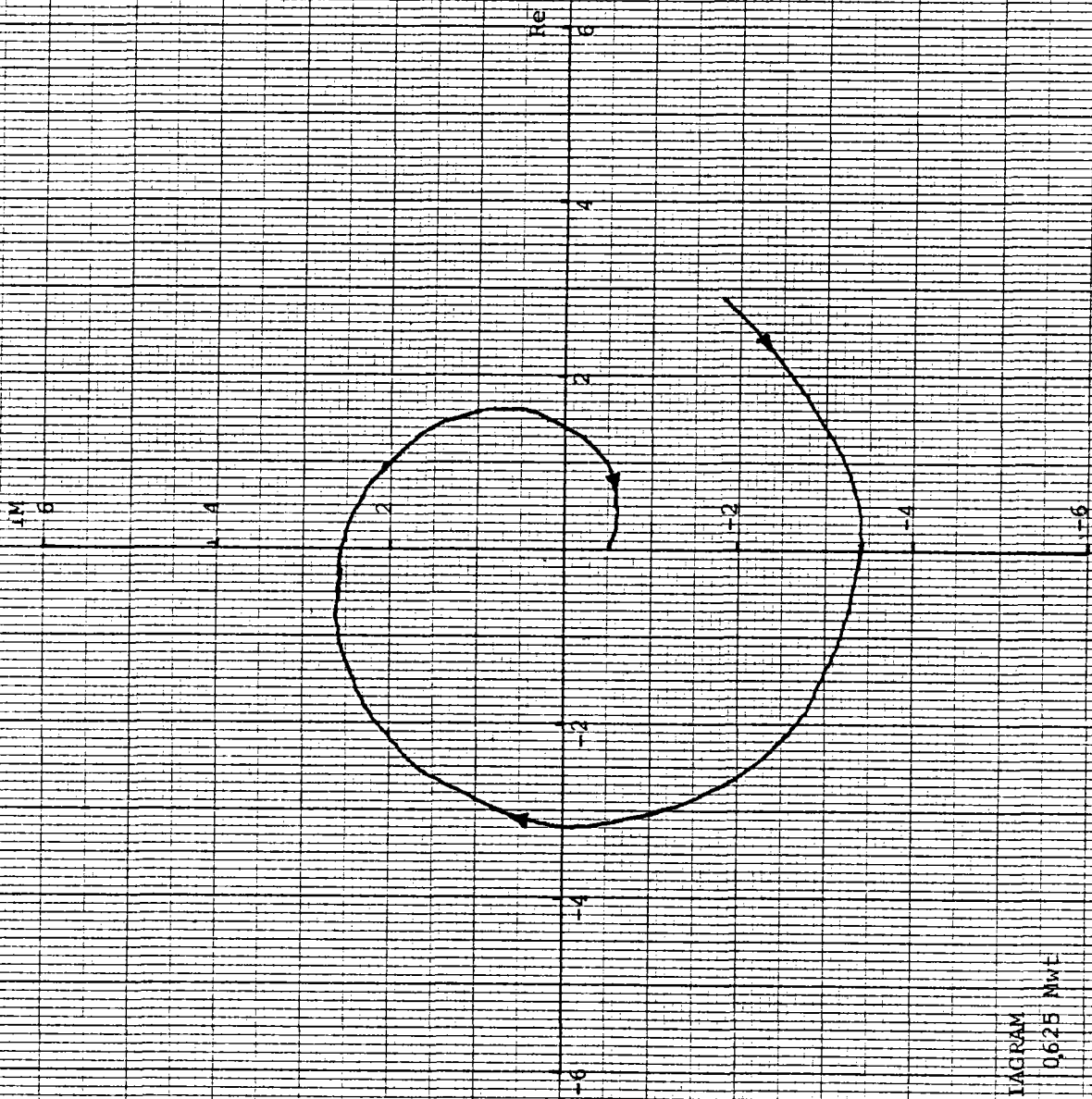


FIG. 9 NYQUIST DIAGRAM  
PANEL 21, 0.625 MWE  
NUFR10



determine the required orifice sizes to stabilize the boiling flow. The same results were obtained from using both computer codes. The required orifice sizes are as follows:

	<u>Maximum orifice I.D. (in.)</u>
Panel 13 with 3.218 Mwt incident power	0.096
Panel 21 with 1.758 Mwt incident power	0.090
Panel 21 with 0.625 Mwt incident power	0.052

Dynamic stability was further investigated for panel 13 and panel 21 by reducing the inlet water subcooling from 50°F to about 1°F. The solar boiler thermal performance computer code was again used to establish the thermal/hydraulic conditions. With inlet water subcooling of 1°F, it was found that the dynamic stability of both panel 13 and panel 21 had improved, but that small inlet orifices were still required.

According to the theory of density-wave dynamic instability, the location of the boiling boundary between the subcooled liquid and the two-phase boiling fluid inside a boiling channel is of primary importance in the determination of dynamic instability. Both theoretical and experimental considerations indicate that a critical boiling length or point of minimum stability exists for a boiling channel. Below this critical boiling length, dynamic stability will increase with a decrease in inlet subcooling. Above this critical boiling length, an increase in subcooling tends to stabilize the system. Since dynamic instability is caused by the existence of the boiling boundary between the single phase subcooling liquid and the two-phase boiling region, this boiling boundary can be eliminated if saturated liquid (i.e., no inlet subcooling) is introduced into the boiling channel. This can be done by redesigning the preheat section so that nearly saturated

water enters boiler panels. However, our study showed that 1°F inlet subcooling does not stabilize the evaporator/superheater panels. Therefore, further re-designing of evaporator/superheater panels should be considered; namely separation of superheating from evaporation.

#### CONCLUSIONS AND RECOMMENDATIONS

The flow stability analyses indicate that the boiler panels are statically stable, but are dynamically unstable under various levels of incident thermal power. Reducing the inlet water subcooling and increasing the water flow rate improved the dynamic stability of the boiling channel, but the results were still not satisfactory. Inlet orificing of individual boiler tube was required to achieve dynamic stability. However, the required orifice sizes were extremely small and were prohibited by the consideration of scale deposition. If the boiler panel configuration could be modified, it is suggested that the heated subcooled section be separated from the evaporator/superheat panel by modifying the preheat panel and the superheat section be separated from the present combined evaporator/superheater panel by introducing a proper plenum between evaporation and superheat. This will require a rearrangement of the boiler circuits. In other words, there would be three groups of flow panels (Preheat, boiling, superheat) in series connection and in each group a number of panels would be connected in parallel.

The CHF/DNB thermal stress analysis needs more precise high cycle fatigue data for Incoloy 800. This task is beyond the present workscope, and further efforts on CHF/DNB thermal analysis are necessary.

Within the limit of current funding, we will continue dynamic stability analysis for separate preheater boiler and superheater panels to find a way to stabilize the flow circuit and perform a limited analysis for the DNB-induced thermal oscillation.

## REFERENCES TO APPENDIX F

1. P. I. Kawano, D. J. Daniels, "Parametric Thermal Analysis of the Central Receiver Boiler/Superheater Panel," MDAC Memorandum A3-228-DELTA-78014, January 23, 1978.
2. F. W. Dittus and L. M. K. Boelter, "Heat Transfer in Automobile Radiators of the Tubular Type," University of California - Publications in Engineering, Vol. 2 No. 13, p. 443-461, 1930.
3. J. R. S. Thom, et al. "Boiling in Subcooled Water During Flow Up Heated Tubes or Annuli," Proceedings of the Institute of Mechanical Engineers, 1965-1966, Vol. 180, Pt. 3C, p. 226.
4. J. C. Chen, "A Correlation for Boiling Heat Transfer to Saturated Fluids in Convective Flow," ASME Paper No. 63-HT-34.
5. L. S. Tong, "Boiling Heat Transfer and Two-Phase Flow," John Wiley & Sons, Inc., New York, June, 1967.
6. A. A. Bishop, R. O. Sandberg, and L. S. Tong, "Forced Convection Heat Transfer at High Pressure After the Critical Heat Flux," ASME Paper No. 65-HT-31.
7. J. B. Heineman, "An Experimental Investigation of Heat Transfer to Superheated Steam in Round and Rectangular Channels," Argonne National Laboratories, Report No. ANL-6213, 1960.
8. R. C. Martinelli and D. B. Nelson, "Prediction of Pressure Drop During Forced Convection Circulation of Boiling Water," Transactions of the ASME.
9. L. G. Efferding, "DYNAM, A Critical Computer Program for Study of the Dynamic Stability of Once-Through Boiling Flow with Superheated Steam," GAMD-8656, 1968.
10. R. T. Lahey, Jr. and G. Yadigaroglu, "NUFREQ, A Computer Program to Investigate Thermo-Hydraulic Stability," General Electric Company, NEDO-13344, July, 1973.